Institut de Sostenibilitat

Sustainability PhD Program

Universitat Politècnica de Catalunya

Bio-based flame retardant for sustainable building materials

Yunxian Yang

Doctoral Degree in Sustainability

Thesis supervisors

Laia Haurie Ibarra

De-Yi Wang

2019 Barcelona

ACKNOWLEDGEMENTS

As an important part in my thesis, there could be no better than gratitude for all the persons who gave me a lot of understanding and supporting during my PhD period. Firstly, I want to express my great acknowledgements to my supervisors, Dr. Laia Haurie Ibarra and Dr. De-Yi Wang, for offering me the opportunity to perform the PhD work. Thanks to their professional and patient guidance as well as encouragement, I enjoyed a fulfilling and interesting time in Spain which would enrich my future life.

I would like to thank all the kind persons in Fire Lab of UPC, who helped me for the scientific work, especially for Ana Maria Lacasta, Xènia Armengol Garin, Alina Avellaneda López, Joaquín Montón Lecumberri, and also thanks for kind persons in UB.

I am grateful to have a chance to work in high performance polymer nanocomposites group in IMDEA, where I worked with Prof. Wen Zhang, Dr. Xin Wen, Dr. Zhiqi Liu, Dr. Wen Da, Dr. Shuang Hu, Dr. Vignesh Babu Heeralal, Dr. Rongkun Jian, Dr. Xiaolin Qi, Xiaomin Zhao, Yetang Pan, Zhi Li, Jing Zhang, Lu Zhang, Can Fu, Wei Liu, Qi Wang, Pablo Acuña, Jimena de la Vega, Abdulmalik Yusuf. As well as great thanks go to Dr. Juan Pedro Fernández, Dr. Miguel Castillo, Vanesa Martínez, and José Luis Jiménez, and my intern students Arthur Ollivier and Haoda Liu.

Special appreciation to my parents, bother, sisters and all my family members for their support and encouragement. Also, thanks for all my friends and all my colleagues in UPC to share the spare time with me. I also feel grateful to China Scholarship Council for the financial support in these three years. Finally, I want to say thanks again for all the precious experience and lovely people, all of them I will treasure.

Yunxian Yang

Barcelona, July 2019

ABSTRACT

Novel bio-based materials are already investigated and applied in various fields due to the issues of environmental contamination and resource depletion, especially in construction sectors. In comparison with the conventional material, this new promising alternative exhibits some attractive advantages, such as biodegradability, low toxicity, sustainability, renewability, and acceptable general properties. Moreover, the flammability related to fire risks should also be concerned, which is also an essential factor to restrict their further application. This thesis focused on the investigation of bio-based material with good flame-retardant performance and corresponding flame-retardant mechanism. The detailed investigation was developed by following stages: synthesis of bio-based flame retardant and its application to PLA (Chapter **3**); effect of bio-based flame retardant on the fire resistance and other properties of natural fiber reinforced PLA (Chapter **4**). Finally, thermal properties and flame retardancy involved smouldering and flaming combustion of thermal insulation material made from corn-pith and bio-based flame retardants were studied in Chapter **5** as well.

1) On the basis of bio-based concept, PA and THAM were selected as raw material to synthesize a novel flame retardant and the chemical structure was confirmed via some characterizations. Afterwards, this phytate product PA-THAM was employed as an efficient additive to PLA by melt mixing. This binary system showed an incompatible morphology and improved flame retardancy, which was achieved by a combination of "heat transfer" effect, slight dilution and barrier action. For example, only 3 wt% loading of PA-THAM imparted PLA-based biocomposite LOI value of 25.8% and UL 94 V-0 level, as well as a significant self-extinguishing ability was observed. Besides, the molten viscosity of biocomposite also demonstrated more reduction compared with neat PLA

due to the lubrication of PA-THAM, while there was little change in the mechanical properties.

2) PA-THAM and corn pith cellulose were combined via in-situ modification and used to prepare a PLA-based biocomposite. After OCC was modified by PA-THAM successfully, which was proved by SEM/ EDS, FTIR, and TGA, the effect of PA-THAM on thermal stability and fire behaviors of natural fiber reinforced PLA biocomposite was also investigated accordingly. In contrast to control sample without additive, 5 phr addition of PA-THAM enabled this biocomposite to possess a 50 °C higher temperature at maximum degradation rate, and the combination of PA-THAM and OCC caused enhanced flame-retardant properties, which exhibited an increase of LOI value, a reduction of PHRR, and more char residue. The predominant flame-retardant mechanism focused on the synergistic effect of PA-THAM and OCC that occurred in condensed phase. Besides, the same level introduction of PA-THAM improved the interfacial affinity between PLA and OCC, which maintained good mechanical properties as well as could play a positive role in thermal stability and fire resistance.

3) A bio-based thermal insulation material was made from corn pith cellulose fiber, alginate, and bio-based flame retardants. After introducing these bio-based additives, the smouldering and flaming combustion behaviors were improved significantly. Compared with the reference sample, thermal insulation particleboard with 8 wt% loading of a mixture of PA-THAM and DOT increased the initial temperature of smouldering ignition by 70 ºC, and meanwhile, the value of PHRR in flaming combustion decreased by 25.5%. Furthermore, the thermal conductivity was hardly affected, while thermal degradation temperature corresponding to the maximum decomposition rate remarkably increased. The improved fire behaviours were attributed to a synergistic effect from both flame retardants, which promoted a formation of more stable charring layer at initial stage.

RESUMEN

Los materiales de base biológica ofrecen una alternativa prometedora para aplicaciones en el sector de la construcción, debido a que se trata de materiales biodegradables, renovables y de baja toxicidad. Sin embargo, su capacidad de inflamar y la necesidad de mantener un bajo riesgo frente a incendios en los edificios es un factor esencial para restringir su posterior aplicación. Esta tesis se ha centrado en el desarrollo de materiales de base biológica con buen comportamiento frente al fuego y la investigación de los mecanismos de los retardantes de llama involucrados. La investigación se desarrolló en tres etapas que se detallan a continuación.

1) Partiendo del concepto de base biológica, se seleccionaron PA y THAM como materias primas para sintetizar un nuevo retardante de llama y la estructura química se confirmó mediante la caracterización del compuesto resultante. Posteriormente, este producto sintético PA-THAM se empleó como un retardante de llama eficiente para PLA mediante mezcla fundida. Este sistema binario mostró una mejora en la resistencia al fuego, que se logró mediante una combinación de los efectos de transferencia de calor, ligera dilución y acción barrera. Por ejemplo, con sólo un 3% en peso de carga de PA-THAM se logró un valor de LOI de 25,8% del compuesto de PLA y un nivel UL 94 V-0, así como una capacidad de autoextinción significativa. Además, la viscosidad fundida del biocompuesto también se redujo en relación a la del PLA puro debido a la lubricación ejercida por el PA-THAM. Por otro lado, la adición del retardante ocasionó pocos cambios en las propiedades mecánicas.

2) El retardante basado en PA-THAM y la fracción fina obtenida triturando la médula de maíz (OCC) se combinaron mediante modificación in situ y se usaron para preparar un biocompuesto basado en PLA. La médula de maíz fue modificada con éxito con el PA-THAM, la cual cosa se demostró por SEM / EDS, FTIR y TGA, el efecto de PA-THAM

sobre la estabilidad térmica y el comportamiento al fuego del material compuesto a base de PLA también fueron investigados. La adición de 5 phr de PA-THAM permitió a este biocompuesto reforzado con fibras naturales (NPC) alcanzar una temperatura 50 °C más alta en el punto de degradación máximo comparado con la muestra de control sin aditivo. También se obtuvo una mejora en el comportamiento al fuego con un aumento del valor de LOI, una reducción del pico máximo del ritmo de liberación de calor (PHRR), y una mayor formación de residuo carbonizado. El mecanismo ignífugo predominante se centró en el efecto sinérgico del PA-THAM y la OCC que ocurrió en la fase condensada. Además, el mismo nivel de introducción de PA-THAM mejoró la afinidad interfacial entre PLA y OCC que también mantuvo buenas propiedades mecánicas.

3) Se prepararon muestras de un material de aislamiento térmico de base biológica a partir de médula de maíz, alginato y retardantes de llama de origen biológico. La adición del retardante de llama de base biológica logró mejorar significativamente el comportamiento al fuego, y el fenómeno de combustión sin llama (smouldering). En comparación con la muestra de referencia, el panel aislante con una carga de 8% en peso de una mezcla de PA-THAM y una sal de borato de sodio (DOT) aumentó la temperatura inicial a la que se produce la combustión sin llama en 70 ºC y, permitió reducir el valor de PHRR en un 25.5%. Además, la conductividad térmica apenas se vio afectada, mientras que la temperatura a la que se produce el valor máximo de degradación térmica aumentó notablemente. El análisis del mecanismo de acción de los retardantes reveló la existencia de un efecto sinérgico de ambos retardantes de llama, que promovió la formación de una capa de carbonización más estable en la etapa inicial.

Contents

Abbreviations

PLA: poly(lactide)

CC: Corn cellulose

APP: ammonium polyphosphate

PA: phytic acid

DOT: disodium octaborate tetrahydrate

THAM: trometamol

SEM: Scanning electron microscopy

EDS: Energy dispersive spectrometer

FTIR: Fourier transform infrared spectroscopy

DMA: Dynamic mechanical analysis

TGA: Thermogravimetric analysis

$T_{5wt\%}$: Temperature at 5wt% mass loss

T_{max}: Temperature at maximum mass loss rate

T_{ig}: Ignition temperature

T_g: Glass transition temperature

T_c: Cold crystallization temperature

H_c: Enthalpy of crystallization

H_m: Enthalpy of melting

χ_c: Crystallization degree

LOI: Limiting oxygen index

MCC: Micro combustion calorimeter

CCT: Cone calorimeter test

HRR: Peak heat release rate

PHRR: Peak heat release rate

THR: Total heat release rate

TTI: Time to ignition

Av-EHC: Average effective heat of combustion

TSP: Total smoke production

TGA-FTIR: TGA coupled with FTIR

Vt-FTIR: Variable temperature FTIR

CHAPTER 1

Introduction

1.1 Background and motivation of this study

1.1.1 Application of bio-based material

Due to the increasing issues of environment and energy problems, the concept of ecological materials has obtained more and more attention, which needs to build a balance to achieve the goals of social benefits and environmental protection [1–3]. In construction sector, the environmental awareness is also considered by the stakeholders, which means some new unconventional materials, such as biodegradable, recycled, and natural resources, are promoted to utilize in this field [4–6].

In comparison with the traditional petroleum-based construction material, these new alternatives usually exhibit attractive merits, such as renewable, biodegradable, abundance, sustainability etc. [7,8]. Among these new generation materials, natural fibers and bio-degradable thermoplastics are the most commonly used materials, which are prepared into natural fiber reinforced plastic composites or thermal insulation boards due to the specific properties. Natural fibers plant-derived mainly include seed, blast, fruit, leaf, stalk, and wood, listed in Fig. 1-1 [9–12], while the bio-degradable thermoplastics which are widely investigated consisted of PLA, PBT, PCL, and PHAs, shown in Fig. 1-2 [13–17].

However, there are also other existing problems due to their intrinsic property, especially for the flammability, which should be highly regarded before using as a construction material due to a great quantity of fire hazard [18,19]. Therefore, the flame-retardant properties of the novel bio-based material should be investigated while

considering the environmental and energy problems. In this work, the thermoplastic and natural fiber are focus on PLA and corn stalk cellulose, respectively.

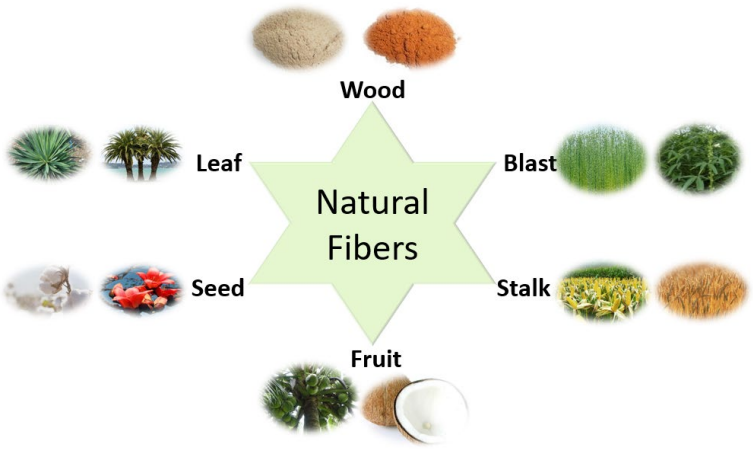

Fig. 1-1 Classification of natural fibers [9–12]

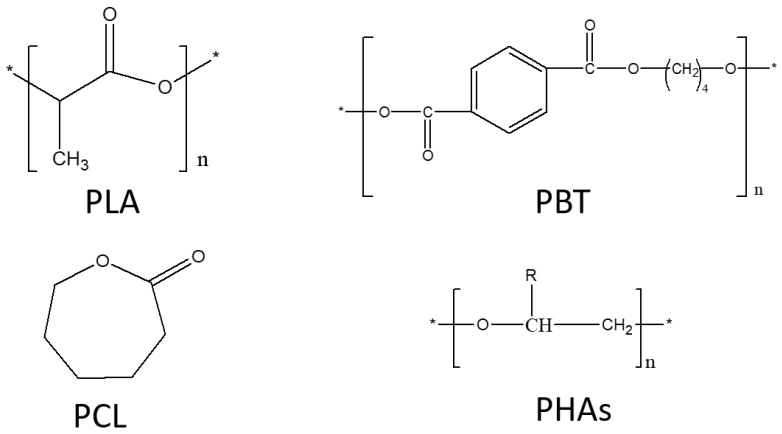

Fig. 1-2 Bio-degradable thermoplastics [13–17]

1.1.2 Thermoplastic polymer PLA and its biocomposite

PLA, as environmental-friendly thermoplastic, is an aliphatic polyester with biocompatibility and biodegradability, which is extracted and made from renewable resources, such as corn starch, cassava, and sugarcane, shown in Fig. 1-3 [20].Owing to the good inherent properties (tensile strength: 60 Mpa, elongation at break: 6%, Young's modulus: 2.4 Gpa, Notched izod impact: 16 J/m, and glass transition temperature: 55-60 ℃

at the extrusion grade) [21], PLA is becoming a promising substitute for petroleum-based polymers in the various applications including medical, packaging, electronic, and engineering areas [22–26].

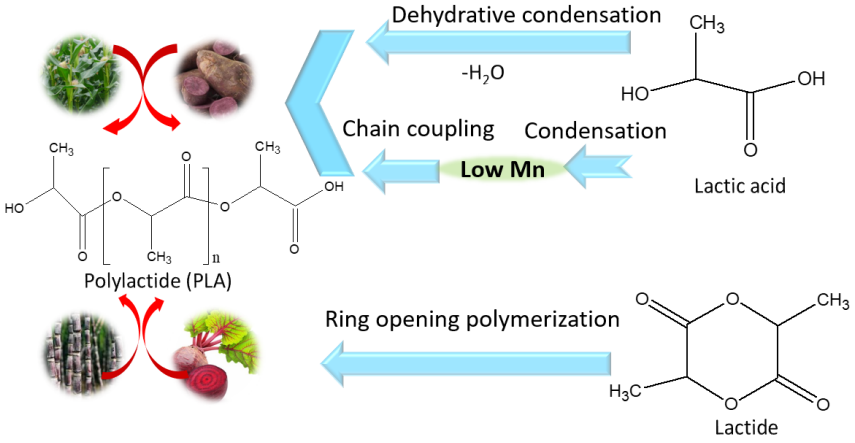

Fig. 1-3 Synthesis routes of PLA [20]

Besides, natural fiber reinforced PLA-based biocomposites are also gaining more and more attention and utilization in some applications such as automobile, aeroplane, and construction applications in consideration of environmental sustainability and energy efficiency [27]. Saurabh [28] used sisal fiber with different fiber size to reinforce PLA via two processing strategies of direct-injection molding (D-IM) and extrusion-injection molding (E-IM), shown in Fig. 1-4. Through the analysis of mechanical properties and the morphology of the biocomposites, D-IM process was recommended to prepare the biocomposites with short fibers; meanwhile E-IM way was suitable for ones with both long and short fibers. Biocomposites with short sisal fiber exhibited superior tensile and flexural properties with uniform dispersion and orientation, while the corresponding impact strength decreased due to the incorporation of short fibers.

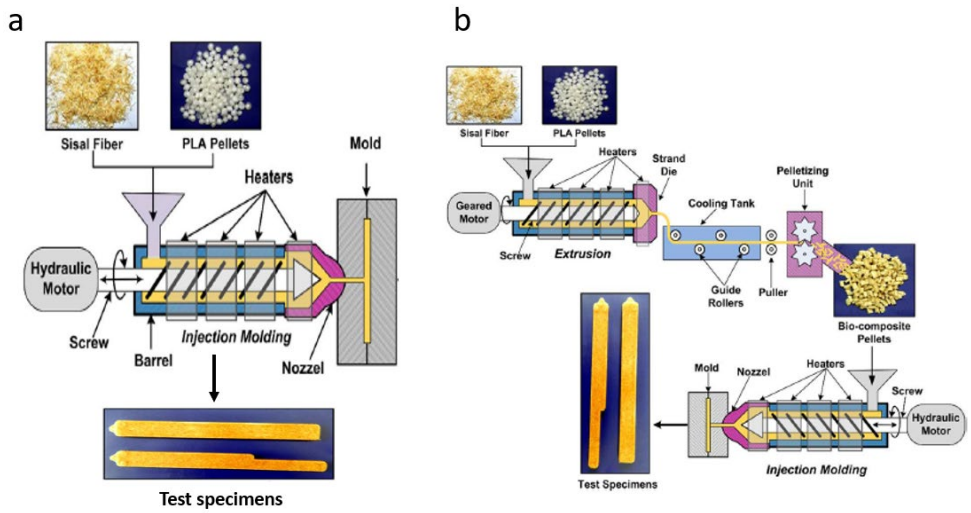

Fig. 1-4 Schematic of two different processing methods: a) D-IM; b) E-IM [28]

Cellulose fibers were used to fabricate the PLA/ fiber composite, and the chemical and enzymatical methods were developed to improve the interfacial affinity between fiber and polymer [29]. After incorporation of modified lignofibre cellulose fibers (LFO) into PLA, the resulting composites illustrated an enhancement in Young's modulus, impact strength as well as thermal stability with a compromising tensile strength, especially for the PLA-based composites with chemically modified fibers. As for the accelerated weathering conditions, which generally gave negative effect on the properties of biocomposites, the enzymatical modification enabled PLA-based composites to preserve the mechanical, thermal and surface chemical performances compared to the reference composite with unmodified fibers. Mazzanti [30] studied the reinforcing mechanisms of natural fibers in PLA-based composites by analyzing the mechanical behavior and fiber-matrix interface. Two types of PLA-based biocomposites were prepared by introducing untreated fiber (UF) and alkali-treated fibers (TF). PLA/TF composite demonstrated better tensile properties than those with UF did, which can be elucidated with interfacial adhesion, fiber-induced crystallization, and crystalline structure of fiber. Besides, the morphology of UF and TF were also investigated, and there was obvious difference between these two fibers,

presented in Fig. 1-5. It was proposed that opening bundle and individualization of fibers after treatment can benefit the mechanical properties.

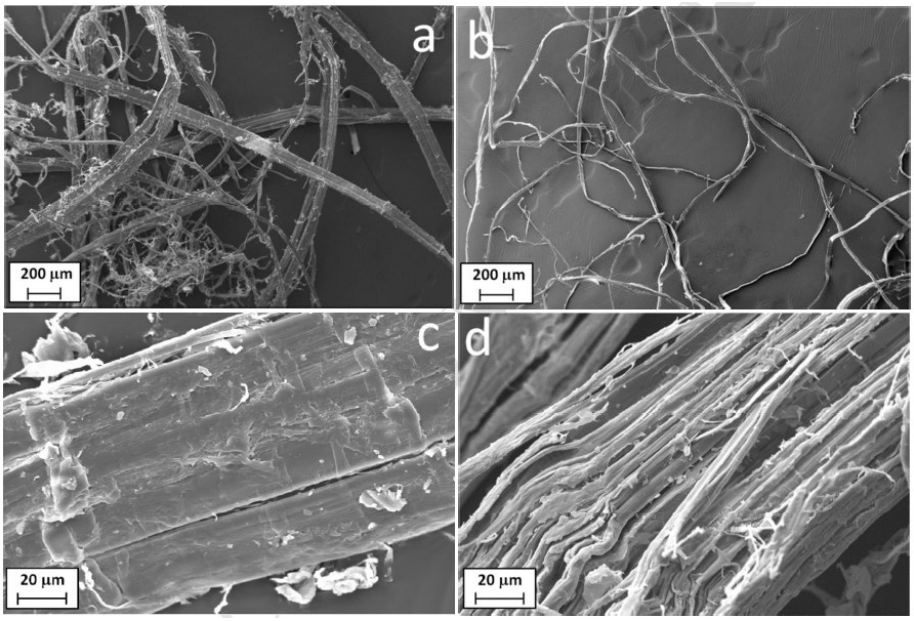

Fig. 1-5 SEM micrographs: a) UF 150X; b) TF 150X; c) UF 2000x; d) TF 2000x [30]

1.1.3 Natural fiber material

Now effective utilization of natural fiber is becoming a promising approach to relieve the environment and energy problems, especially for the by-products and surpluses of the crops. With regard to the construction applications, the natural fiber from crops can be used as the alternative for petroleum-based thermal insulation materials, which need a low thermal conductivity [31]. Except some factors that affect the final thermal conductivity, such as product density, temperature-humidity conditions, and granulometric structure, the internal structure of material also determine the value of thermal conductivity. VĖJELIENĖ et al [32] evaluated the relationship between thermal conductivity and internal structure for straw and stalk of natural fibers, and pointed that the internal porous structure played an important role in the thermal conductivity of materials. Sample made with bent grass possessed much higher density (110 kg/ m^3) than

the one with reed did (76.5 kg/ m^3), but a lower thermal conductivity (0.06 W/ mK) were observed in bent grass than that in reed (0.085 W/ mK). This was because the bent grass stalk comprised an inner layer with a pore size of 0.1 μm -1.0 μm, while the reed wall was consisted of voids less than 0.1 μm. Consequently, at conditions of the same loading, sample with high porosity was conductive to decrease the heat transfer coefficient. As the common and abundant agricultural by-products, barley straw, corn stalk and rice husk are used to prepare the novel thermal insulation materials due to their availability and morphology structure, which were investigated in our laboratory [33] and listed in Fig. 1-6 and Fig. 1-7. Barley straw, which is comprised by stalk and leaf tissue with parenchymal cellules and vascular bundles with fibrous structure, exhibited a 0.6 μm thickness for cellular wall and plasma membrane of parenchymal cellules, as well as the intercellular space was about 3 μm. Corn pith that is the interior spongy tissue of the corn stalk, is mainly consisted of parenchymal cellules with a larger size of 100-140 μm and intercellular space of 10 μm. Rice husk, from dry outer part of the rise, showed a less porous structure with 2-5 μm of cellule diameter and 3 μm thickness of cellular wall. On the basis of internal structure, corn pith was more adaptable to be a thermal insultation material, which was supported by following research.

Fig. 1-6 Digital photos of natural fibers of barley straw, corn pith, and rice husk (from left to right) [34]

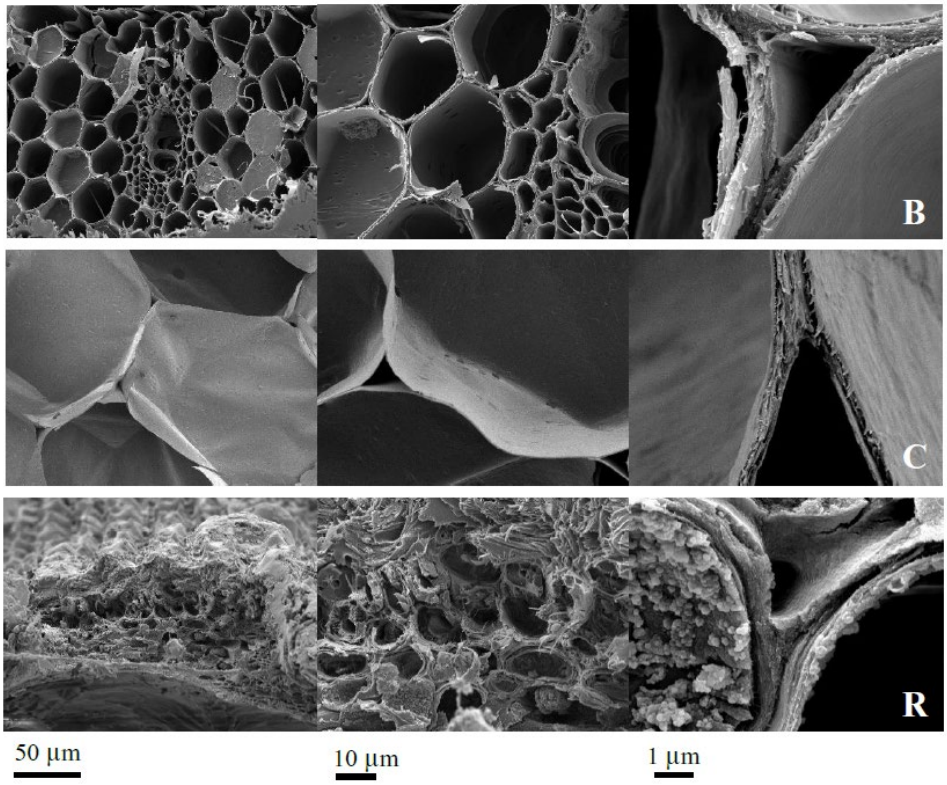

Fig. 1-7 SEM images of natural fibers at 500x, 1500x, 15000x from left to right: B) barley straw, C) corn pith, R) rice husk [34]

Besides, some achievements are already reported about these novel thermal insulation materials. A stem fiber from cotton stalk was used as raw material to produce thermal insulation fiberboard without binder and chemical additives by using high frequency press [35]. This binderless cotton stalk fiberboard (BCSF) presented good potential for insulating component due to a low thermal conductivity, which had a linear correlation with the board density. Although the fiber moisture content and pressing time hardly affected the value of thermal conductivity, IB, MOR, and MOE were improved obviously with the increase of these two parameters, and this phenomenon was attributed to the enhanced lignin repolymerization and hydrogen bonding formation. Fig. 1-8 is the curves of thermal conductivity and board density for BCSF.

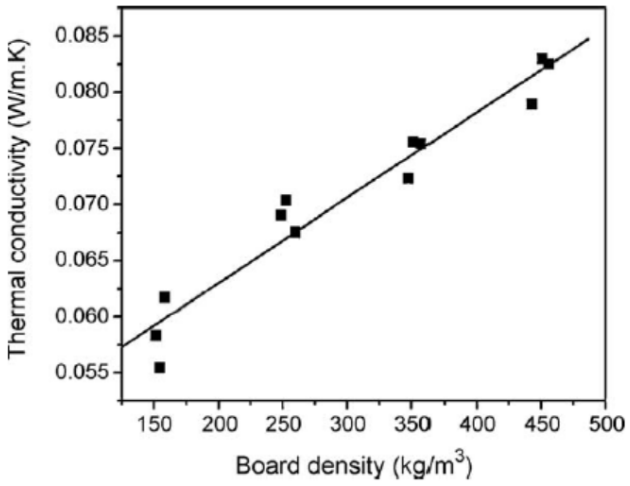

Fig. 1-8 Thermal conductivity of BCSF as a function of board density [35]

Zhou et al. [36] developed a new thermal insulation material made from rice straw (RSTIB) by high frequency hot-pressing. Through this high frequency hot-pressing, the thermal insulation boards demonstrated optimum properties of a low density of 250 kg/ m^3, thermal conductivity of 0.051-0.053 W/ mK, as well as a higher IB value than that of sample made by the conventional hot-pressing method, and the relative data were listed in Table 1-1. Furthermore, other factors affected the thermal conductivity also studied such as the particle size, boards' density, and ambient temperature.

Table 1-1 Comparison of properties for RSTIB in different manufacturing methods [36]

	IB/ (MPa)	MOR/ (MPa)	TS/ (%)	Thermal conductivity (W/ mK)
Conventional hot pressing	0.0096	0.89	13.52	0.0524
High frequency hot pressing	0.0132	0.56	17.49	0.0517

Boonterm et al. [37] treated the cellulose fiber from rice straw with chemical modification and thermal steam explosion; then thermal insulation boards were made from these two types of natural fiber, shown in Fig 1-9. This straw fiber insulation board illustrated the conductivity coefficients in the range of 0.11-0.14 W/mK, which are

similar with that of gypsum boards and bricks but higher than that of EPS foam. In comparison with the chemical modification, the steam explosion can remain a higher fiber yielding and larger remaining of lignin and hemicellulose; moreover, a lower thermal conductivity was obtained in thermal insulation boards made from steam-exploded fiber.

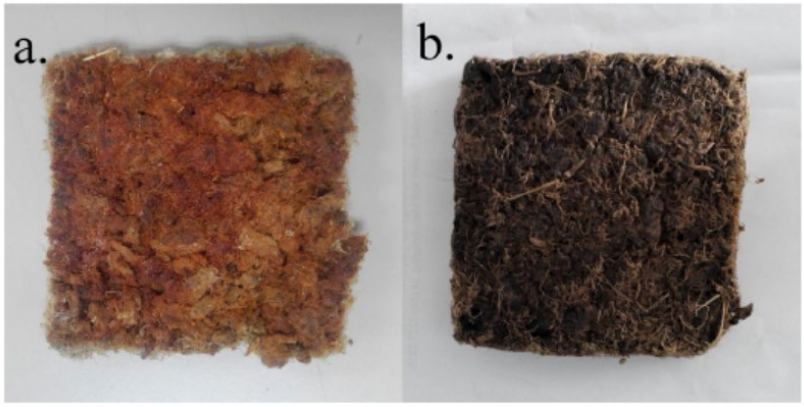

Fig. 1-9 The insulation boards made from straw fiber: a) treated by NaOH solution, b) treated by steam explosion [37]

1.1.4 Flame retardants

In terms of flame retardants, there are general principles of the flame-retardant mode, which involves chemical or/ and physical actions occurred in solid or gas phase. The physical retarded action mainly occurs by the ways including formation of carbonaceous layer, cooling and dilution effects during degradation process, while the chemical reactions act by interfering with combustion process in the condensed or/ and gaseous phase [38,39]. In most cases, the fire resistance behavior of the flame retardants take place as a complex process with several individual stages and one dominating simultaneously. In general, the flame retardants can be classified as the major types according to the containing elemental content: halogenated compounds, inorganic additives, phosphorus-containing flame retardants, and chemicals involved boron or nitrogen elements.

Halogen-containing compounds, as a common flame retardant with advantages of processability, miscibility, low negative effect on other properties, and low-cost, act mainly in gas phase by capturing radicals to retarded the combustion process. Although an amount of halogenated chemicals in various formulations are developed for thermoplastic and thermoset, some of them are already restricted to use in some countries due to the released toxic products that are hazard to environmental and health [40].

Inorganic additives, especially for ATH or MDH, are widely used in industrial applications with a combination of halogen-containing compound owing to the remarkable synergistic effect. These compounds can undergo some endothermal degradation processes, such as dehydration reaction, to cool down the surface temperature, which cannot reach the critical value for sustaining combustion, and form an oxide protective layer to improve the flame-retardant properties. However, a large loading in thermoplastics, which would change the inherent nature of matrix, limits the further application in some fields [41,42].

Phosphorus-containing flame retardants, containing phosphorus with trivalent from -3 to +5, include inorganic PFRs, organic PFRs, and halogenated PFRs, are considered as suitable alternatives for BFRs. The flame retardant mechanism of these compounds can be focus on the condensed phase, the gas phase, or the both phases, which varies depending on the type of additives and polymers [43,44]. As the representative of the first group, RP and APP functioned in solid phase are frequently reported in the academic research. Dogan et al. [45] incorporated an microcapsulated RP into TPU composite with huntite & hydromagnestite. This TPU based composite showed an obvious enhancement in flame retardant behaviours, increasing LOI value to 32.5%, passing UL-94 V-0 rating, decreasing PHRR by 76.7%. The synergistic interaction between flame retardant system increased the formation of charring layer in condensed phase and action of radical capture

in gas phase; this combination of both phases prevented remaining material from further combustion. APP, as a typical IFR, was combined with phosphorylated sodium alginate and dipentaerythritol to improve the flame retardant propertied of polypropylene [46]. This novel effective IFR system demonstrated a good flame-retardant ability for composite due to char layer-protecting mechanism, which is an isolating barrier with low thermal conductivity to reduce heat transfer and flame propagation.

With regard to the organic PFRs, there are three primary structures of these compounds, which are listed in Fig. 1-10 [47]. A series of flame retardant formulations (in Fig. 1-11) containing phosphates, phosphonates, and phosphinates were utilized for PET and the corresponding flame retardant mechanism was analyzed via TGA, TG-MASS, and TG-FTIR as well [48]. Composite with PCO 910 exhibited a gas phase flame-retardant mechanism, where the NOR-FR acted as a radical-forming agent and the pyrolysis mechanism was presented in Fig. 1-12 [49]; a condensed phase activity was found in the material system with SPDPP; and combination of condensed and gas phase actions was for the formulation with SPDPDOM. Moreover, Qian et al. [50] synthesized a DOPO derivative named ABD, and applied it into epoxy resins. This thermoset system illustrated an increased in flame retardancy due to the existence of 3 wt% ABD, which was supported by a LOI value of 36.2%, UL-94 V-0 rating, as well as a reduction of PHRR and THR. This improvement in flame retardant performance was attributed to quenching activity from phosphaphenanthrene group and charring effect caused by phosphaphenanthrene group and hydroxyl group, and the conjoint behaviours in condensed and gas phases imparted epoxy material good flame-retardant properties. The chemical structure of ABD and its pyrolysis route were demonstrated in Fig. 1-13 [50].

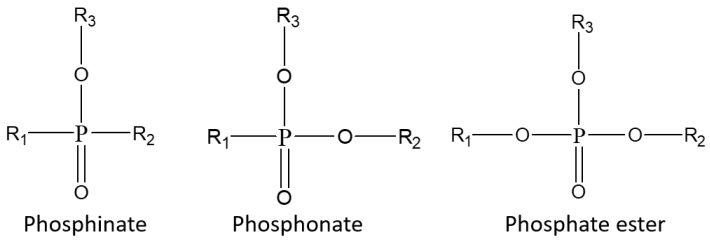

Fig. 1-10 General structure of organophosphorus flame retardants [47]

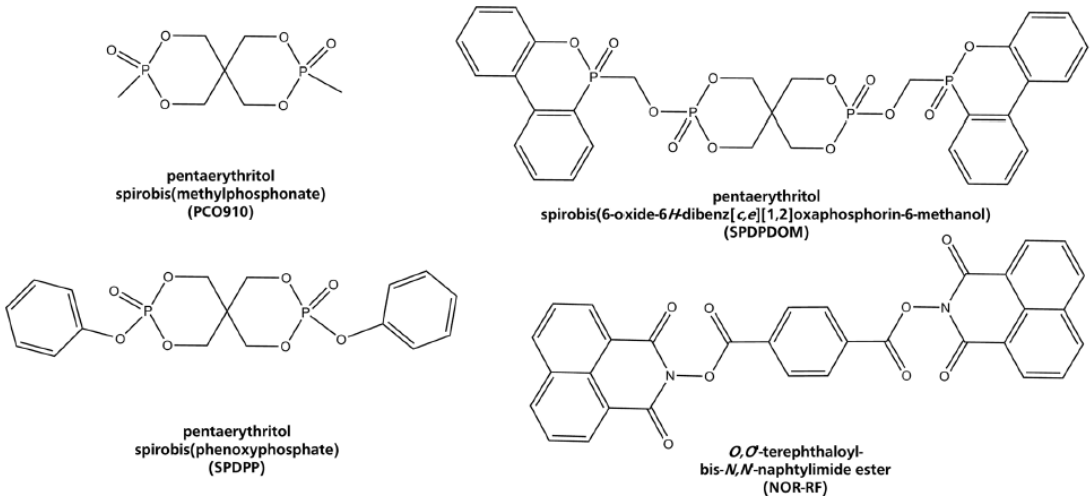

Fig. 1-11 Molecular structures of three organophosphorus flame retardants and NOR-RF agent [48]

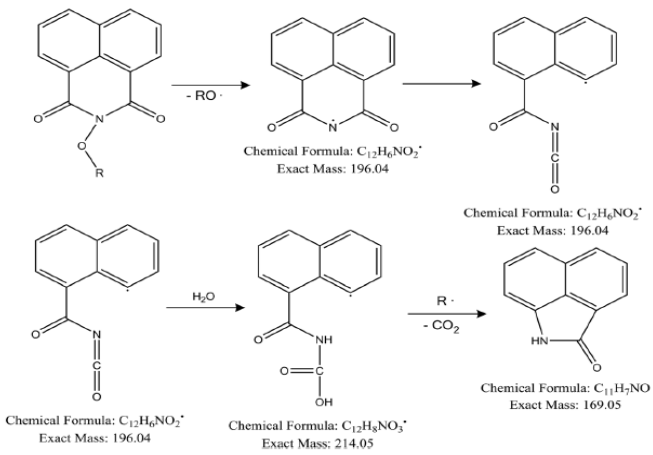

Fig. 1-12 Radical dissociation mechanism of NOR-RF [49]

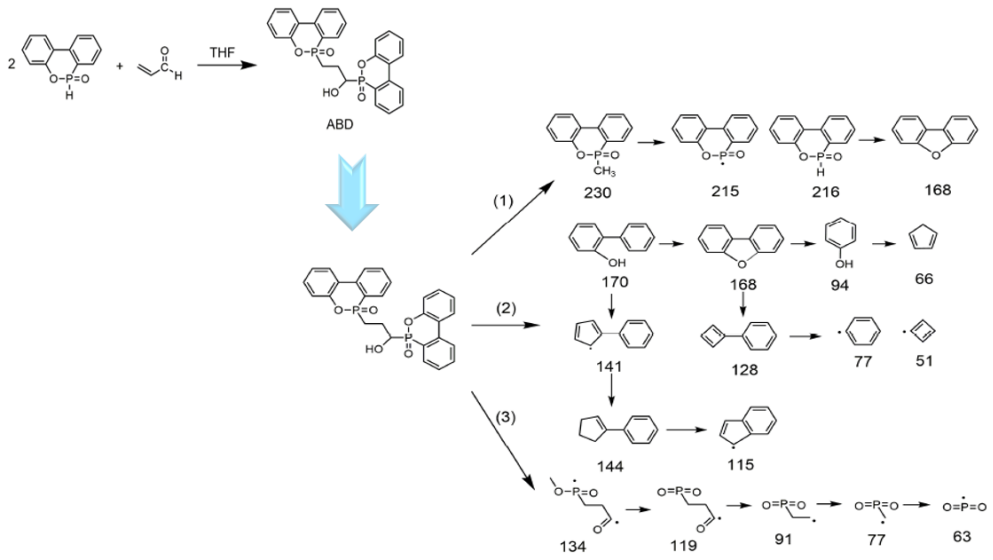

Fig. 1-13 Chemical structure of ABD and its pyrolysis route [50]

Nitrogen-containing and boron-based compounds, as halogen-free flame retardants, also attract much attention due to their synergistic effect with other additives. The flame retardant action of nitrogen-containing chemicals acts by diluting the concentration of oxygen and/ or promoting the dripping of polymers [51–53], and also used as a combination with phosphorus to enhance the charring ability. Boron-based products are active in the condensed phase by changing the decomposition process to induce the formation of carbonaceous layer instead of CO or CO_2 [54,55]. A highly efficient flame retardant (RGO-AZOB/ SMB) of boron-containing graphene oxide was prepared and introduced into PLA [56]. Due to the flame retardant effect of this hybrid, which was based on the glassy charring process of boron-containing groups and the blocking effect of inherent lamellar, PLA-based nanocomposite exhibited an improvement in flame retardant performance with a significant reduction of PHRR by 76.5%, THR by 76.9%, TSR by 55.6%, as well as passing UL-94 V-0 rating and increased LOI value 31.2%. Fig. 1-14 is the synthesis process and proposed flame retardant mechanism of RGO-AZOM/ SMB.

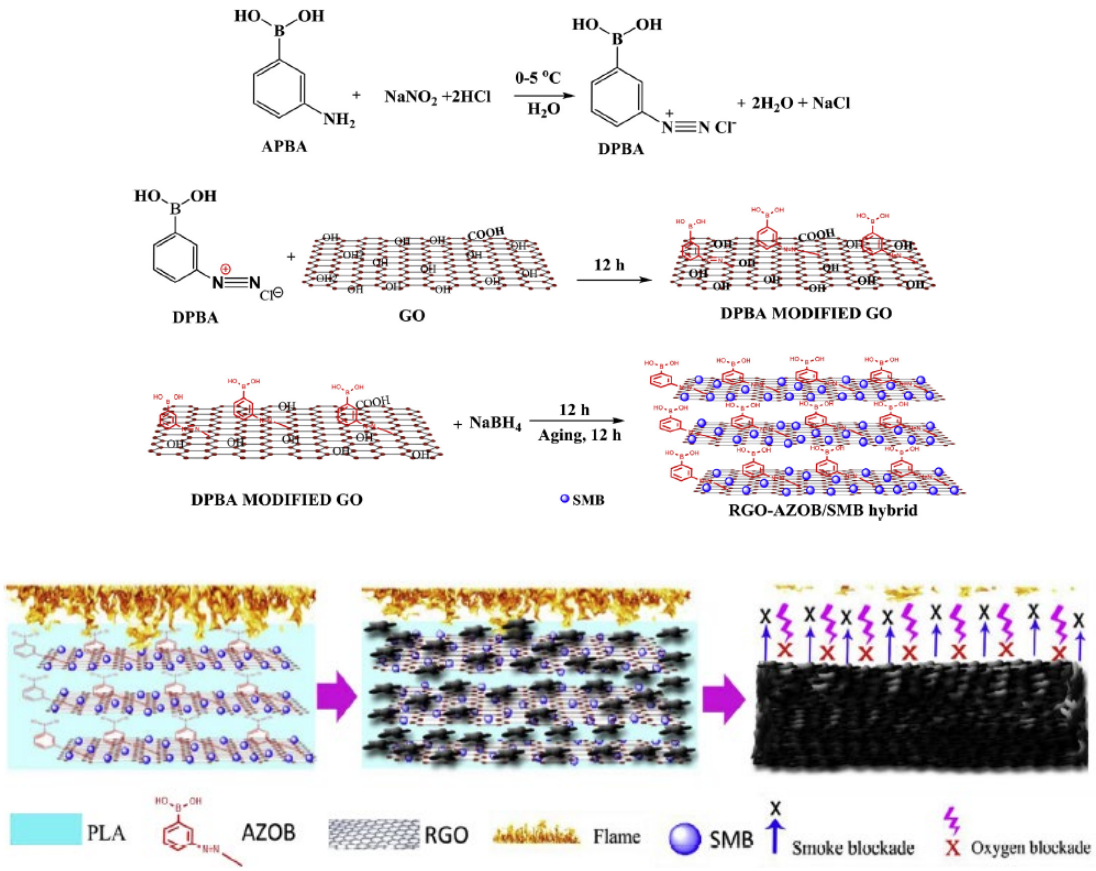

Fig. 1-14 Synthesis of RGO-AZOM/ SMB and the propose flame retardant mechanism [56]

Yang et al. [57] improved the flame retardant properties of epoxy resins by incorporating a novel phosphorus/ nitrogen-containing compounds (DMT), listed in Fig. 1-15. When the DMT with 1.25% phosphorus content was loaded, the EP composite showed decreased values for PHRR by 59.4% and THR by 27.4%. Through analyzing the volatile products and residue composition, it was elucidated that DMT acted in both condensed and gas phases, which was achieved by the free radical-quenching effect and incombustible volatiles from DMT in gaseous phase, as well the charring catalyzation effect in solid phase.

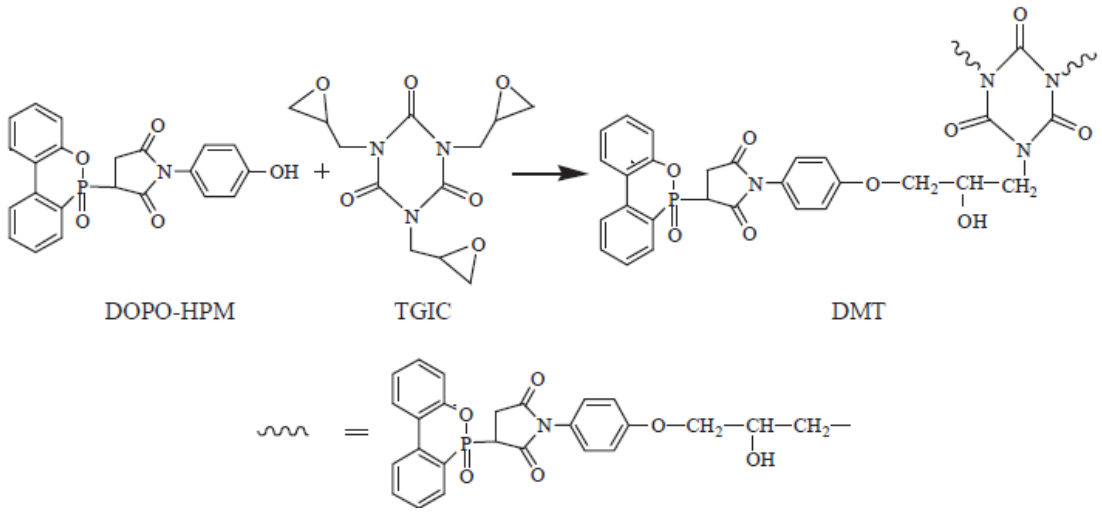

Fig. 1-15 Synthesis route of DMT [57]

1.2 State of the art

1.2.1 Bio-based flame retardant

In terms of bio-based and ecological concept, some bio-based flame retardants are already reported by previous investigations [58–60]. For example, a series of environmentally friendly flame retardants (SPCs) with varying degrees of phosphorus and nitrogen were prepared by some ecological substances [61], and the reaction scheme is listed in Fig. 1-16. Through analyzing the thermal degradation behavior, it was found that SPCs decomposed in three stages. In the first step, ammonia and phosphoric acid were generated, and the latter can promote the charring behavior of SPC due to the dehydration of starch backbone; then a thermal stable and compact char layer formed by crosslinking reactions of starch with liberated phosphoric acid and formation of polyphosphate. During the degradation process, the volatile products such as ammonia, water, and carbon dioxide can dilute the concentration of fuels to lead flame extinguishment, and meanwhile, the existence of carbonaceous layer can act as an obstruction for heat transfer and gas exchange, which play an essential role to keep sustaining combustion. Therefore, this

novel SPC can be used as an efficient bio-based flame retardant for some material. Tang et al. [62] used PA to treat PLA nonwoven fabric via pad-dry-cure technique. In comparison with the control sample, the modified PLA nonwoven fabric illustrated a significant flame retardant properties with a reduction of PHRR, THR, and HRC contributed by a good condensed phase mechanism. Phloroglucinol was chosen as bio-based raw substance to synthesize a reactive PFR and epoxy monomer [63]. With regard to the fully bio-based system, PFR-free epoxy presented a good thermal stability and 38 wt% content of chat residue. On the other hand, the incorporation of PFR in epoxy decreased the thermal stability but increased the char yield at high temperature.

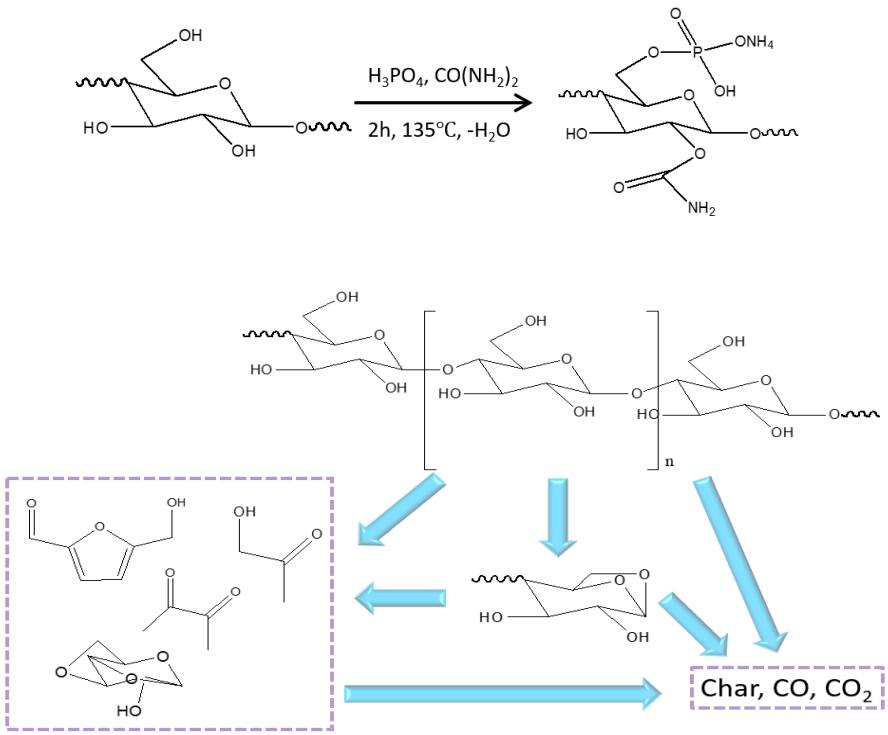

Fig. 1-16 Synthesis route of SPC and pyrolysis behavior of starch [64]

Concerning the scheme of reaction mechanism of phosphorus-containing compounds, condensed or/and gas phase reaction (shown in Fig. 1-17) should be analyzed depending on different material system. Flame retardant activities occurred in gas-phase are mainly based on the effect of radical phosphorus species, as the flame inhibitors, on the

recombination of hydrogen and hydroxyl radicals, which can decrease the concentration of combustible gas that is required for sustaining combustion [65–68]. As for the solid-state fire resistance mechanism, char formation plays a key role to improve the flame retardant properties, and this physical barrier can act as a thermal insulation and obstruction of gaseous fuels to reduce the volatile mass and heat flux. As a result, the underlying material is protected from further degradation [69–72]. However, in a real scenario, it is hardly to considered that one single action mechanism exists for PFRs during the combustion process [73].

Besides, the fire behavior of materials can be evaluated by some important factors, such as burning rate (degradation rate, heat release rate), spread rate (pyrolysis, smouldering), ignition performance (time to ignition, ignition temperature, critical heat flux), gas products (volatile species, concentration), and smoke production, etc. According to the present research, compounds involved phosphorus element can exhibit a charring ability, especially for those with a high oxygen content [74–76]. Consequently, this study is aiming at synthesizing a halogen-free phosphorus-containing compound by using bio-based raw materials. PA, as a bio-based phosphorus-containing chemical extracted from seed, stem, and germ of plant, was selected as a raw material to prepare novel flame retardant. Besides, nature fiber was also chosen for the flame retardant system due to the inherent char formation of lignin, cellulose, and hemicellulose when exposed to heat [77]. Afterward, the effect of this bio-based phosphorus-containing compound on the flame retardant properties of the PLA-based composites and thermal insulation particleboards are evaluated via different measures including LOI, UL-94, CCT, MCC, and smouldering test, as well as the correlative flame retardant mechanism of different material systems are analyzed by using TGA-FTIR, vt-FTIR, and SEM-EDS.

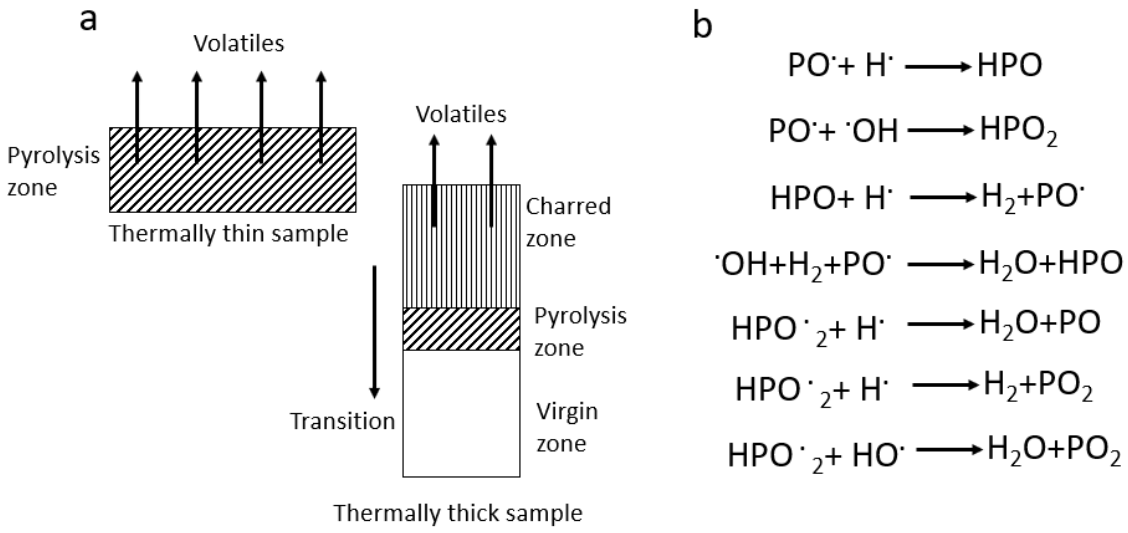

Fig. 1-17 Flame retardant mechanism: a) intumescent mechanism, b) radical capture mechanism [69,78]

1.2.2 Flame retardant PLA-based polymer

As for the flammability of PLA-based composite, which is an essential factor to restrict the application of PLA and its composites, it is also investigated by material scientists. With regard to improving the flammability of PLA and its composites, some approaches can be considered [79]: (1) chemical modification, (2) incorporation of flame retardants, (3) surface treatment. Jiang et al [80] grafted 9,10-dihydro-9-oxy-10-phosphaphenanthrene-10-oxide (DOPO) onto the surface of sepiolite (SEP) via chemical reaction of amino groups and salicylaldehyde, and this product SEP-DOPO with a grafting ratio of 12.8% was used to improve the fire resistance of PLA. In the presence of SEP-DOPO, PLA-based composite with 10 wt% additive presented an improvement in flame retardant properties: a 40.7% reduction of PHRR, passing V-0 rating in UL-94, reaching 31.5 % in LOI value. This was due to the synergetic effect of DOPO and SEP to catalyze the char formation in the condensed phase, and the proposed flame retardant mechanism was shown in Fig. 1-18. Boday et al. [81] prepared a flame retardant PLA-

backbone copolymer via ring-opening polymerization (ROP). This copolymer was synthesized by a lactide-functionalized macromonomer bearing phosphorus groups, which may be obtained from the atom transfer radical polymerization (ATRP) between phosphorus-containing monomer and brominated lactide initiator. The reaction scheme is listed in Fig. 1-19. Feng et al [82] improved the fire resistance of PLA by introducing intumescent flame retardants IFR (APP, CNCA-DA: an efficient oligomeric charring agent) and La_2O_3. The results showed that a synergistic effect between La_2O_3 and IFR promoted to form a compact and homogeneous carbonaceous layer, which possessed a crosslinking structure with good strength and barrier properties to protect the material during combustion.

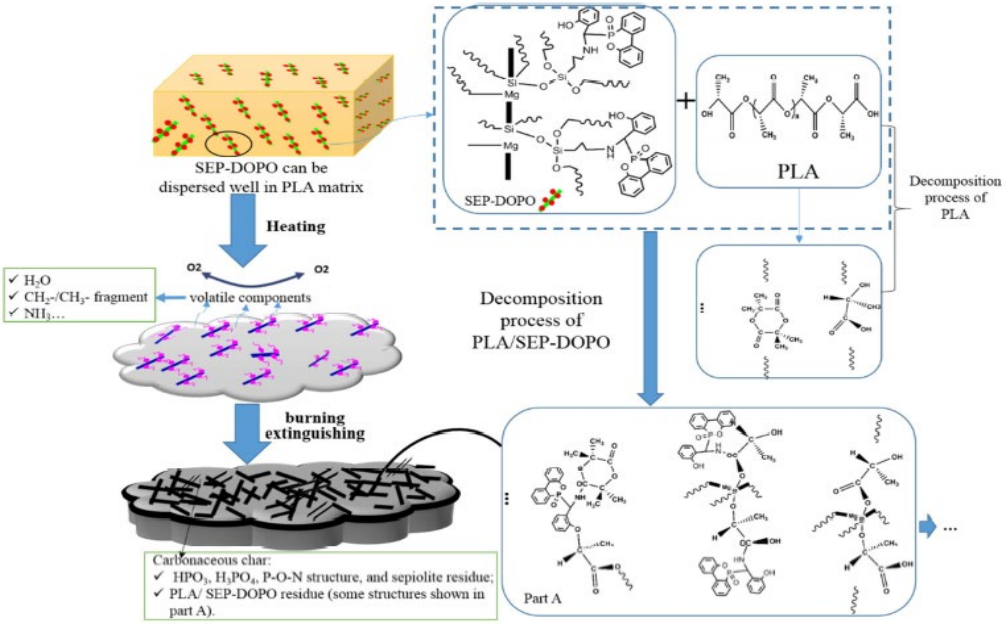

Fig. 1-18 Proposed flame retardant mechanism of PLA/SEP-DOPO composite [83]

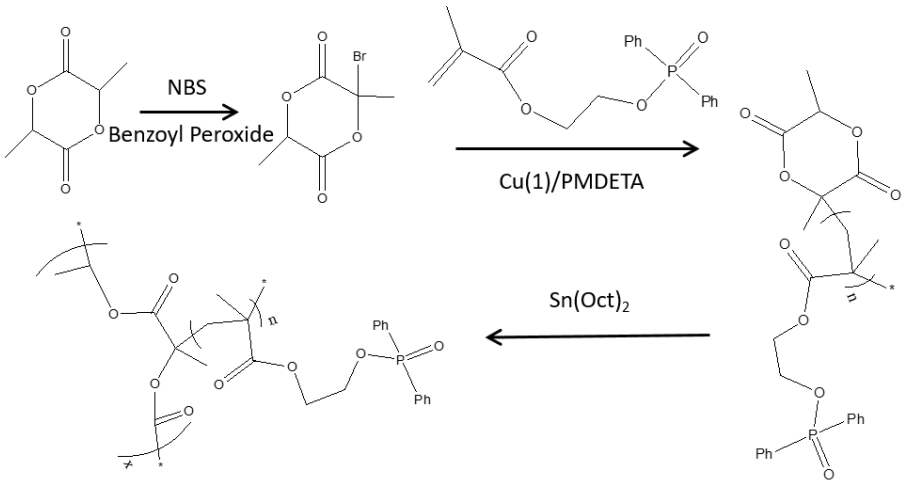

Fig. 1-19 Reaction scheme of flame retardant PLA-backbone copolymer [81]

However, the present research mainly focused on the mechanical properties or flame-retardant performance separately, while the improvement of both aspects for PLA and its composites is rarely reported. Therefore, this work is aiming to find a good balance between the thermal stability, mechanical properties and flame-retardant performance for PLA and its composites via varying the loading of these additives in PLA.

1.2.3 Flame retardant thermal insulation material

Concerning the thermal insulation material made from crop by-product, which are already reported by some papers (shown in part **1.1.3**), current investigations are primarily focused on the thermal conductivity performance, while few papers reported the flammability of the novel material, and this aspect still needs to pay more attention. Consequently, this work investigates the effect of bio-based phosphorus-containing substance not only on the thermal properties (thermal conductivity, thermal stability) of thermal insulation particleboard, but also on fire behaviors, especially for the smouldering performance.

Smouldering combustion, which can take place in porous fuels including polyurethane foam, charring polymers, cellulosic insulation particleboard and so on, also leads to a substantial fire hazard [84,85]. In contrast to the flaming combustion, which usually accompanies by high temperature (1500 ℃), low EHC (16-30 kJ/ g), and oxidation in gas phase, smouldering combustion is a flameless, persistent phenomena with characteristic of slow speed, low temperature (from 450 ℃ to 700℃), low EHC (6-12 kJ/ g), as well as oxidation in solid phase. A simple form of chemical reactions for solid fuel can be summarized by pyrolysis (Equation 1-1) followed by oxidation (Equation 1-2a or 1-2b) to present the difference between smouldering and flaming combustion [86]. In the terms of smouldering spread, which is determined by the oxygen supply and heat transfer, there are different propagation modes between forward and opposed smouldering phenomena, listed in Fig. 1-20 [87]. In forward mode, where the ignition takes place on the top of the fuel bed, smouldering will spread along the lateral and downward directions. On the contrary, the smouldering propagates in a slow and upward way in opposed mode, in which the occurrence of smouldering is observed in the interior of the fuel bed and the nearest top is virgin part. Therefore, some fire retardant strategies can be conducted in a combination of fire spread mechanism and smouldering kinetics, which consists of three step for cellulose material: cellulose pyrolysis, cellulose oxidation, and char oxidation [88].

Pyrolysis: [86]

$$\text{Fuel (solid)} + \text{Heat} \rightarrow \text{Pyrolyzate (gas)} + \text{Char (solid)} + \text{Ash (solid)} \quad \text{1-1}$$

Heterogeneous oxidation:

$$\text{Char (solid)} + O_2\ \text{(gas)} \rightarrow \text{Heat} + CO_2 + H_2O + \text{other gases} + \text{Ash (solid)} \quad \text{1-2a}$$

Gas-phase oxidation:

$$\text{Pyrolyzate (gas)} + O_2\ \text{(gas)} \rightarrow \text{Heat} + CO_2 + H_2O + \text{other gases} \quad \text{1-2b}$$

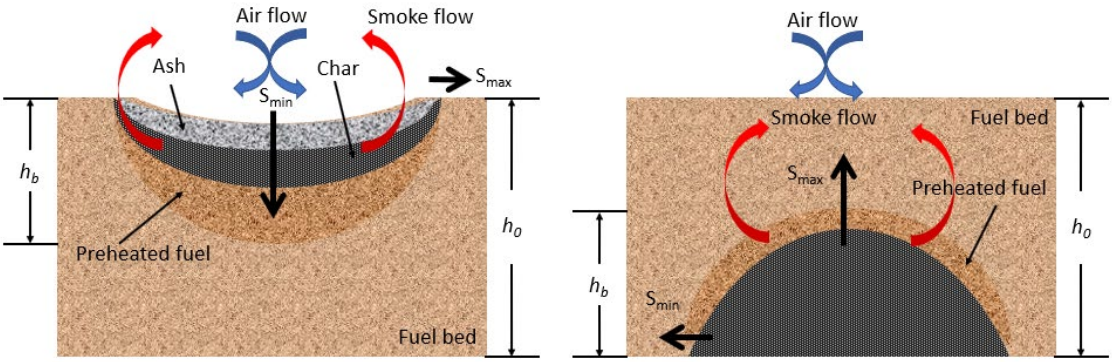

Fig. 1-20 Scheme of smouldering propagation in two different initiation modes: a) downward propagation; b) upward propagation [89]

With regard to the smouldering initial ignition, there are four types of initiation including radiant, conductive, ember, and self-heating, and all the four modes already are investigated by some groups [90–93]. In this study, thermal insulation particleboard made from corn-pith fiber with porous structure possesses a large specific surface area, and this feature can promote the reaction between fuel and oxygen as well as permit the transfer of oxygen and heat [84]. As a consequence, smouldering test is necessary performed to investigate the effect of bio-based flame retardant on this flameless burning property of the thermal insulation board. In this assay, the thermal insulation board specimens are prepared by the corn-pith particles with an appropriate size, which is also a factor for the balance of heat generation and heat loss [94]; meanwhile conductive initiation is utilized to ignite the samples, in which mode smouldering occurs by heat conduction and heat convection when porous fuel bed is in a direct contact with a heater. Besides, some flaming combustion tests are also carried out to study the fire performance of this novel thermal insulation material.

1.3 Objectives

On the basis of the previous research and analysis, this study is aiming to develop a novel bio-based flame-retardant material and clarify the corresponding flame-retardant mechanism, which was listed as following in detail.

1.3.1 To study the flame-retardant mechanism of PLA-based biocomposite with conventional flame retardant

In order to analysis the flame-retardant mechanism of natural fiber and phosphorus-containing flame retardant, PLA-based biocomposite with a combination of OWF and APP was prepared firstly, in which the OWF acted as an ecofriendly charring agent and APP as flame retardant. The effect of incorporation of OWF and APP on fire resistance behaviours of this biocomposite was investigated systematically, and simultaneously the flame-retardant mechanism was analyzed. The results of this preliminary work have been published in: Yunxian Yang et al., *Effect of oxidized wood flour as functional filler on the mechanical, thermal and flame-retardant properties of polylactide biocomposites*, Industrial Crops and Products, Volume 130, 2019, 301-309.

1.3.2 To study the relationship between structure and properties of PLA-based biocomposite

In consideration of the environmental protection and phosphorus-containing flame-retardant concept, a bio-based flame retardant (PA-THAM) was synthesized via sample salt formation reaction. The chemical structure of PA-THAM was determined and then

applied to PLA. The flame-retardant performances of this biocomposite were studied in detail, and the flame-retardant mechanism of PA-THAM was analyzed as well.

1.3.3 To study the flame-retardant mechanism of natural fiber reinforced PLA biocomposite

With regard to the results of previous material system, the natural fiber reinforced PLA biocomposite (NPC) system was prepared, which included corn-pith fiber pretreated with PA-THAM via in-situ modification. Meanwhile, a control sample, which comprised corn-pith fiber alone, was also designed to compare with the flame-retardant formulation. After analyzing the flame-retardant properties of these NPCs, the synergistic effect between corn-pith fiber and PA-THAM on flame-retardant mechanism of NPC system was also evaluated.

1.3.4 To study the flame-retardant mechanism of ecological thermal insulation material

In terms of natural fiber thermal insulation material, a bio-based thermal insulation material system prepared with corn-pith cellulose fiber and PA-THAM was designed to improve the flame retardancy. In addition to investigation of fire behaviours including both smouldering and flame combustion of this thermal insulation material system, the corresponding flame-retardant mechanism was elucidated through analyzing the actions in gas and condensed phases.

1.3.5 To evaluate other properties of these bio-based composites

In accordance with the aim of good balance, other performances of these different bio-based flame-retardant material systems, such as thermal properties, micro morphology,

molten viscosity and mechanical properties, were also investigated, and an optimum loading of additives was proposed.

CHAPTER 2

Materials and Experimental Methods

2.1 Materials

Polylactide (PLA, 4043D), a multi-purpose extrusion grade, was supplied by NatureWorks (Minnesota, USA). Corn stalk was kindly supported by northern farm in Cataluña. Phytic acid (PA, 50 wt%), trometamol (THAM), and sodium hydroxide (NaOH) were obtained from Sigma-Aldrich Corporation. Solubor (DOT) and ammonium pyrophosphate (liquid: APP) were bought from U.S. Borax and Budenhiem, respectively. Other chemicals including sodium alginate, plaster, and citrate were purchased from the Cargill SA. All the materials were used without any further purification and dried at 80 °C for 8 h before processing.

2.2 Experimental methods

2.2.1 Preparation of materials

Melt-mixing and hot-pressing processes

The thermoplastic materials were prepared by melt-mixing and hot-pressing processes (Fig. 2-1). A micro-compounder (MC 15, Xplore) with two screws was performed to mix PLA and fillers and the procedures were as following: preheated the chamber to 170 °C and started rotation at 80 rpm; fed PLA until it was melted; added other fillers into the melting PLA and mixed them for 2-3 min; then cut the strip-materials into granules. Afterwards, all the granulates were filled into molds and shaped by a hot press (LabPro 400, Fontijne Presses) according to relevant testing standards. This technology was conducted at 170 °C for 5min.

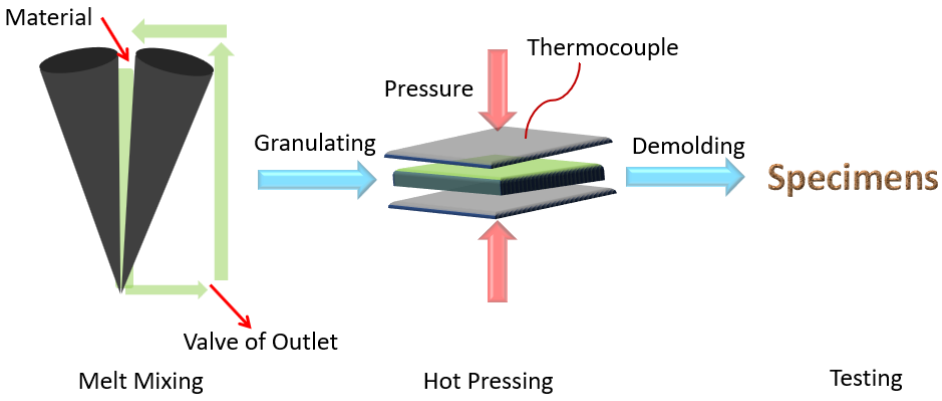

Fig. 2-1 Scheme of fabrication for thermoplastic materials

Curing process

The curing process was carried out to fabricate the cellulose insulation particleboards. As listed in Fig. 2-2, the wetted cellulose was thoroughly mixed with other additives; then transferred the mixture into the mold to press sample for 30min. After that, demolded sample and removed it into an oven at 50 ℃ for 2 days. Moreover, the relevant alginate films were obtained via the same method and all the specimens were kept at constant conditions (25 ± 1 ℃, 50% ± 3 R.H) for 2 days before testing.

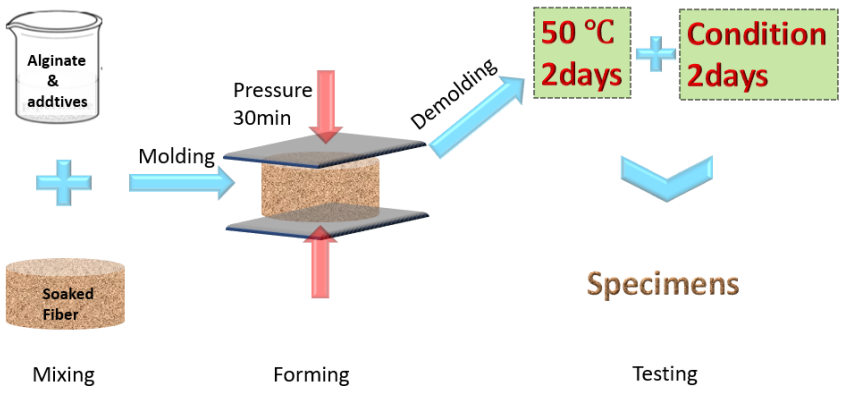

Fig. 2-2 Scheme of fabrication for cellulose insulation particleboards

2.2.2 Structural characterization

Nuclear magnetic resonance spectroscopy (NMR)

^{1}H NMP, ^{13}C NMR, and ^{31}P NMR spectra were performed on an equipment (Varian Infinity AS400, Bruker Co., Germany) with D_2O as solvent. Spectra was referenced by the standard experiment setup with a chemical shift (δ) in ppm.

Fourier transform infrared spectroscopy (FTIR)

FTIR (Nicolet iS50, TA Instrument) spectrum was recorded by scanning a range from 4000 cm^{-1} to 500 cm^{-1} with the resolution of 4 cm^{-1}. Each pellet was prepared by KBr powder and tested after background scanning with pure KBr.

Scanning electron microscopy (SEM)

SEM and Scanning electron microscopy-energy dispersive spectra (SEM/ EDS) were used on an apparatus Helios NanoLab 600i, FEI. The polymer-based specimen was observed after cryo-fracture and powder sample was scattered on the conductive tape; then the surface was gold-coated with 15 nm thickness at 10 kV accelerating voltage.

2.2.3 Properties characterization

Mechanical properties

Tensile test

Tensile test was carried on an apparatus INSTRON 3384, MA, and USA to investigate the tensile properties of materials. At leat five dumbbell-shapped samples were tested according to ASTM D 638-2014 measurement with a crosshead speed of 5 mm/ min.

Impact test

Charpy impact test was conducted by using CEAST impact machine. Un-notched specimen was hot-pressed on basis of ISO 179-1-2010 and data were recorded from five specimens for each formulation.

Dynamic mechanical analysis (DMA)

Dynamic mechanical analysis (DMA), which is a technique to characterize the relationship between mechanical properties and time, temperature, and frequency for plastic materials, was applied on an instrument TA Q800 in single-cantilever mode. The testing was programmed as: amplitude 20 μm; frequency 1 Hz; heating rate 2 ℃/ min with a range from -40 ℃ to 120 ℃.

Thermal properties

Differential scanning calorimetry (DSC)

As a thermo-analytical measurement, differential scanning calorimetry (DSC) was used to examine the thermal transitions for polymeric materials, such as glass transition temperature (T_g), cool crystallization temperature (T_c), and melting temperature (T_m). The procedure was set up in three stages on an equipment (Q200, TA Instruments): heated up to 160 °C to remove the thermal history; cooled down to -40 °C; increased temperature to 160 °C again at 10 °C/ min under nitrogen atmosphere. All the data were acquired from the second heating process.

Thermogravimetric analysis (TGA)

Thermogravimetric analysis (TGA) was executed to determine the decomposition behavior of materials on an instrument (Q50, TA Instruments). The mass was recorded continuously with the variation of temperature, which was increased from room temperature to 700 °C at a heating rate of 10 °C/ min in both N_2 and air atmosphere.

Flammability

Smouldering test

The smouldering behavior of corn pith particleboard was investigated according to the procedure that was similar to the one from Hagen and Mariana [95–97]. The experiment was carried out in a specimen with the dimensions of 40 × 40 × 160 mm, which was

located on the top of a hot plate. Five K-type thermocouples were fixed every 3 cm along the length centerline of the sample starting from the contact surface of hot plate and specimen.

As described in Fig. 2-3, the hot plate was heated up to the initial pre-determined temperature at the rate of 8 ℃/ min, and then cooled down to room temperature. Consequently, specimens started to smolder and the test continued until the temperature of ash or remaining sample fell down to less than 100 ℃. In this case, smouldering phenomena for all the particleboards would not take place until the temperature increased up to 280 ℃ at least. Besides, the evolution of smouldering process was visualized by infrared camera and propagation velocity was calculated by determining the time when the thermocouple position's temperature reached 200 ℃.

Fig. 2-3 Schematic diagram of smouldering test

Ignition time and extinguishability test (Epiradiator)

Ignition and extinction performance of particleboards with the size of 100 × 100 × 10 mm were observed by dripping test on the basis of Spanish standard UNE 23.725-90. In this experiment, a radiator device was performed to assess the occurrence of flame, from which samples were placed on a metallic grid 3 cm. Specimens were exposed to the radiator with a constant 500 W heat source, which was removed and replaced repeatedly

after each ignition and extinction during 5 min. The diagram of this assay was presented in Fig. 2-4, and some important parameters were recorded throughout the whole process.

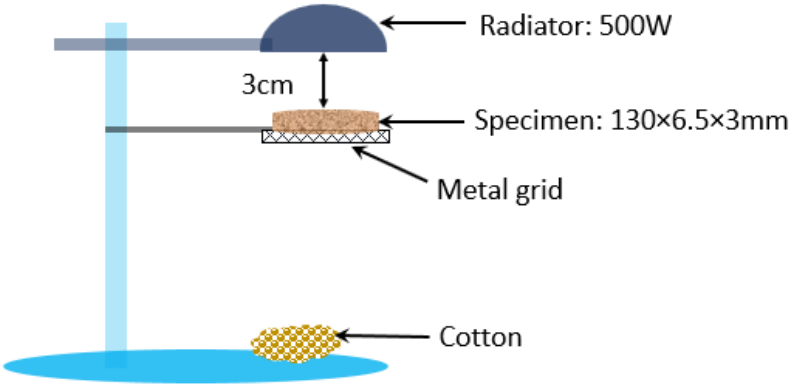

Fig. 2-4 Schematic diagram of dripping test

Limiting oxygen index (LOI)

Limiting oxygen index (LOI) (Fig. 2-5), which was described as a quantitative measure [98], was applied to evaluate the plastic's flammability by measuring the minimum concentration of oxygen to support combustion. Samples with dimension of 130 mm×6.5 mm×3.0 mm were tested in an oxygen index tester (FTT, UK) according to ASTM D 2863-2013. The LOI value can be calculated from the following equation.

$$\text{LOI}\ (\%) = {}^{O_2}/_{(O_2 + N_2)} \qquad (1)$$

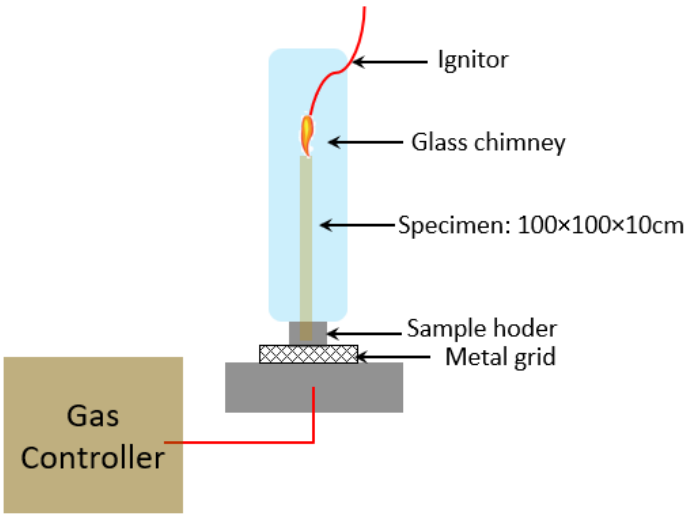

Fig. 2-5 Schematic diagram of limiting oxygen indexer

UL-94 vertical burning test

UL-94 vertical burning test is a way to indicate the flammability of polymeric materials by determining the extinguish ability, propagation of flame and dripping performance after specimen was ignited. Samples with 130 mm×13 mm×3.0 mm were prepared on the basis of ASTM D 3801-2010 standard and measured on a flame chamber (FTT, UK). As listed in Fig. 2-6, the samples were persisted on the 10s-flame for twice and the afterflame time was recorded as t1 and t2, while t3 was written as the aftergrow time after the second 10s-flame application. The UL-94 vertical burning ratings was shown in Table 2-1.

Table 2-1 Ratings in UL -94 vertical burning test

Criteria	V-0	V-1	V-2
Afterflame time for each specimen t_1 or t_2	≤ 10s	≤ 30s	≤ 30s
Total afterflame time for five specimens (t_1+t_2)	≤ 50s	≤ 250s	≤ 250s
Afterflame + afterglow time for each specimen after the second 10s-flame (t_2+t_3)	≤ 30s	≤ 60s	≤ 60s
Afterflame or afterglow of any specimen up to the holding clamp	No	No	No
Cotton underneath ignited by flaming particles or drops	No	No	Yes

*Note: If only one specimen from the group with five specimens does not meet the requirements, another group is to be tested. As well as an additional group need to be test if the total recorded flaming time is in the range of 51-55 s for V-0 and 251-255 s for V-1 and V-2.

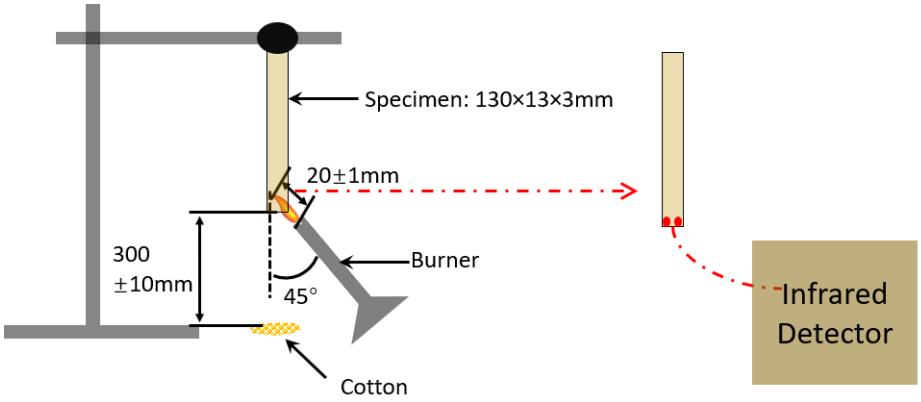

Fig. 2-6 Schematic layout of UL-94 vertical burning test

The surface temperature (T_s) of the sample was detected during the UL-94 vertical test by IR temperature detector, illustrated in Fig. 3-6. The infrared probe should detect the bottom of specimen, so it is necessary to move the probe with the burning condition. In order to keep the same testing conditions, the emissivity was set at 0.950 for IR thermometer.

Micro combustion calorimeter (MCC)

As an evaluation of combustibility for small samples, such as alginate films, micro combustion calorimeter (MCC, Fire Testing Technology, UK) was performed to analyze the flammability by oxygen consumption of the pyrolysis products [99]. From the Fig. 2-7, it can be observed that the solid state and gas phase processes were generated separately in micro combustion calorimetry. Samples of 10 ± 0.2 mg was heated to 800 ℃ at the rate of 1 ℃/ s in an inert gas stream. The volatile thermal degradation products were conveyed to the 900 ℃ combustor and mixed with excess oxygen to complete the oxidation of the fuel. The amount of heat release rate (HRR, W/ g) can be obtained via calculating the heat from per unit mass of sample.

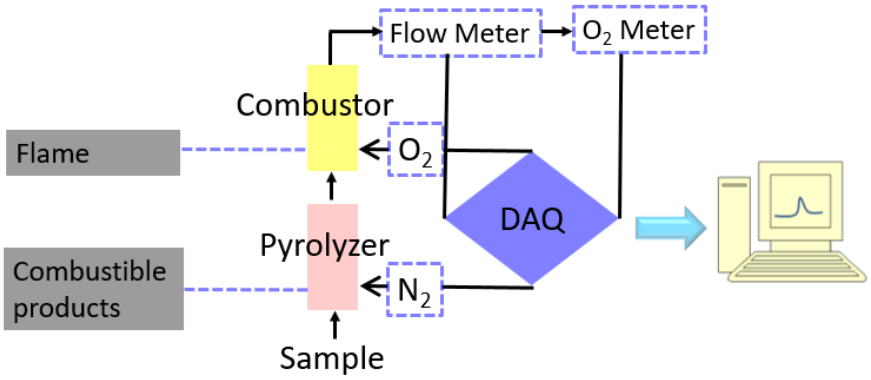

Fig. 2-7 Schematic layout of UL-94 vertical burning test

Cone calorimeter test (CCT)

Cone calorimeter test (CCT) is considered as a bench scale fire test due to a good simulation of real fire scenario. CCT was carried out on an FTT apparatus in accordance with the standard ISO 5660-1-2016. Samples with 100 mm×100 mm×3.0 mm for thermoplastic materials and ones with 100 mm×100 mm×10 mm for cellulose particleboards were wrapped by aluminum foil; then placed on a ceramic sample-holder with 25 mm distance with the cone base. All the tests were executed under the 35 kW/ m^2 of heat flux.

In the CCT, piloted ignition, which is the way to ignite materials by an external sparker located at the cone calorimetry, is characterized by some parameters, including time to ignition (TTI), heat flux for ignition, and ignition temperature (T_{ig}). The ignition behavior was investigated by measuring the TTI and T_{ig}. External thermocouples were used to detect the temperature of relevant parts of specimens before ignition, and the values were logged by an extra device. The schematic layout for CCT and ignition test was presented in Fig. 2-8.

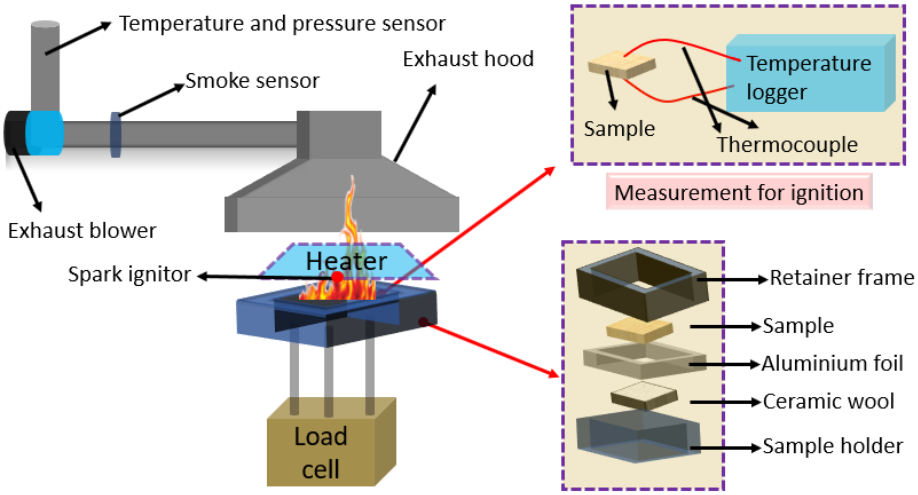

Fig. 2-8 Schematic layout of CCT and ignition test

Other properties

Melt flow index (MFI) test

Melt flow index (MFI) test, from which the molecular weight can be evaluated indirectly, was described in ASTM D 1238-2013. All the samples were measured at 170 °C with a loading weight of 2.16 kg on a Melt Indexer (KJ-3092) manufactured by Dongguan Kejian Instrument Co. Ltd.

Rheology test

Rheology test was carried out to study the plasticity of plastic materials, which can indirectly predict the mechanical behavior based on the microstructure of material, on a stress-controlled rheometer (AR2000EX, TA instruments) with a parallel plate geometry (diameter 25 mm, gap 1 mm) under air atmosphere. Specimens were placed between the parallel plates and tested in modes of viscosity-temperature and frequency-sweep. The former conditions were experimented with the 1 rad/s frequency and the 5% constant strain at the temperature range from 150 °C to 200 °C. With regards to the latter, the frequency varied from 0.1 to 100 rad/s in a fixed 5% strain at 170 °C.

2.2.4 Analysis for flame retardant mechanism

Thermogravimetric analysis coupled with FTIR (TG-FTIR)

Thermogravimetric analysis coupled with FTIR (TG-FTIR) was performed to study the volatile products from the thermal degradation of samples. As shown in Fig. 2-9, sample of 10 ± 0.5 mg was placed in the furnace of TGA; the evolved products were transferred into the cell of FTIR under nitrogen atmosphere through a heated pipe, which was maintained above 250 °C to avoid the deposition of decomposed products during transferring. The conditions in TGA-FTIR were set as same as the previous one when TGA and FTIR were used alone.

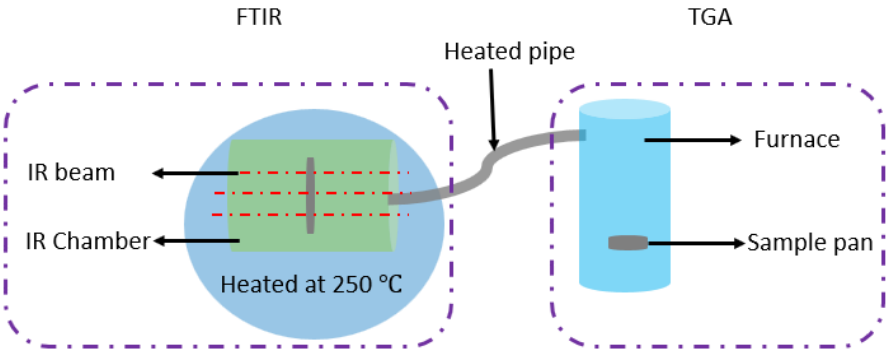

Fig. 2-9 Schematic illustration for TG-FTIR

Variable-temperature connected with FTIR (VT-FTIR)

Variable-temperature FTIR (VT-FTIR), shown in Fig. 2-10, was carried out by FTIR connected with a heating device to analyze the condensed phase with variable temperature. The heating procedure was set as: from 50 °C to 300 °C in 10 °C/ min with isothermal stage at 300 °C for 15 min; meanwhile, the FTIR was programming at the same conditions as above.

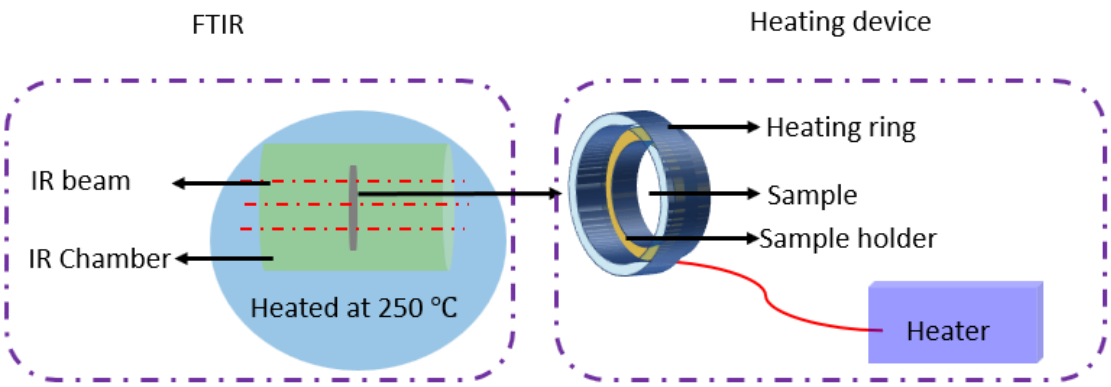

Fig. 2-10 Diagram of key components for VT-FTIR

CHAPTER 3

Synthesis and characterization of novel bio-based flame retardant (PA-THAM) and its application to PLA

3.1 Introduction

Nowadays, environmental and energy issues make bio-based materials develop to meet more and more applications. Meanwhile, the fire hazards of these new generation materials, which concern the security of life and property for everyone, should also be attached more importance to by government, researchers, consumers and manufactures [53,100,101]. With regard to the enhancement of flame-retardant properties in materials, there are two typical approaches referred to 'additive' type and 'reactive' type. As a physical incorporation, 'additive' method is considered as a more widespread, economical and expeditious way to improve the flame retardancy for fire safety materials [102,103].

Among the additive flame retardants, phosphorus-containing flame retardants (PFRs) are the versatile and extensive ones owning to the diversity of the elements existing in several oxidation states. For example, inorganic PFRs, including red phosphorus and APP; organic PFRs involving organo-phosphate esters, phosphonates, and phosphates; and halogenated PFRs, which combine both halogen and phosphorus elements [44,47,104–107]. Because of the ecological and sustainable concept, some halogen-free phosphorus-containing flame retardants were investigated to apply for various materials in the past years. Z. Guo etc. [108] reported that a phosphorus-nitrogen intumescent flame retardant (DPPM) was synthesized and added into rigid polyurethane foams (RPUFs). This DPPM-RPUF composite illustrated a 29.5 % LOI value and passed UL-94 V-0 rating, as well as achieved a high char residue. S. Gaan etc. [109] prepared a series of DOPO-based flame

retardants, which were incorporated into polyesters via thermal processing. These flame-retardant blends showed a higher thermal-oxidative stability and flame retardancy compared to the neat polyesters. A novel halogen-free flame retardant (DTB) integrating phosphorus, nitrogen and boron was introduced into epoxy resin system [110]. This flame-retardant epoxy thermoset presented a significant improvement in fire resistance and smoke inhibition performance.

As a typical bio-based thermoplastic, PLA is also studied to enhance the flame retardancy by introducing some flame-retardant fillers. Ammonium polyphosphate (APP) combined with a charring agent (CNCA-DA) was used to modify the flame retardant properties of PLA [111], and this composite system demonstrated a very effective flame retardancy with a high LOI value of 32.8 % and V-0 rating in UL-94 test at the loading of 20 wt% fillers. P. Jiang etc. [83] used the sepiolite (SEP) modified with DOPO to increase the fire performance of PLA, and there was a significant decrease in peak of heat release rate (PHRR) after adding 10 wt% SEP-DOPO into PLA. Y. Chen etc. [112] found a flame-retardant PLA composite, which involved bio-group additives containing phosphazene-triazine and APP, possessed a 34.3 % LOI value and passed UL-94 V-0 rating without dripping, as well as a large amount of residual char. On the basis of previous research [113–116], although the fire resistance of PLA-based composites can be improved via adding some efficient phosphorus-containing flame retardants, the incorporation of additives might also lead to negative effect on mechanical properties, which was studied by a few articles.

In view of bio-based concept, this work aims to synthesize a novel bio-based flame retardant involving phosphorus element, and study its effect on both mechanical properties and flame-retardant behaviors of PLA.

3.2 Synthesis and characterization of bio-based phosphorus-containing flame retardant (PA-THAM)

3.2.1 Synthesis of PA-THAM

Phytic acid (PA), which bears six-fold dihydrogenphosphate ester groups, is extracted from the plant tissues, such as bran, seeds, legumes and grains. Trometamol (THAM) containing a reactive primary amine is usually used as a buffer for biochemistry and molecular biology. These two raw materials were selected to prepare PA-THAM, and the synthesis rout is depicted in Fig. 3-1. In a three-neck flask with condenser pipe, THAM (60 mmol) was firstly dissolved in ethanol at 70 °C; then PA (5 mmol) was added into the solution drop by drop with stirring until the reaction completed. After the mixture cooled down to room temperature, filtered the precipitate and washed it with ethanol to remove the residue by several times. Finally, the light-yellow flame-retardant PA-THAM (80% yield) was obtained after drying at 150 °C for 2 h.

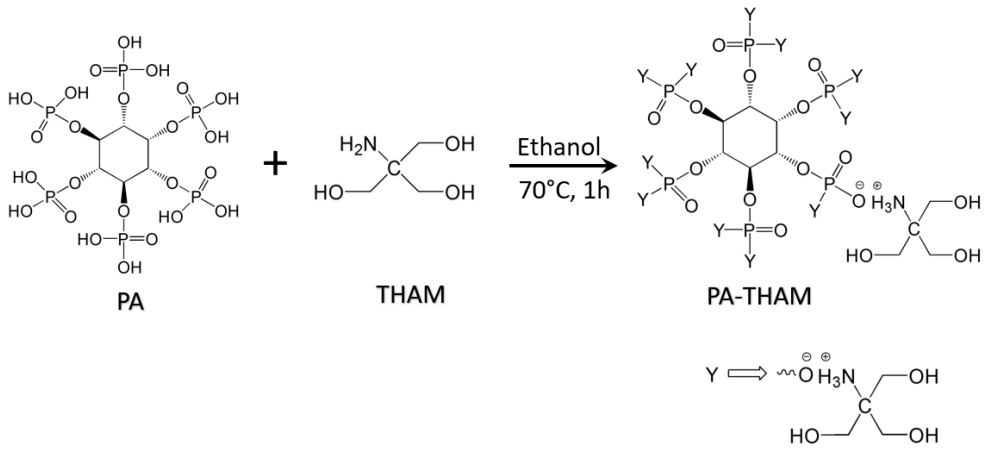

Fig. 3-1 Scheme of possible reaction route between PA and THAM

3.2.2 Characterization of PA-THAM

As shown in Fig. 3-2, PA-THAM was characterized by NMR test. In ^{1}H NMR spectra, shift at 3.43 ppm was attributed to the protons of the methene group (H_{β}), while the

protons from phytic acid (H_γ) overlapped with the ones from H_β. Other protons of the structure, which was due to hydroxyl groups and ammonium salt, were exchanged with D_2O solvent. Meanwhile, the ^{13}C-NMR and ^{31}P-NMR were also employed to confirm the structure, and the assignments of relevant peaks were observed as following, respectively: (D_2O, ppm: 74.2, 61.3, 59.3) and (D_2O, ppm: 2.28, 0.06) [117–119].

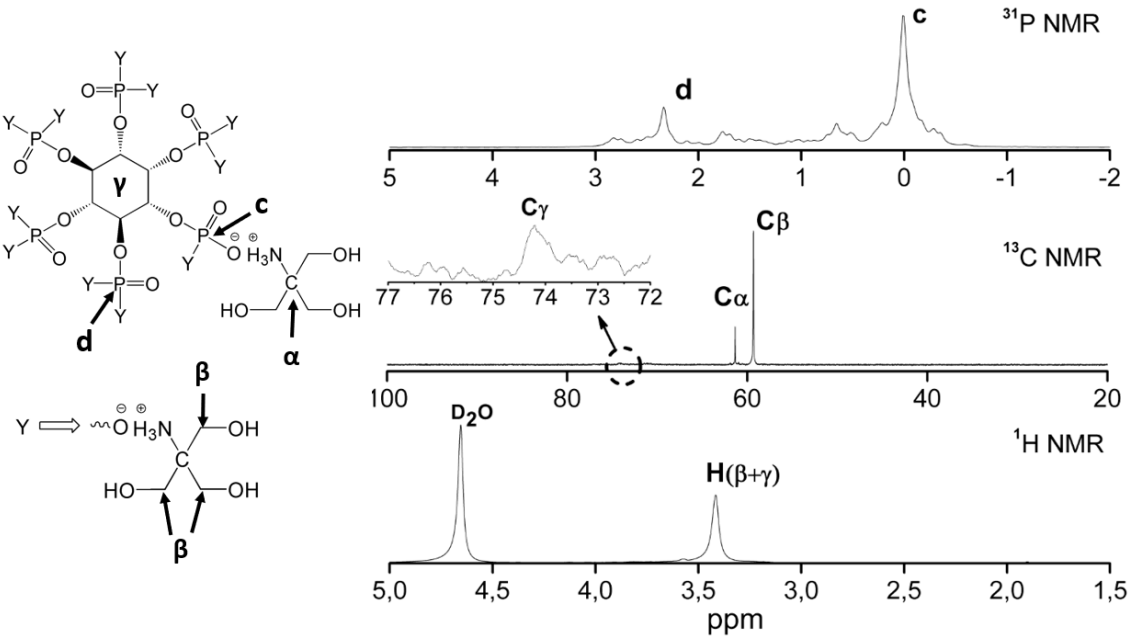

Fig. 3-2 ^1H-NMR, ^{13}C-NMR and ^{31}P-NMR spectra for PA, THAM, and PA-THAM

From the infrared spectrum in Fig. 3-3, some characteristic peaks were observed. With regard to PA, an absorption at 3400 cm^{-1} was due to the stretching vibration of hydroxyl group, and the spectral peak at 1000 cm^{-1} was attributed to P=O bond [120]. Meanwhile, typical double peaks of THAM between 3500 cm^{-1} and 3400 cm^{-1} can be explained as the stretching vibration of primary amine [121]. However, in PA-THAM spectrum, a wide and strong absorption peak between 3400 cm^{-1} and 2500 cm^{-1} derived from stretching vibration of ammonium salt was detected, which overlapped with the bond of aliphatic hydroxyl and methylene groups; while the corresponding double peaks caused by primary amine group disappeared. Furthermore, other characteristic peaks were detected, such as

double bands at 1630 cm^{-1} and 1533 cm^{-1} assigned to ν_{as}(O-P-O) and β(N-H) as well as strong absorbance from 1160 - 960 cm^{-1} due to the bands from P=O, and P-O [122]. These alterations indicated that the reaction occurred between carboxyl and amino groups.

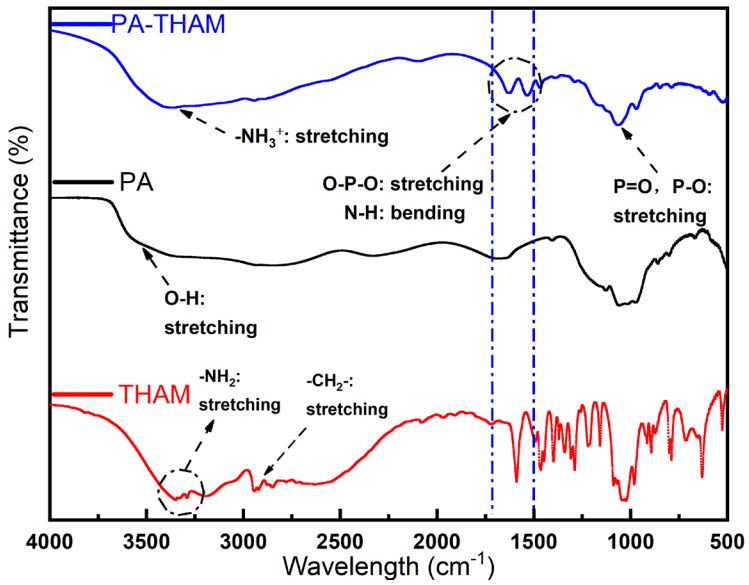

Fig. 3-3 FTIR curves for PA, THAM, and PA-THAM

Additionally, Fig. 3-4 gave the TGA curves for PA, THAM and PA-THAM. As for PA, there were four stages during thermal degradation. The first stage around 100 °C corresponded to the removal of water in solution; the following two events of mass loss between 190 °C and 450 °C were attributed to occurrence of dehydration and carbonization processes. At 850 °C, only 5 wt% residue left due to the decomposition of char formed previously and phytate group [123,124]. As concerns the THAM, which contains hydroxyl groups, demonstrated a single degradation process and no residue left after 200 °C, this was because of the volatilization around the melting point [125]. Nevertheless, a significant improvement was observed in PA-THAM curve. Compared with PA, the value $T_{5\%}$ of PA-THAM corresponding to 5% mass loss rose up to 217 °C,

as well as three stages resulted from dehydration of ionic bond, carbonization, and oxidation of char layer, respectively.

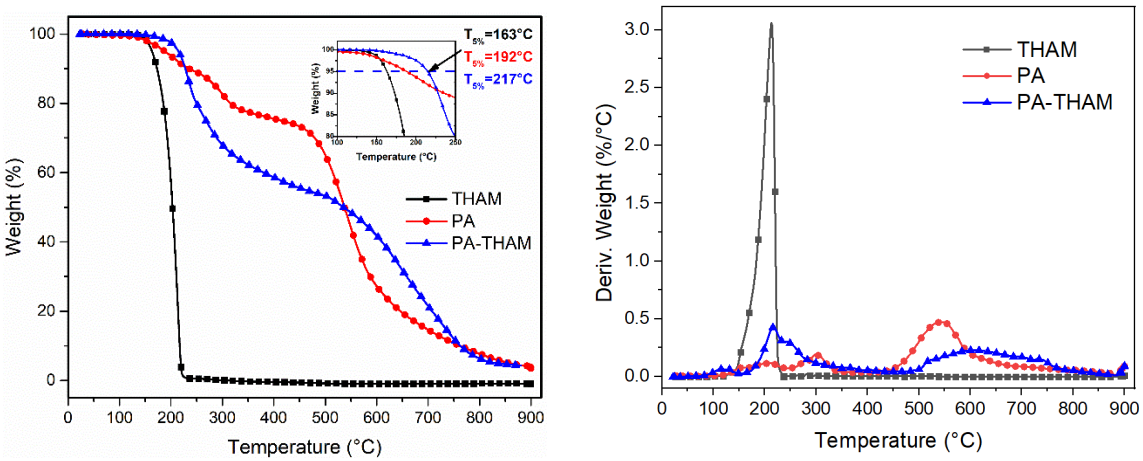

Fig. 3-4 Curves of thermal stability for PA, THAM, and PA-THAM in air atmosphere: a) weight loss curve; b) differential thermogravimetric curve

In conclusion, a novel bio-based flame-retardant PA-THAM was synthesized successfully via reaction between PA and THAM.

3.3 Effect of PA-THAM on the properties of PLA

3.3.1 Preparation of PLA/PA-THAM biocomposites

Table 3-1 presented the design of PLA and its biocomposites, which were fabricated via melt mixing method in a micro-compounder at 170 °C for 2 min. As the reference sample, pure PLA was prepared under the same procedure conditions. All the test samples were shaped by mold forming according to relevant standards at 170 °C for 5 min. Before processing, a vacuum oven was used to dry materials at 80 °C for 8 h at least.

Table 3-1 Formulation of PLA and its biocomposites

Sample	PLA /(wt%)	PA-THAM /(wt%)
B1	100	0
B2	99	1
B3	97	3
B4	95	5

3.3.2 Mechanical properties of PLA/PA-THAM biocomposites

Tensile and impact properties

Tensile and un-notched Charpy impact properties of PLA and its biocomposites were summarized in Table 3-2. There was a slight change in the aspect of mechanical properties when the loading of PA-THAM was no more than 3 wt%. After introducing 3 wt% PA-THAM into PLA, biocomposite B3 showed a little decrease of tensile strength from 67.3 MPa to 64.8 MPa. In parallel, the value of elongation at break was not affected, and that of impact strength only varied from 23.6 KJ/m^2 to 23.8 KJ/m^2. These little difference on mechanical properties can be explained as the slight alteration of molecular weight on the condition of low weight percentage of PA-THAM. Moreover, with the addition of 5 wt% PA-THAM into PLA, a clear reduction was detected in both tensile strength and impact strength. These results indicated that optimum loading levels of PA-THAM in PLA would maintain the mechanical properties.

Table 3-2 Mechanical properties of PLA and its composites

Sample	Elongation at break/ (%)	Tensile Stress/ (MPa)	Impact Strength/ (KJ/m^2)	Melt Flow Index/ (g/10min)
B1	4.1±0.1	67.3±1.5	23.6±2.0	3.4±0.5
B2	4.1±0.1	65.3±2.0	22.3±1.0	5.3±0.5
B3	4.1±0.1	64.8±1.5	23.8±2.0	7.1±0.5
B4	3.9±0.2	60.2±1.0	15.0±2.0	11.7±0.5

Dynamic mechanical analysis

Dynamic mechanical analysis was also carried out to analyze the thermo-dynamic behaviors of PLA and its biocomposites. From the curves of DMA (Fig. 3-5), each formulation presented double peaks during relaxation process. The first peak associated

with the glass-to-rubber transition varied from 65 °C to 63 °C, and the corresponding value of Tan Delta, which is related to the relaxation of polymer chains, also showed a downward trend while the content of flame retardant increased. Compared with neat PLA, the blend B4 with 5 wt% loading of PA-THAM illustrated about 35% reduction for δ value at the primary-transition temperature; meanwhile, the storage modulus at glass state also decreased significantly. This phenomenon pointed that this flame retardant with low molecular weight acted as a lubricant and weakened the intermolecular forces, which led to enhance the mobility of PLA molecular chain [126,127].

The occurrence of second small peak at a higher temperature around 100 °C were attributed to secondary transition behavior correlated with the crystal phase, and the values also decreased to lower temperature after introducing additives. Besides, an increasing trend from B1 to B4 was detected for tan δ at melting-transition area, especially for formulation B4, this was probably because the presence of PA-THAM improved the crystallization of biocomposite.

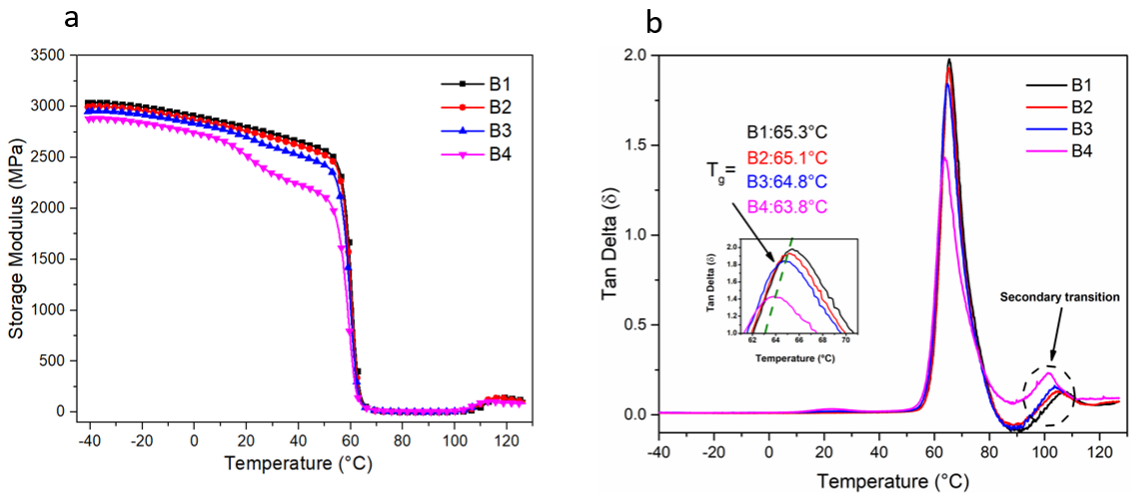

Fig. 3-5 DMA data of PLA and its composites: a) Storage Modulus vs Temperature curves; b) Tan δ vs Temperature curves

Morphology and molecular weight analysis

In order to further study the effect of PA-THAM on mechanical properties of PLA, micro morphology and melt flow index (MFI) of PLA and its biocomposites were exhibited in Fig. 3-6 and Table 3-2, respectively. In comparison with pure PLA, two phases can be observed in the micrographs of three biocomposites with PA-THAM, where the discrete phase of PA-THAM in the form of micron sizes uniformly dispersed in continuous phase of PLA. Three types of morphological features were demonstrated in this binary system, including (a) cavities from droplets, (b) droplets of PA-THAM, and (c) holes filled with PA-THAM. In parallel, the amounts of cavities increased with the content of PA-THAM, which might cause more possibility of defect-forming [128]. This "sea-island" morphology was probably attributed to the incompatibility between PA-THAM and PLA.

Additionally, data from melt flow index for PLA and its biocomposites, which can be used to indirectly measure molecular weight, demonstrated a slight change when the incorporation of PA-THAM was no more than 3 wt%. Therefore, it can be concluded that small loads of PA-THAM can determine the optimum levels for the mechanical properties [129].

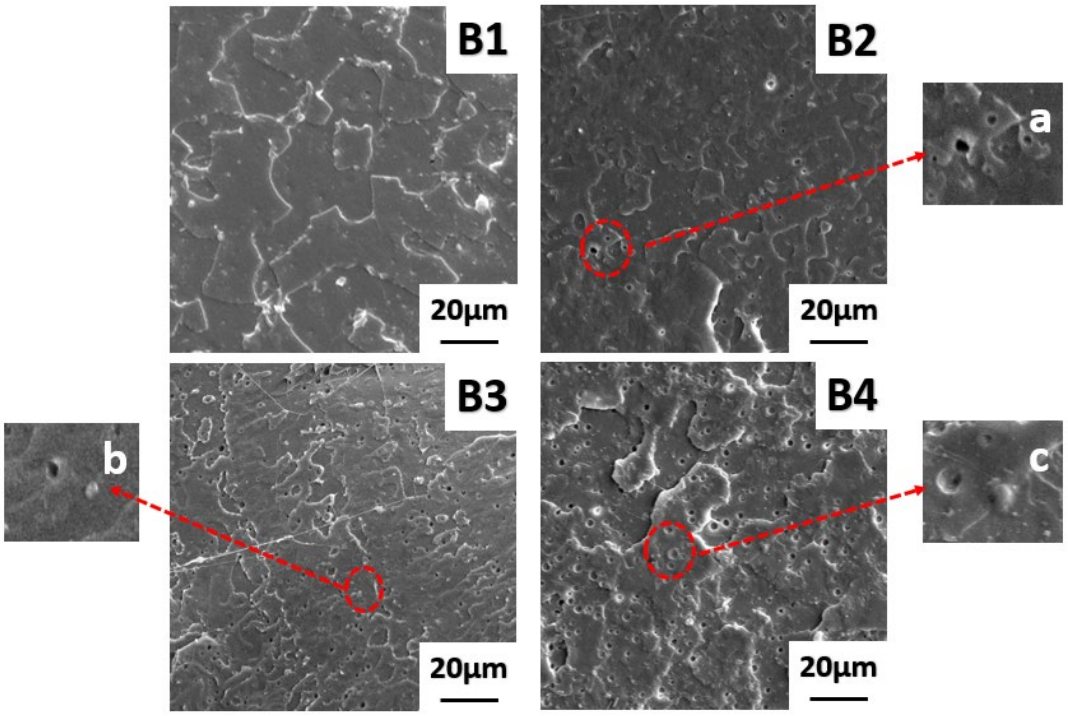

Fig. 3-6 SEM micrographs of cryo-fracture at magnification 1000×: B1) PLA, B2) PLA/ PA-THAM 1 wt%, B3) PLA/ PA-THAM 3 wt%, B4) PLA/ PA-THAM 5 wt%

3.3.3 Rheology behavior of PLA/PA-THAM biocomposites

The rheology behavior at molten state was measured by two experimental modes in view of no effect for morphological structure [130,131]. The variation of complex viscosity for PLA and its biocomposites can be observed from the viscosity-temperature curves in Fig. 3-7 a). Compared with neat PLA, which presented complex viscosity of 5973 Pa.s at 170 °C, the formulation B3 with 3 wt% flame retardant showed a significant reduction for that parameter by 90.4% at the same conditions. It was suggested that the processing temperature for pure PLA can be set at above 180 °C [132,133], whereas the introduction of 1 wt% PA-THAM enabled PLA biocomposites to reach the same viscosity value at lower 165 °C. This can be elucidated that PA-THAM, as an incompatible additive with comparatively small amount and low molecular weight in PLA matrix, played a

lubricating role in this binary system, and reduced the molten viscosity significantly [134,135] [136,137].

Another frequency sweep mode was utilized to study the correlation between complex viscosity and angular frequency of PLA and its biocomposites at a fixed temperature, shown in Fig. 3-7 b). As for pure PLA, a typical rheological curve was obtained, which exhibited Newtonian behavior at low frequency and shear-thinning performance at high value [138]. The complex viscosity of biocomposite loaded with 3 wt% additives reduced remarkably at the same testing range, where the melting viscosity was almost independent of frequency with a constant value. This obvious improvement of rheological properties in PLA-based biocomposites can be clarified by the lubrication of PA-THAM. As an additive with low molecular weight, the presence of PA-THAM weakened the intermolecular forces or ruptured the selective secondary bond between polymer molecules and left the shaping or flexing of the material [139,140].

Through the investigation of rheology behaviour, PA-THAM can be used as lubricating additive to decrease the melting fluidity and improve the processing temperature of biocomposites simultaneously.

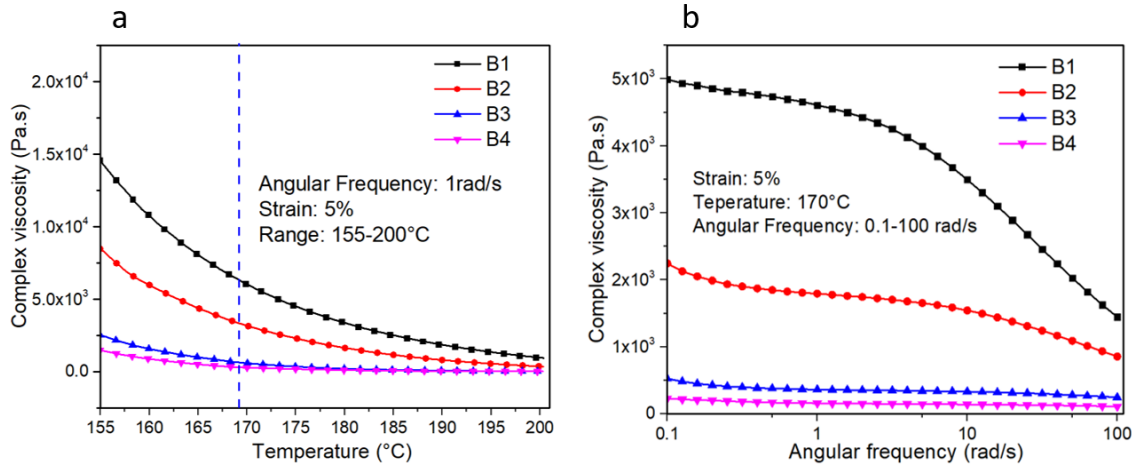

Fig. 3-7 Rheology behaviour of PLA and its composites at different temperatures and frequencies: a) Complex viscosity vs Temperature; b) Complex viscosity vs Angular frequency

3.3.4 Thermal properties of PLA/PA-THAM biocomposites

Differential scanning calorimetry

Due to the addition of PA-THAM into PLA, the miscibility, which can be stated in the material system with only one glass transition temperature in DSC traces, also produced some changes in the crystallinity of blenders, which was displayed in Table 3-3. In addition, Fig. 3-8 demonstrated the different thermograms for PLA and its biocomposites during the second heating processing and the relevant crystallization degree was calculated based on Eq. (3-1).

$$x_c = (\Delta H_m - \Delta H_c)/((1-\varphi)\Delta H_m^0) \quad (3\text{-}1)$$

Where φ described weight percentage of fillers in composites, and the melting enthalpy of 100% crystalline PLA (H_m^0) is (93.0 J/g). ΔH_m and H_c are the melting enthalpy and crystallization enthalpy (J/g), respectively.

Both PLA and its biocomposites exhibited exothermic peak correlated with cold crystallization and endothermic peak corresponding to melting processing. The pure PLA had a weak ability to crystallize, which yielded a cold crystallization peak at 115 °C and single melting peak at 150 °C. After blended with PA-THAM, PLA-based biocomposites showed a double melting peak from 140 °C to 151 °C, as well as the temperature value at both glass transition (T_g) and cold crystallization (T_c) shifted to lower temperature. Meanwhile, the enthalpy related to crystallization and melting (H_c and H_m) increased with the content of the additives, and a little increase was also observed for crystallinity that was in experimental error.

When the percentage of flame retardant rose up to 5 wt%, T_g and T_c dropped to 63 °C and 108 °C with an increase of 28.7 J/ g and 36.7 J/ g for H_c and H_m, respectively. These phenomena indicated that PA-THAM, as a nucleator, slightly facilitated the chain mobility and crystallization rate of PLA during the heat history [141,142]. Additionally,

as an impurity, the presence of flame retardant disturbed the order orientation of molecular chains and resulted in a characteristic of double-melting peaks, which was attributed to the formation of different crystal structures and melting point at a different temperature [143–146].

Based on a little reduction of these transition-temperature value, the incorporation of small loads of PA-THAM slightly altered the mobility of polymer segments [147,148].

Table 3-3 Thermal properties' data of PLA and its composites

Sample	T_g/ (°C)	T_c/ (°C)	H_c/ (J/ g)	T_m/ (°C)	H_m/ (J/ g)	χ_c/ (%)
B1	65	115	18.7	149	26.6	8.5
B2	65	111	22.5	146-151	31.3	9.5
B3	64	109	26.7	144-151	34.9	9.1
B4	63	108	28.7	143-151	36.7	9.0

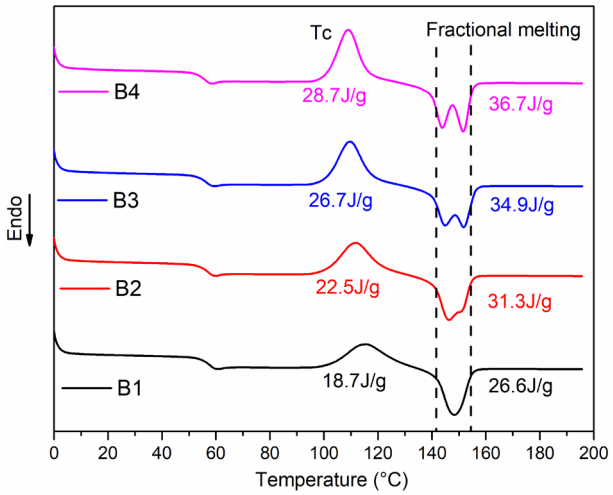

Fig. 3-8 DSC curves of PLA and its composites

Thermogravimetric analysis

Thermal decomposition behaviors of PLA and its biocomposites were investigated in both air and nitrogen atmosphere. Fig. 3-9 displayed that all the materials underwent a similar degradation process in both conditions, which started to degrade at a temperature 320 °C corresponding to 5 wt% weight loss and the maximum weight loss occurred at approximate 350 °C. This little change between the formulations was because that the

dominant decomposition of PLA and its biocomposites, which was induced by the loss of end group of the polymer chain or ester exchange [149], was hardly affected by the surrounding atmosphere.

Besides, a little premature degradation appeared after incorporation of PA-THAM. This was contributed by the poor thermal stability from additives. However, the residue content of the biocomposites with PA-THAM presented more amount at high temperature (above 400 ºC), while the pristine PLA left no residue. This performance was attributed to the formation of char layer due to the carbonization ability of PA-THAM at high temperature [150]; which played a barrier-role in combustion process. Furthermore, the presence of PA-THAM did not improve the charring behavior of PLA according to the theoretical amount of char residue.

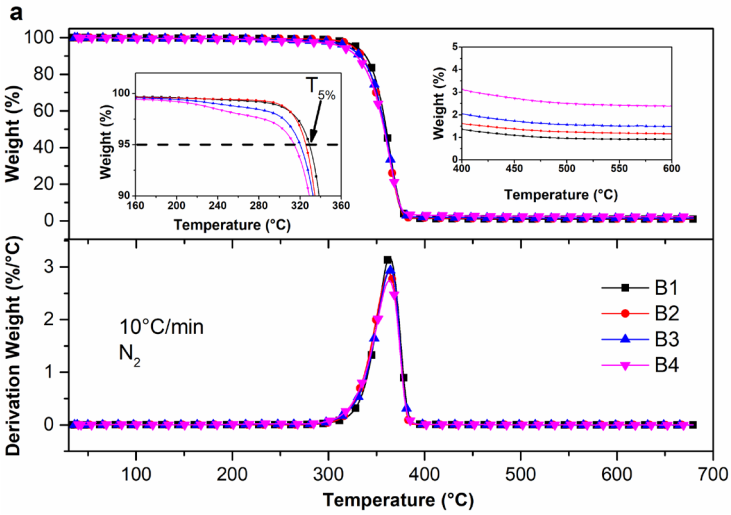

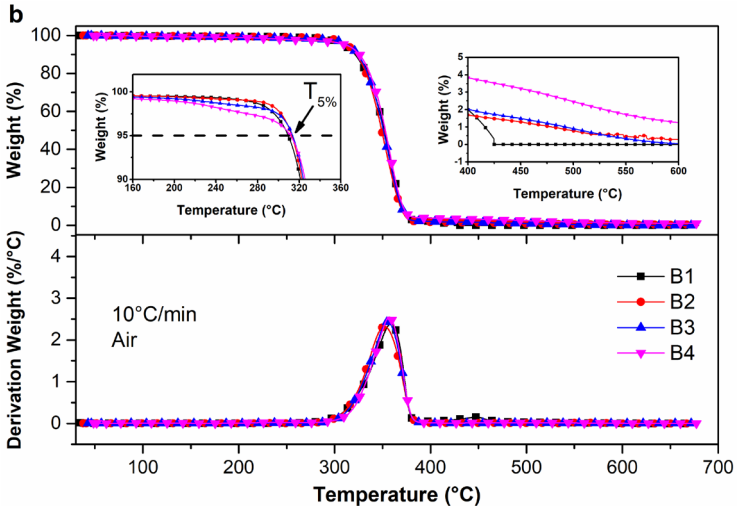

Fig. 3-9 PLA and its composite TGA curves in (a) nitrogen and (b) air obtained at 10 °C/min

3.3.5 Flammability of PLA/PA-THAM biocomposites

LOI and UL-94 tests

LOI and UL-94 were executed to compare the flammability between PLA and its biocomposites, and the results were listed in Table 3-4. Pure PLA exhibited a typical flammable behavior with a 19.9% LOI value and no rating in UL-94 test. However, the flammability of other formulations was enhanced significantly due to the incorporation of PA-THAM. With a 3 wt% loading of PA-THAM, the biocomposite possessed a higher LOI value with 25.8%. Impressively, an enhancement in dripping performance and excellent self-extinguishing were observed in UL-94 test, which signified that the material was difficult to be ignited and the flame cannot be maintained after the 10-second ignition when the igniter was removed. As a result, the V-0 rating with a little dripping-droplets was achieved for this formulation.

In order to clarify this “anti-dripping” behavior, an infrared thermometer was utilized to record the evolution of surface temperature (T_s) for neat PLA and its biocomposite B3 during the UL-94 test. Fig. 3-10 illustrated the screenshots of combustion phenomenon and the curves of T_s versus time. As for neat PLA, the T_s continued rising to 370 °C with

a 30s sustaining flame at the first ignition. On the contrary, the introduction of PA-THAM enabled B3 to present an interesting self-extinguish ability, which was not ignited at the first 10-second and only maximum 290 °C of T_s was reached at the second ignition. Besides, self-extinguishing behavior can also be supported by the results from screenshots of combustion.

With regard to the results form LOI and UL-94 tests, the satisfactory improvement of flammability was owing to the "heat transfer" effect of PA-THAM. When specimen B3 flamed, the heat was transferred quickly from bottom to other parts, and this "heat runaway" diminished the surface temperature to prevent the further flame-occurrence. The following cone calorimeter test further proved this excellent behaviour.

Table 3-4 Flame retardant properties of PLA and its biocomposites

Sample	LOI (%)	UL-94			
		Rating	$\overline{t1}$ / $\overline{t2}$ (s)	Dripping/ (Droplets/ 20s)	Ignition
B1	19.9±0.2	No rating	burned out	Serious	YES
B2	23.0±0.2	V-2	18 / 3	21	YES
B3	25.8±0.2	V-0	1 / 1	3	NO
B4	27.9±0.2	V-0	0 / 1	1	NO

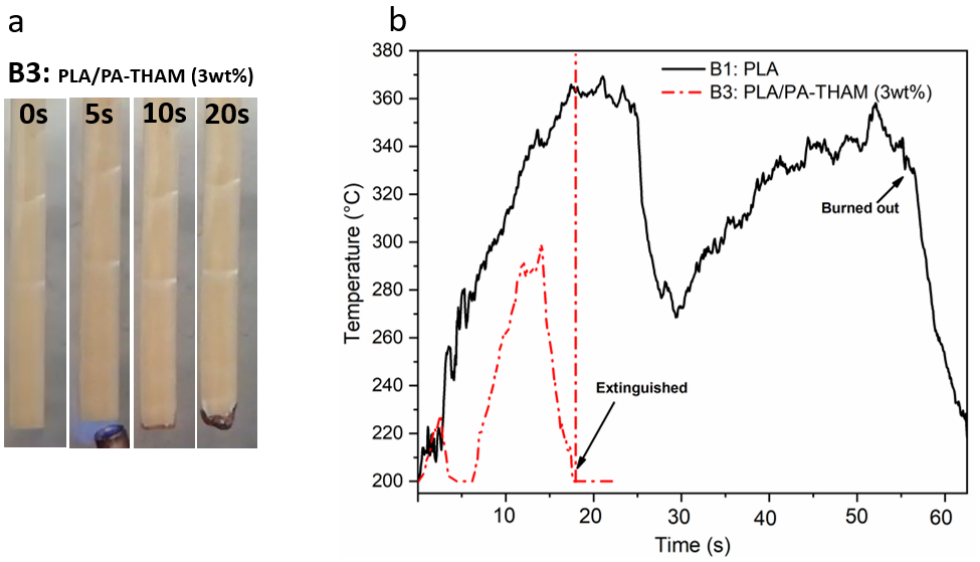

Fig. 3-10 Results for PLA and its biocomposite from the UL-94 test: a) screenshots during the UL-94 test; b) surface temperature vs time curves

Cone Calorimeter Test (CCT)

As a bench-scale fire test, CCT was applied to assess the flammability of PLA and its biocomposites, and the correlative parameters were recorded, such as heat release rate (HRR), peak heat release rate (PHRR), total heat release rate (THR), time to ignition (TTI), average effective heat of combustion (Av-EHC) and mass loss, et al, which were listed in Table 3-5 and Fig. 3-11 in detail.

The reference sample B1 exhibited a typical combustible performance with 410 kW/m² PHRR and only 0.6 wt% residue after the test. Nevertheless, other formulations loaded with PA-THAM showed an enhancement in flame retardant properties. The incorporation of 3 wt% PA-THAM imparted biocomposite B3 lower PHRR (366 kW/m²), higher residue (2.5 wt%), as well as little change for THR and Av-EHC. This alteration can be elucidated by the carbonization of PA-THAM, which acted as a barrier for the exchange of the heating and oxygen [151]. The residue from digital photos also proved that charring layer was formed after introducing PA-THAM.

Furthermore, a postponed ignition behaviour was observed in TTI value, which was affected by chemical and physical factors. In comparison with pure PLA, biocomposite B3 was delayed to ignite by 10s. Because of little effect of PA-THAM on the thermal degradation of this material system, chemical factor referred to composition and concentration of degradation volatile products can be negligible during ignition process. Thus, as physical parameter, temperature-rising rate was considered as an important role to affect the ignition time. Aiming to analyse this parameter, the relationship between temperature and time was investigated before ignition. Fig. 3-12 (a) showed that all the samples were ignited at the same surface temperature (334 °C) [152–154], while more time was needed to reach this value for samples with flame retardant, and an upward trend

was observed in ignition time from B1 to B4. From Fig. 3-12 (b), the curves of bottom temperature versus time demonstrated an opposite trend, in which the sequence of temperature value under the same time was: B4>B3>B2>B1. This can be explained by the reduced molten viscosity due to the introduction of PA-THAM, which facilitated a better "heat transfer" in-depth and decreased the heating rate of the surface; then more time was needed to ignite material [155,156]. Moreover, the flame-retardant mechanism was also analysed by the following methods.

Table 3-5 Data from cone calorimeter test for PLA and its composites

Sample	PHRR/(kW/m²)	TTI/(s)	THR/(MJ/m²)	Av-EHC/(MJ/kg)	Residue/(wt%)
B1	410±5	61±1	70±1	15.7±0.1	0.6±0.2
B2	379±4	65±2	68±1	15.6±0.2	1.1±0.1
B3	366±3	71±1	64±1	15.5±0.1	2.5±0.2
B4	349±5	73±2	63±1	14.5±0.2	4.9±0.5

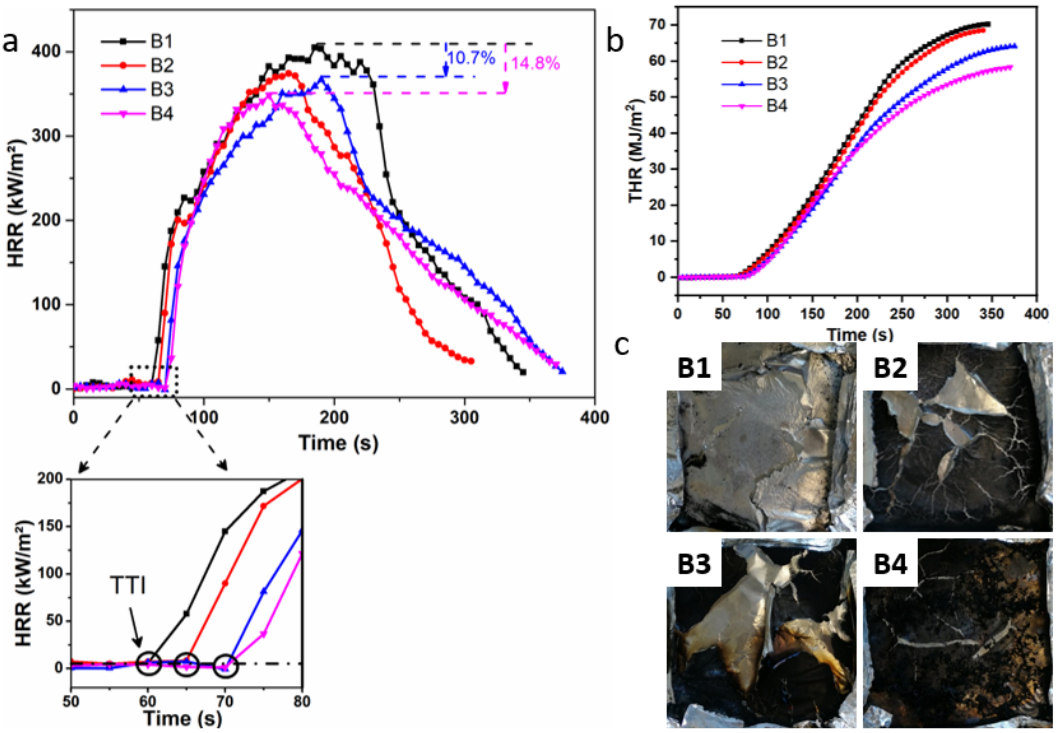

Fig. 3-11 Results of PLA and its composites after cone calorimeter test: a) HRR vs Times curves; b) THR vs Times curves; c) digital photos after combustion: B1) PLA, B2) PLA/ PA-THAM 1wt%, B3) PLA/ PA-THAM 3wt%, B4) PLA/ PA-THAM 5wt%

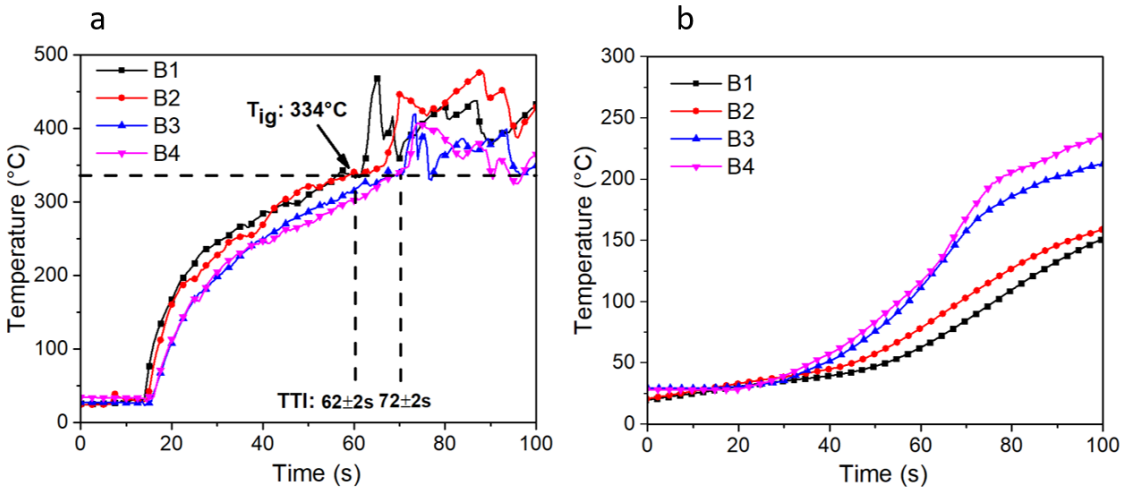

Fig. 3-12 Curves between temperature and time before ignition during the cone calorimeter test: a) Surface temperature vs Times curves; b) Bottom temperature vs Times curves

Analysis of flame-retardant mechanism

TGA-FTIR technique was used to analyse the gas phase behaviour of PLA and PLA/PA-THAM (3 wt%) during thermal degradation, which can monitor the evolution of gas products from the thermal decomposition process. Fig. 3-13 (a) demonstrated that both material systems pyrolyzed almost similar gas products, and this meant a little amount of flame retardant hardly changed the dominant thermal decomposition process of PLA except the peaks at 2358 cm^{-1} (CO_2) and 1244 cm^{-1} (C-O stretching) [157].

Due to exist some difference for PLA and its biocomposite, Fig. 3-13 (b) and (c) listed the curves of relative intensity versus temperature for total pyrolyzed gas and absorption peak at 1244 cm^{-1}, respectively. Both materials released quite equal amount of total gas products, while the maximum intensity of C-O absorbance showed an obvious reduction and postponement, which was related with the reduction of concentration of ether compounds [158]. The delayed decomposition behavior and decreased amounts of correlative C-O products were attributed to the charring effect of PA-THAM, which played a physical-obstruction role at high temperature.

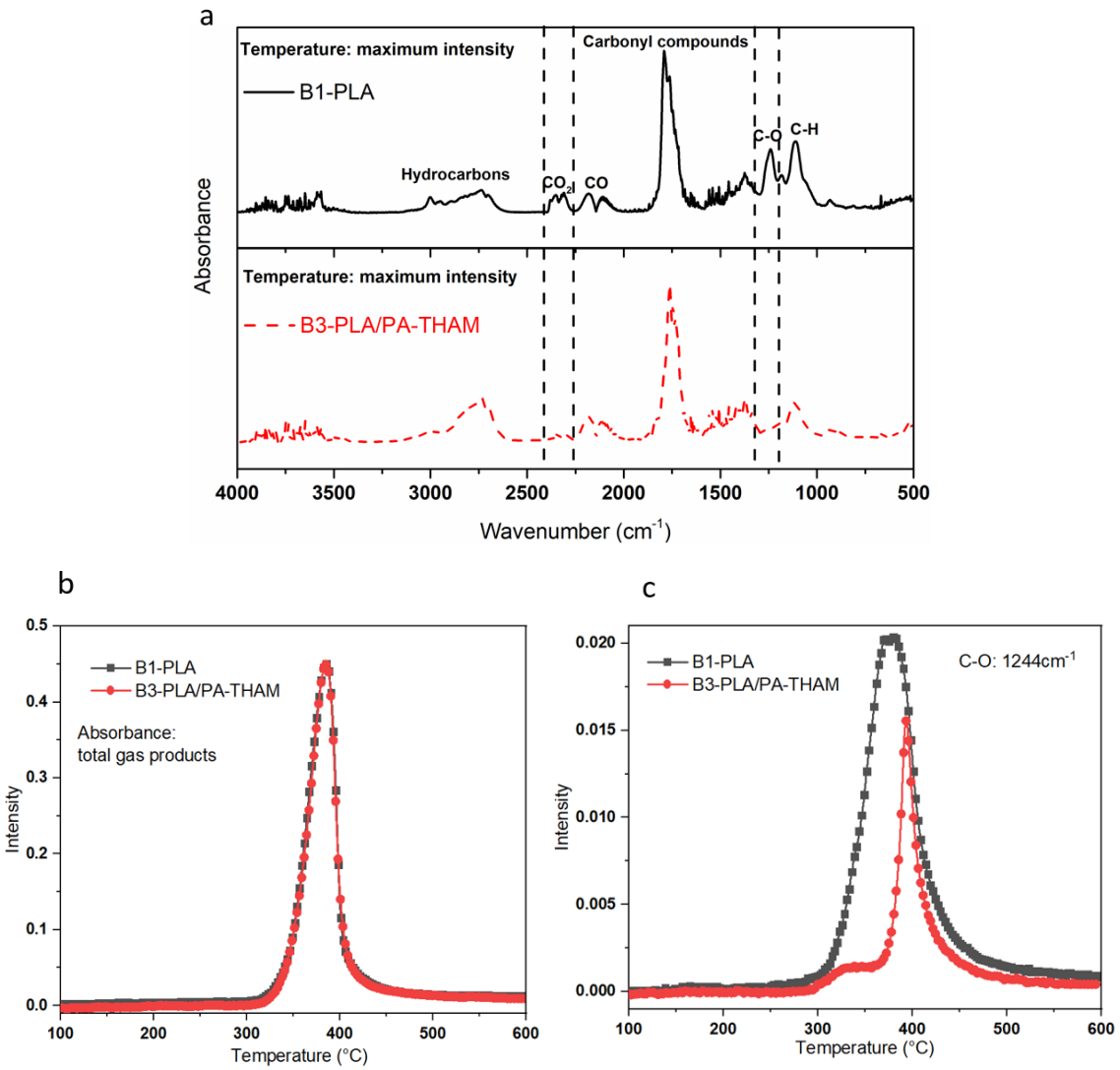

Fig. 3-13 TGA-FTIR spectra of decomposed products for PLA and PLA/PA-THAM: (a) comparison of evolved gas for PLA and PLA/PA-THAM (3wt%) at 400°C; (b) absorbance vs temperature from total decomposition gas for PLA and PLA/PA-THAM (3wt%); (c) absorbance at 1244cm^{-1} vs temperature for PLA and PLA/PA-THAM (3wt%).

The measure of Various temperature coupled with FTIR was also utilized to investigate the thermo-oxidative decomposition by detecting the condensed phase of PLA and its biocomposite. Fig. 3-14 presented the FTIR spectra of different time for PLA and PLA/PA-THAM (3 wt%) at the same temperature 300 °C. As the previous result in TGA-FTIR, both samples illustrated similar evolved gas products and degradation trend that the intensity of characteristic peaks decreased with the increasing time at the same testing conditions [159,160]. However, some alteration appeared in degradation behaviours at

higher temperature after adding flame retardant. With respect to pure PLA, barely peaks were detected after 10 min at 300 °C. On the contrary, the skeleton absorptions with relative spectra intensities were evidently observed in PLA/PA-THAM at the same conditions. Besides, the absorption belonged to phosphorus-containing bands were hard to detected because of the small PA-THAM loading.

According to the previous report [161], the primary decomposition process of PLA involved intra- and intermolecular ester exchange, cis-elimination, radical and concerted non-radical reactions, and selective depolymerization. In the case of PLA and PLA/PA-THAM, the principle reversible reations still mainly consistecd of ester exchange and cis-elimination. Consequently, on the basis of the investigation from gaseous and condensed phases, the presence of PA-THAM cannot change the thermal degradation products of PLA, but its carbonizing ability can promote char-formation and protect the material at high temperature.

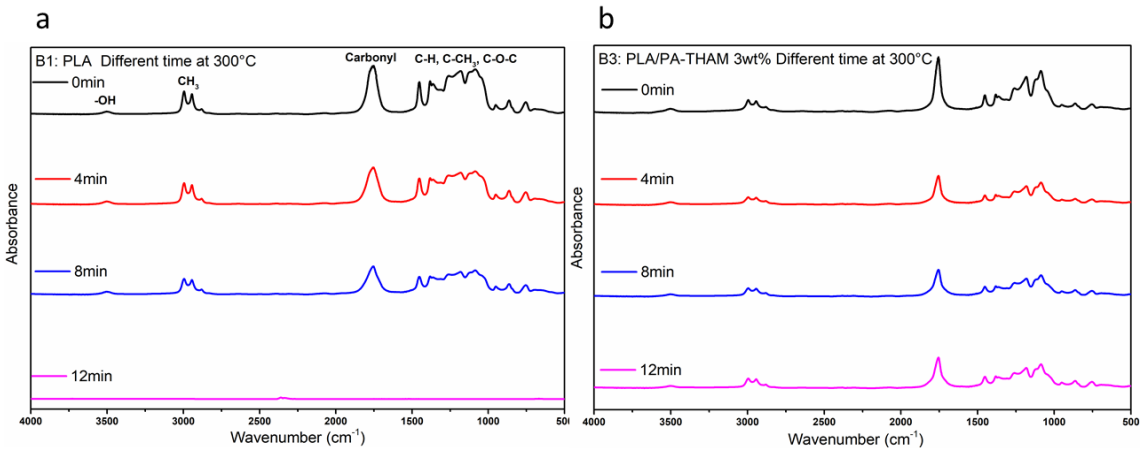

Fig. 3-14 FTIR spectra of pyrolysis products of different times at 300°C for PLA and PLA/PA-THAM: (a) B1 PLA; (b) B3 PLA/PA-THAM (3wt%).

Based on the analysis of gaseous and condensed phases as well as the results from flame combustion tests, a possible flame-retardant mechanism of PA-THAM can be proposed as following. At the early stage, some incombustible products, such as H_2O,

were generated from the dehydration of PA-THAM and decomposition of ionic bonds, and released into the gas phase. Meanwhile, other pyrolyzed acid compounds promoted thermal degradation of PLA, which can cause the reduction of molten viscosity and facilitate the heat transfer. Along with the further decomposition of PA-THAM, the carbonization led to forming a protective layer in condensed phase. As a consequence, the flame-retardant mechanism of PA-THAM focused on the combination of "heat transfer" effect, dilution action and slight barrier protection by physical properties.

3.4 Conclusion

In this work, a novel bio-based flame retardant (PA-THAM) was synthesized successully via salt formation reaction. The fire resistance of PLA was improved after introducing this novel phytate, which were supported by the corresponding results. In contrast with the neat PLA, only 3 wt% addition of PA-THAM significantly enhanced the ignition-resistance performance of PLA-based biocomposite, possessing a LOI value of 25.8%, passing UL-94 V-0 rating, exhibiting excellent self-extinguish behaviour, and delaying the time to ignition (TTI). Moreover, the complex viscosity of this biocomposite illustrated a 90% less than that of pristine PLA at 170 °C, and little change in mechanical properties were observed. When the percentage of PA-THAM was added up to 5 wt%, the correlative biocomposite showed a slight increase in flame retardant performance as well as evident reduction in mechanical properties. Therefore, PA-THAM, as a bio-based additive with small molecular weight, can act as a synergist to improve the flame-retardant properties and a lubricant to decrease molten viscosity for PLA simultaneously; moreover, the biocomposite would achieve a good balance between mechanical properties and fire resistance at optimum loading levels.

CHAPTER 4

Study of flame-retardant natural fiber reinforced plastic biocomposite: PLA/OCC/PA-THAM

4.1 Introduction

Due to the issues of environmental pollution and energy depletion, natural fiber reinforced plastic biocomposites (NPC) are becoming new promising alternatives to replace the conventional materials in building applications [162–164]. This new generation substitute can benefit both economy and environment by converting the residues of corps into a new product with low-cost, green, biodegradable, and acceptable properties, which can meet the demand in construction field [165–167].

Natural fibers can be derived from both plant and animals, and the one obtained from plants are developing a potential market, which are already applied to residential construction sectors, such as furniture or railing systems [31,168]. As a by-product of corn, which is a widespread industrial crop in many countries, a large amount of corn stalk is left after harvest every year. Thus, recycling this residue as a reinforcement material in composites is an economical and effective method. A new biocomposite prepared with magnesium phosphate cement and corn stalk was reported for the application in the insulation and structure field, which showed better thermal performance and mechanical properties than the one comprised hemp and cement did [169]. Kaya et al. [170] extracted a xerogel from corn stalk and introduced it into epoxy system; this xerogel imparted epoxy nanocomposite good thermal stability and more char residue at high temperature. Binici rt al. [171] found that many engineering properties of concrete can be improved via adding partial bio-based fillers such as corn stalk.

With regard to the NPCs, matrix is an essential part in the fiber reinforced biocomposite, and thermoplastics are used as the matrices in most cases. On the basis of the concept of bio-based material, polymers obtained from renewable sources should be the primary choice. Among these biopolymers, polylactide (PLA) is a typical acceptable thermoplastic in NPCs system, which is already reported in previous papers [29,172]. Compared with reference sample PLA, biocomposite with natural fibers exhibited a better tensile specific strength and stiffness with an increase of 116% and 62%, respectively [173]. After adding natural cellulosic fiber into PLA, this biocomposite demonstrated an improvement in crystallinity and melt strength due to the nucleation of filler [174]. 5 wt% loading of flame retardant with a metal-organic framework (MOF) structure enabled natural fiber/ PLA system to possess a 43% reduction in smoke production and enhancement in mechanical properties [175].

Moreover, as residential construction material, the flammability is also an important aspect to be considered. In order to improve the fire resistance, incorporating flame retardants, especially the ones bearing “flame-retardant elements” with synergistic effect, such as phosphorus and nitrogen, into material system is regarded as an highly efficient way to achieve this objective [176–178]. In the precious work, a novel eco-friendly flame retardant (PA-THAM) containing phosphorus and nitrogen was synthesized and applied for PLA. The study showed that 3 wt% incorporation of PA-THAM in PLA exhibited improved flame-retardant properties and significant lubricating effect simultaneously, whilst the mechanical properties were hardly impacted. Furthermore, another problem that should not be neglected is the interfacial affinity between matrix and fillers, which plays a crucial role for general properties in multi-phase system. Therefore, PA-THAM was proposed to enhance the affinity and flame-retardant properties of NPC system simultaneously.

This work aims to prepare a PLA-based biocomposite reinforced by corn-pith cellulose fiber, which was pretreated with this eco-friendly additive (PA-THAM) via in-situ modification. The effect of fillers on relevant mechanical properties, thermal stability, and fire behaviors of biocomposite is investigated systematically.

4.2 Modification and characterization of corn-pith fiber

4.2.1 Pretreatment of corn-pith fiber (CC)

Corn-pith derived from the interior part of corn stalk is a natural fiber with spongy tissue and noticeable low density. The physical and chemical pretreatments were carried out to improve cellulose reactivity prior to modification [179]. Firstly, the exterior hard surface of corn stalk was peeled off, while the interior soft part was milled mechanically. Then CC with millimeter size was selected by sieving. After that, the CC was oxidized in NaOH solution (PH=11) at room temperature for 12 h with continuous stirring [180]. Finally, oxidized corn-pith cellulose fiber was dried after filtrating and washing with deionized water.

4.2.2 Modification of oxidized corn-pith fiber (OCC)

Fig. 4-1 illustrated the rout of in-situ modification for OCC. As a raw material of flame retardant, THAM was dissolved in ethanol solvent at 70 °C; then OCC was added with stirring for a good dispersion. Based on Table 4-1, the correlative amount of another reactant PA was introduced dropwise into the well-dispersed solution until the reaction was complete; the precipitate in solution was washed with ethanol to remove the residual reagents. Finally, OCC modified with different content of PA-THAM was acquired after drying in vacuum oven at 80 °C.

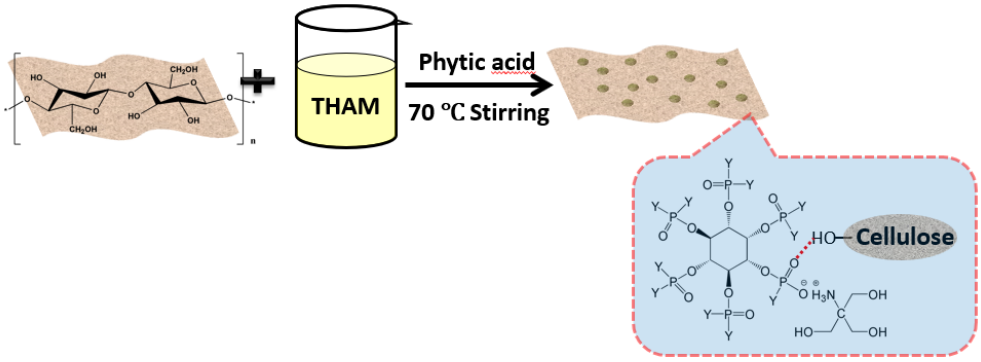

Fig. 4-1 Scheme diagram of OCC modification with PA-THAM

4.2.3 Characterization of modified OCC

Different micro-morphologies for the surface of OCC with and without PA-THAM were observed in Fig. 4-2. OCC showed a smooth surface with 73.31 wt% of carbon, 26.66 wt% of oxygen and little phosphorus that might result from the original composition in corn pith. However, in-situ modification endowed a rough surface of OCC with many small particles of flame retardant, as well as additional elements consisted of 6.07 wt% of phosphorus and 0.47 wt% of nitrogen were detected except carbon and oxygen.

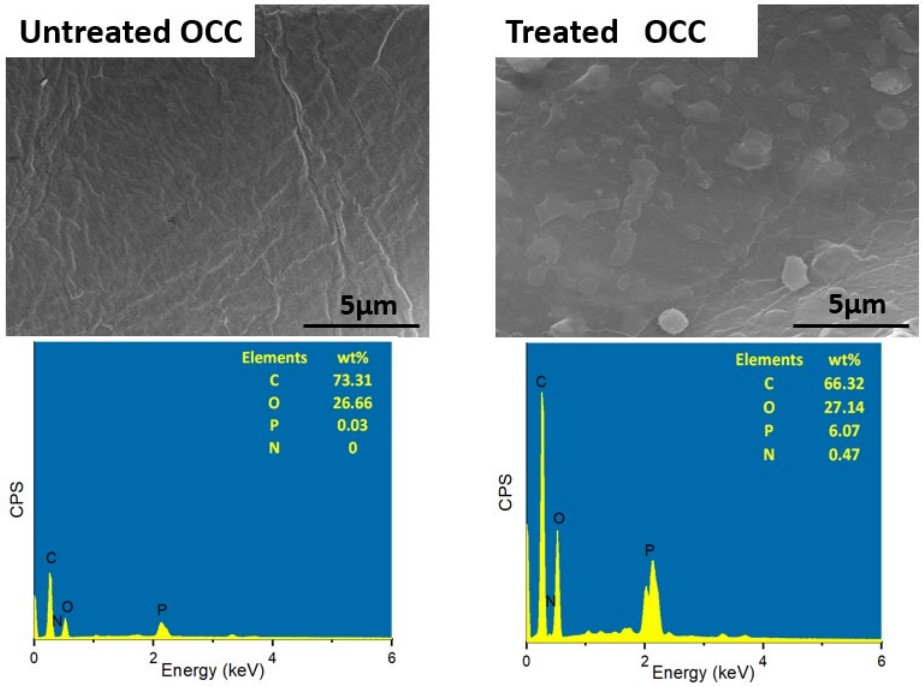

Fig. 4-2 Images from SEM/ EDS for the surface of OCC before and after modification

Furthermore, FTIR was utilized to confirm the chemical components of cellulose fiber surface by comparing the difference of OCC before and after modification. (shown in Fig. 4-3). OCC without PA-THAM exhibited a typical absorption spectrum of cellulose [181,182], in which bands at 4000 - 3000 cm^{-1} were attributed to hydrogen-bonded O-H stretching, absorption at 2900 cm^{-1} was due to C-H stretching, peaks around 1600 cm^{-1} can be assigned to O-H bending vibration, and out-of-plane bending mode of C-O caused the appearance of peaks at 1055 cm^{-1} [183,184]. On the contrary, some changes were observed in absorption peaks of modified OCC. For example, broader and stronger absorbances appeared at wavelength from 4000 cm^{-1} to 3000 cm^{-1} probably resulted from the more hydrogen-bonded bands between PA-THAM and OCC [185]. An obvious change was also observed at 1630 cm^{-1} due to the stretching vibration of O-P-O. Bands at 2940 cm^{-1} and 1530 cm^{-1} was caused by the ammonium salt and bending vibration of N-H, respectively, whilst peak from P-O-H stretching vibration was detected at 890 cm^{-1}. Another wide and strong characteristic band occurred around 1060 cm^{-1}, which was

shifted to higher wavenumber caused by the formation of hydrogen-bonded bands, was attributed to the overlap from bending modes of C-O and C-N bonds [186,187]. These alterations in treated OCC spectrum further proved that the PA-THAM was coated onto the surface of OCC.

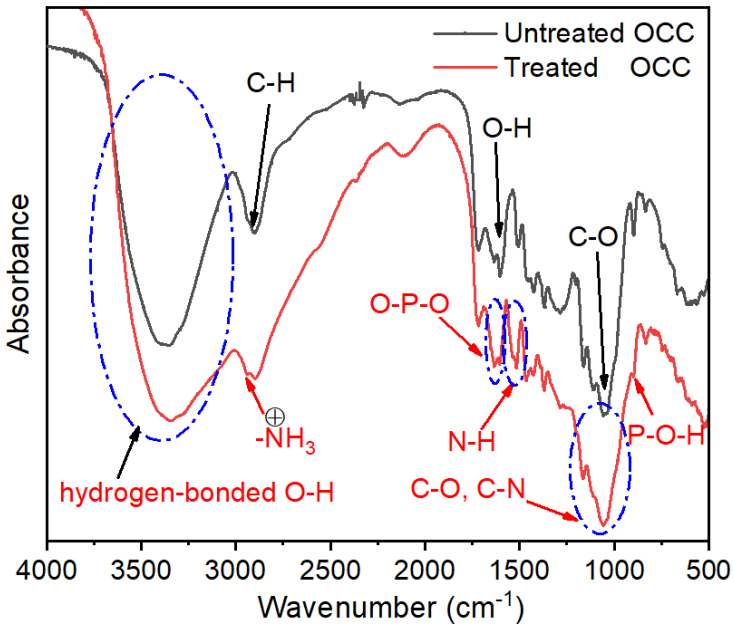

Fig. 4-3 Infrared spectra of FTIR for untreated and treated OCC

The effect of PA-THAM on the thermal stability of natural fiber was also investigated via thermogravimetric analysis, shown in Fig. 4-4. Both samples degraded in three stages during temperature-rising process [188]. The first stage was due to the evaporation of free water which occurred around 100 °C. The following stage caused by hemicellulose and cellulose decomposition took place between 200 °C and 350 °C. Finally, lignin pyrolyzed above 700 °C. Although, the incorporation of PA-THAM in OCC led to a lower initial degradation temperature, which was owing to the poor thermal stability of PA-THAM, a reduction in maximum degradation rate and an increase in residue at high temperature were observed in the samples with additives. This changes can be elucidated that PA-THAM decomposed products at lower temperature to catalyze carbonization of the

cellulose by dehydration reaction [189,190]; then the char layer prevented the cellulose from further decomposition.

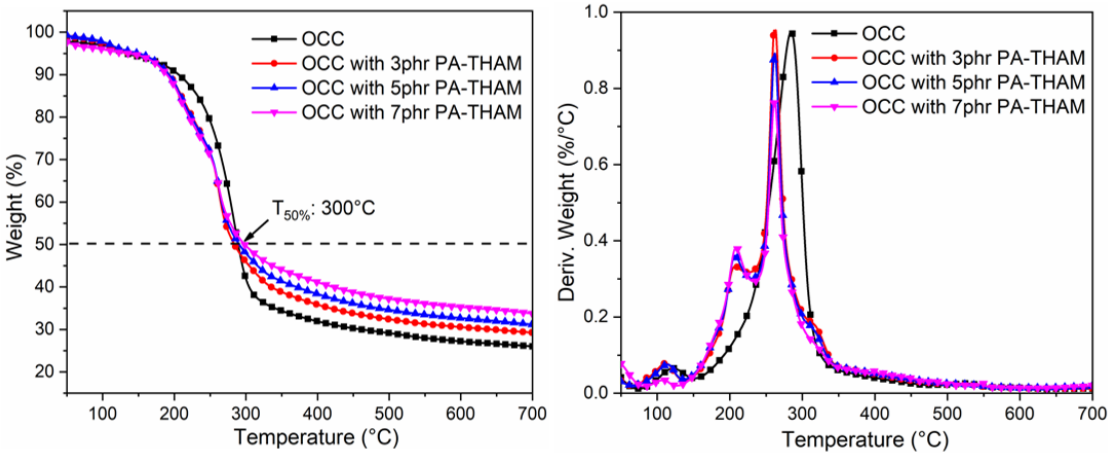

Fig. 4-4 Results from thermogravimetric test for OCC before and after modification

On account of the analysis from micro morphology, infrared spectra, and thermal stability, the OCC was modified with flame retardant successfully and can be used as the filler for PLA biocomposite.

4.3 Preparation and characterization of natural fiber reinforced plastic biocomposites (NPCs)

4.3.1 Preparation of natural fiber reinforced plastic biocomposites (NPCs)

Table 4-1 showed the design of the PLA-based NPCs with different content of flame retardant. The NPCs were prepared via melt mixing under the processing conditions mentioned in previous part. All involved samples were tested after being shaped into the required dimensions and drying in a vacuum oven at 80 °C for 8 h before use.

Table 4-1 Formulation of PLA and its biocomposites

Sample	PLA/ (wt%)	OCC/ (wt%)	PA-THAM*/ (phr)
NPC0	90	10	/
NPC1	90	10	3
NPC2	90	10	5
NPC3	90	10	7

*PA-THAM was fixed with phr on the basis of total composite mass.

4.3.2 Mechanical properties of NPCs

Tensile and impact properties

The tensile and un-notched impact properties of PLA-based NPCs were investigated firstly. As shown in Table 4-2, the reference sample NPC0 generally showed a typical change in mechanical properties with poor affinity between matrix and filler. However, almost no variation was observed in the tensile properties after introducing flame retardant less than 7 phr. Especially for sample NPC2 with 5 phr content of PA-THAM, the elongation at break varied from 3.1% to 3.0%, and tensile strength changed from 54.1 MPa to 53.7 MPa with same value of Young's Modulus. This phenomenon was probably due to little effect of small loading PA-THAM on the crystallinity of biocomposite.

With regard to impact strength, the value increased firstly and then declined in all the NPCs. Compared with NPC0 (11.7 kJ/m^2), the incorporation of OCC modified with 5 phr PA-THAM in biocomposite exhibited a higher value of 13.0 kJ/m^2, while sample NPC3 with further addition of 7 phr PA-THAM presented a decrease in impact strength. Aiming to clarify this change, the micro morphology of NPCs, which played an important role for impact property in multiphase material system, was analyzed by SEM technique.

As shown in Fig. 4-5, NPC0 demonstrated morphology with many smooth hole and clean cellulose surface due to poor compatibility between matrix and filler. Consequently, a premature failure and debonding behavior occurred because of these defects in weak

region. In contrast, formulations with modified OCC exhibited a better interface conditions, in which there were more celluloses adhered with PLA resin instead of debonding holes. Moreover, the continuous phase consisted of PLA matrix altered from smooth surface to rough one, and the natural fiber was embedded well in matrix with fuzzy boundaries. When the flame retardant was loaded up to 5phr in biocomposite, a homogeneous morphology with a few aggregations was achieved. This indicated that appropriate dosage of PA-THAM improved the interfacial affinity as well as caused a good dispersion in this ternary system [191–193]. When this additive was further loaded into the biocomposite material, some large agglomerates and obvious droplets resulted from PA-THAM were observed in biocomposite NPC3. This was probably caused by the ratio of fillers, which played a key role in the shape and amount of agglomerate in multiphase material system [194–196]. Therefore, the optimum addition of 5 phr PA-THAM can enable PLA-based biocomposite to reach good interfacial adhesion and dispersion.

Table 4-2 Mechanical properties of PLA-OCC NPCs

Sample	Elongation at break / (%)	Tensile Strength/ (MPa)	Young's Modulus/ (GPa)	Impact Strength/ (kJ/m^2)
NPC0	3.1±0.1	54.1±2.0	2.4±0.1	11.7±1.0
NPC1	2.9±0.1	52.4±1.0	2.4±0.2	12.1±0.5
NPC2	3.0±0.1	53.7±1.0	2.4±0.1	13.0±0.2
NPC3	2.1±0.2	45.7±2.0	2.3±0.1	11.8±0.2

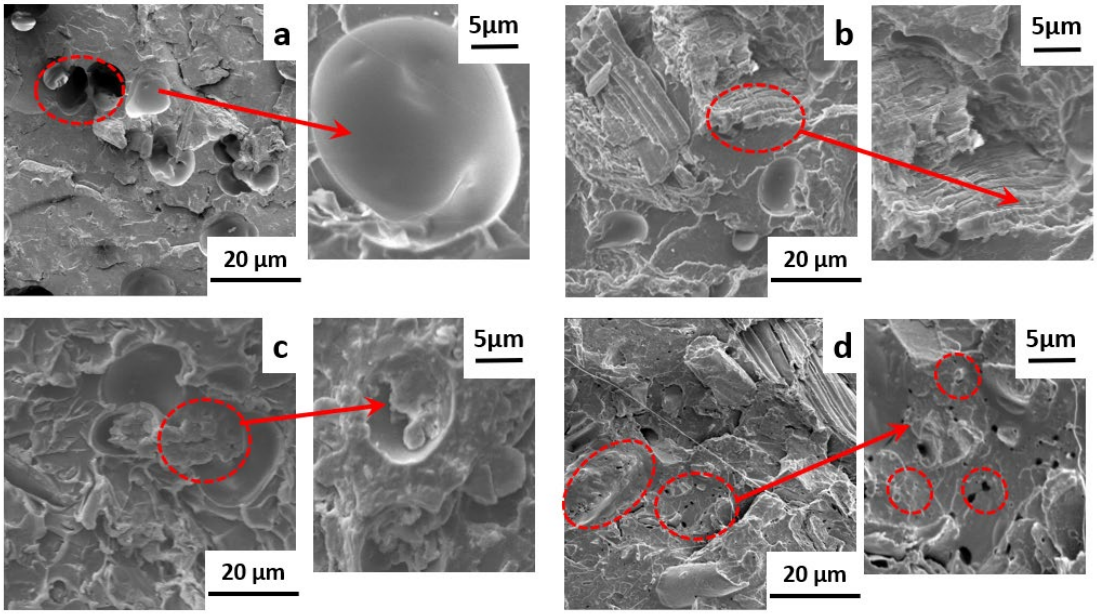

Fig. 4-5 SEM morphology of impact-fracture surface for PLA-based NPCs: a) NPC0; b) NPC1; c) NPC2; d) NPC3

Dynamic mechanical analysis

The dynamic mechanical properties of PLA-based biocomposites were displayed in Fig. 4-6. All the formulations demonstrated two thermo-dynamic relaxation processes at similar temperatures. The first relaxation occurred at 60 °C was caused by glass-to-rubber transition, and the another one derived from secondary transition of the crystalline region took place around 100 °C. As for the curves of storage modulus versus temperature, the value of storage modulus for all NPCs was almost constant in glassy region. Along with the increase of temperature, the occurrence of glass-transition led to a significant reduction in storage modulus, which also showed a little increase correlated with the cold crystallization [197,198].

Nevertheless, there was obvious alteration in the value of Tan Deltas for all the NPCs, which indicated the mobility of polymer chains. The introduction of PA-THAM in the biocomposites illustrated a higher value of tan δ peak height. This increase can be elucidated with the polar groups introduced by PA-THAM to bring about more friction

between molecular chains and more time was needed to overcome it [199]. The peak intensity of tan δ decreased with the addition of PA-THAM, which was because that the lubrication effect from PA-THAM weakened the intermolecular interaction [200,201].

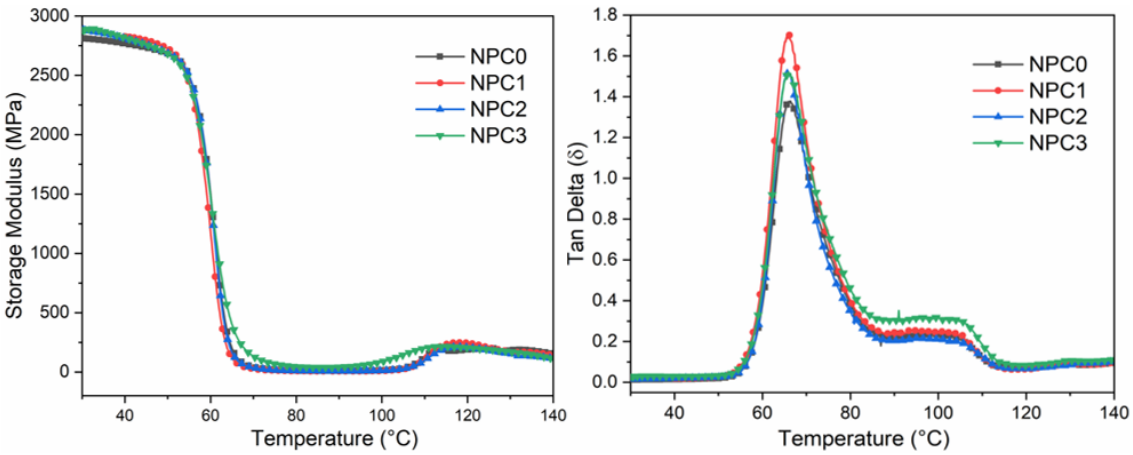

Fig. 4-6 Results from DMA test for PLA-based NPCs

4.3.3 Thermal stability of NPCs

From Fig 4-7, it can be seen that the thermal stability of PLA-based biocomposites was enhanced significantly after adding flame retardant. When OCC was incorporated alone into PLA, the biocomposite decomposed at a lower temperature ($T_{10\%}$: 255°C) due to poor thermal stability of corn-pith cellulose. On the contrary, the corresponding decomposition temperature of other formulations increased by 50 °C due to the combination of OCC and PA-THAM. This significant improvement was because of the phosphorylation of cellulose by reacting with PA-THAM rather than premature thermal degradation of PLA induced by cellulose, and this reaction between OCC and PA-THAM promoted to forming a thermal stable char layer which acted at later stage [202,203]. Besides, the formation of char layer prevented the penetration of pyrolyzed volatiles out from the material at early stage and slowed down further degradation [204].

With the gradually increasing temperature, further degradation of PLA occurred as well as volatile products from additives released; consequently, biocomposites with flame retardant exhibited more weight loss at the maximum decomposition stage than the one filled with only OCC did [205]. Moreover, the existence of PA-THAM in PLA-based biocomposites increased the amount of char residue at high temperature (above 400 °C).

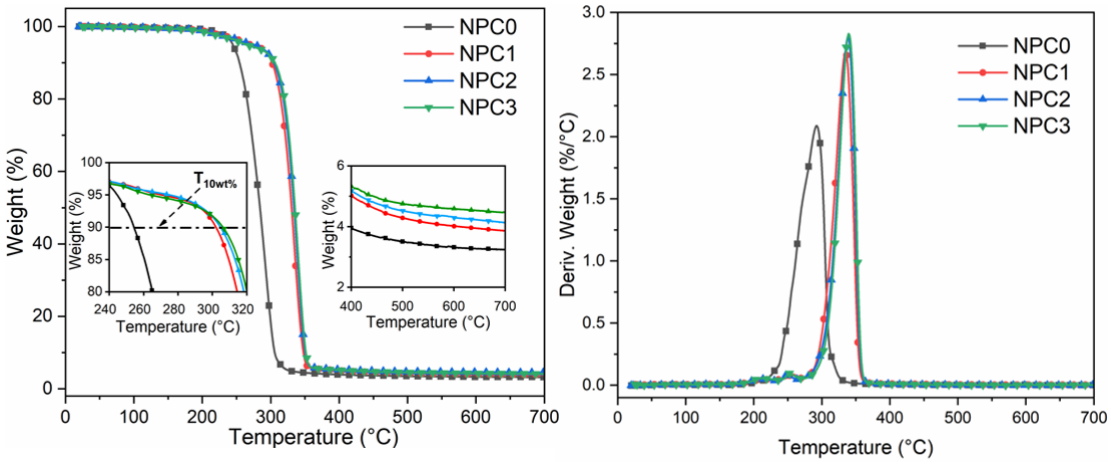

Fig. 4-7 Results from thermal gravimetric analysis for PLA-based NPCs

Aiming to explain the evident improvement in the thermal behavior, TGA coupled with FTIR technique was performed to investigate the evolution of volatile compounds from PLA-based biocomposites during the degradation process. Fig. 4-8a) illustrated the same decomposed products for NPC0 and NPC2, which indicated the presence of PA-THAM did not change the primary thermal degradation behaviour of PLA reinforced with OCC [206]. But the reduced intensity of volatiles from NPC2 at the same temperature (300 °C) demonstrated that the combination of OCC and PA-THAM delayed thermal degradation. Additionally, the curves of intensity versus time was listed in Fig. 4-8b), which represented the evolution of hydrocarbons' concentration in the whole degradation process [207]. The results showed that the incorporation of modified OCC with PA-

THAM not only postponed the degradation behavior, but also inhibited the release of hydrocarbons.

According to the analysis of thermal performance, it can be deduced that the combination of OCC and PA-THAM can form a thermal stable char layer at early stage that enabled biocomposite to avoid a premature degradation and acted as a barrier for exchange of heat and volatiles, and finally improve the thermal stability [208–210].

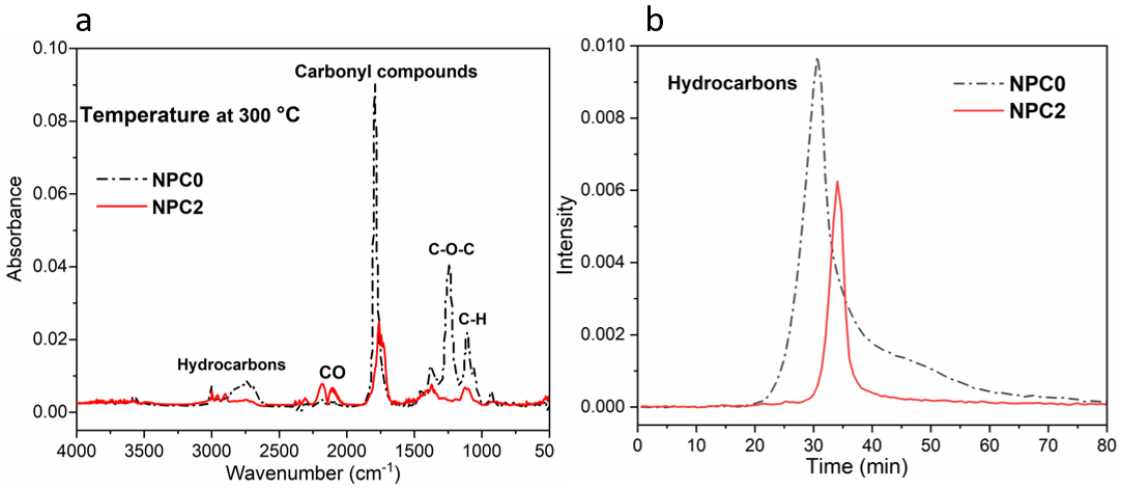

Fig. 4-8 Curves from TGA/ FTIR test for NPC0 and NPC2: a) FTIR spectrum for volatiles at 300 °C; b) evolution of hydrocarbons component at the whole heating process

4.3.4 Flammability of NPCs

LOI and UL-94

As testing measures of the flammability, LOI and UL-94 were operated to evaluate the combustion behaviors of PLA-based biocomposites. Table 4-3 exhibited that sample modified with PA-THAM had better results in LOI and UL-94 tests than the one with corn-pith cellulose fiber alone. The controlled sample NPC0 presented 19.0% for LOI value and no rating in UL-94. Along with the rising content of flame retardant, the flame-retardant properties of NPCs improved as well, possessing 25.2 % LOI value, passing

UL-94 V-2 rating at the content of 5phr PA-THAM. This enhancement was attributed to the synergistic effect of OCC and PA-THAM [211–213]. 7 phr loading of PA-THAM further declined the total flaming time in UL-94, but the result still maintained V-2 rating due to flaming dripping during combustion, which can take flame away from the specimen and ignite cotton below at the same time [214].

Table 4-3 Results from LOI and UL-94 tests for PLA-OCC biocomposites

Sample	LOI/ (%)	$\overline{t1+t2}$/ (s)	UL-94		
			Rate	Ignition	Dripping
NPC0	19.0±0.2	Burt out	NR*	Yes	Yes
NPC1	22.0±0.2	10+60	NR	Yes	Yes
NPC2	25.2±0.1	13+14	V-2	Yes	Yes
NPC3	26.1±0.1	14+0	V-2	Yes	Yes

*NR: NO Rating

Table 4-4 and Fig. 4-9 summarized the results from cone calorimeter test, which was considered as a useful assay to simulate a real fire scenario [215,216]. The fire behavior of materials can be evaluated by some important parameters, such as heat release rate (HRR), peak heat release rate (PHRR), time to ignition (TTI), total heat release (THR), average effective heat of combustion (Av-EHC) and residue.

Compared with neat PLA, the reference sample NPC0 presented worse fire behavior, which showed an 35s TTI value, THR of 65 MJ/ m^2 with a PHRR of 428 kW/ m^2, and 0.5 wt% residue [217,218]. These performances were attributed to the poor thermal stability and little charring ability of natural fiber, which led to a reduced TTI value and little residue, respectively. By contrast, the incorporation of PA-THAM in biocomposite increased the flame-retardant properties, especially for NPC2 with 5 phr PA-THAM. In comparison with NPC0, the PHRR of NPC2 reduced by 21.3%, char residue increased to 6.2 wt%, and TTI postponed by 8s.

Ignition of polymer material is a complex issue, which can be divided into two stages including temperature-rising and ignition temperature processes affected by physical and chemical factors, respectively [219]. As thermally thin sample, the TTI of PLA-based biocomposite can be analyzed according to the equation 4-1 [220].

$$\mathrm{TTI} = \iota\rho c\frac{T_{ig}-T_0}{q''_{ext}-CHF} \qquad (4\text{-}1)$$

Where ι is the sample thickness, ρ the density, c the heat capacity, T_{ig} and T_0 are the ignition temperature and initial ambient temperature, respectively, q''_{ext} is the experimental heat flux as well as CHF the critical heat flux.

In this case, the physical parameters (ιρc), which mainly played role at temperature-rising stage, can be considered constant due to the small loading of additive. In consideration of the same experimental conditions, T_0 and q''_{ext} did not change for all the samples. As for the chemical aspects, chemical composition and concentration of volatiles made effect on the T_{ig} and CHF. In order to analyze the ignition temperature T_{ig}, samples NPC0 and NPC2 were selected to monitor the top-surface temperature, shown in Fig 4-10. From the curves of temperature versus time, it can be seen that both samples started to ignite at same temperature, which indicated that the incorporation of PA-THAM did not alter the ignition temperature due to the little effect on the decomposition behavior of natural fiber reinforced PLA biocomposite at ignition process [220,221]. Consequently, as the remaining parameters, the critical heat flux CHF, which can be utilized to evaluate the ignitability of each material, is related to the thermal stability [222]. According to the results from TGA test above, the thermal stability was improved significantly after incorporation of flame retardant, whilst the volatile species did not change. This further implied that the increased TTI value was due to higher thermal stability. Taking into account of these comprehensive physical and chemical parameters, the delayed TTI was

because of the barrier effect of thermal-stable carbonaceous layer to reduce volatile concentration at later process [213,217].

Table 4-4 Results from CCT for PLA-based biocomposites

Sample	PHRR/ (kW/m²)	TTI/ (s)	THR/ (MJ/ m²)	Av-EHC/ (MJ/ kg)	Residue/ (wt%)
NPC0	428±6	35±2	65±2	16.5±0.1	0.5
NPC1	375±5	43±2	62±1	16.6±0.1	3.9
NPC2	337±3	43±2	58±1	16.4±0.1	6.2
NPC3	335±4	44±2	57±2	16.1±0.2	6.4

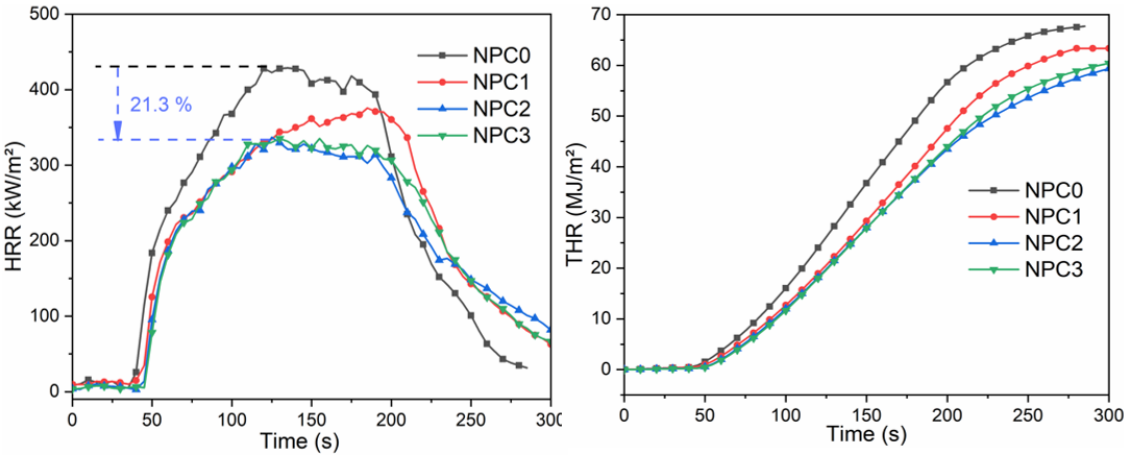

Fig. 4-9 Curves of HRR and THR vs time from cone calorimeter test for PLA-based NPCs

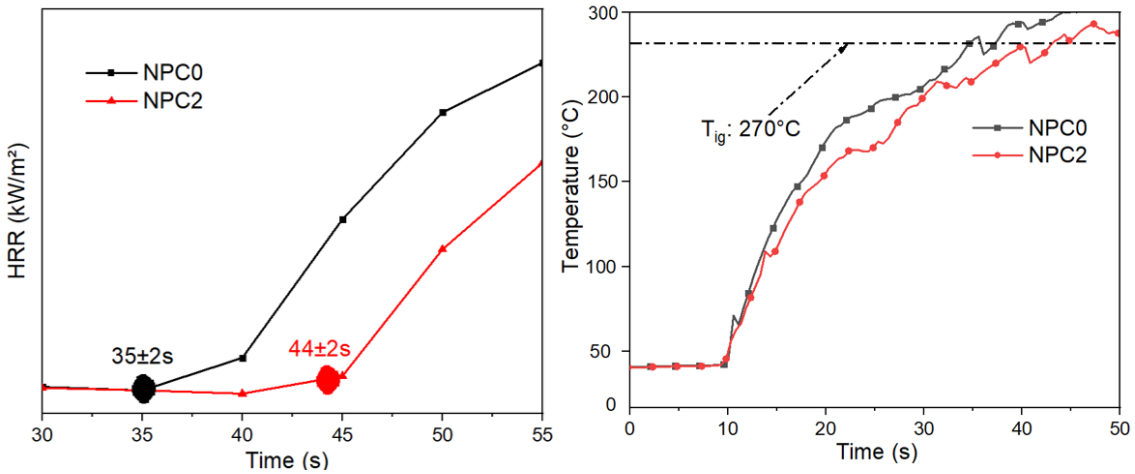

Fig. 4-10 Curves of temperature versus time before ignition and weight loss versus time: a) HRR versus Time at ignition; b) Top-surface temperature vs Time curves

4.3.5 Study of flame-retardant mechanism for NPCs system

Another essential parameter Av-EHC, which was used to describe the released volatiles in the cone calorimeter, almost showed little change in amounts of volatiles for all the samples. Thus, it can be considered that the primary flame retardant mechanism was concentrated in condensed phase, and the char residue of PLA-based biocomposites was investigated after combustion [223,224].

From the digital photos in Fig. 4-11, sample with unmodified OCC almost burnt out with only 0.5 wt% char left. Comparatively, the quantity of char residue increased in other formulations with flame retardant, and the value rose up to 6.2 wt% when the 5 phr of PA-THAM was added into biocomposite. Besides, Fig 4-12 illustrated the micro-structure of external and internal surface for NPC0 and NPC2. In contrast to reference sample NPC0, which presented a loose morphology with large voids, a more continuous and compact micro-structure was observed in both external and internal surface for biocomposite NPC2, as well as more phosphorus and nitrogen elements were detected in char residue. Based on the analysis of char layer, it can be inferred that the efficient combination of OCC and PA-THAM can improve the flame retardant properties of PLA-based biocomposite due to the barrier effect in condensed phase [225–227].

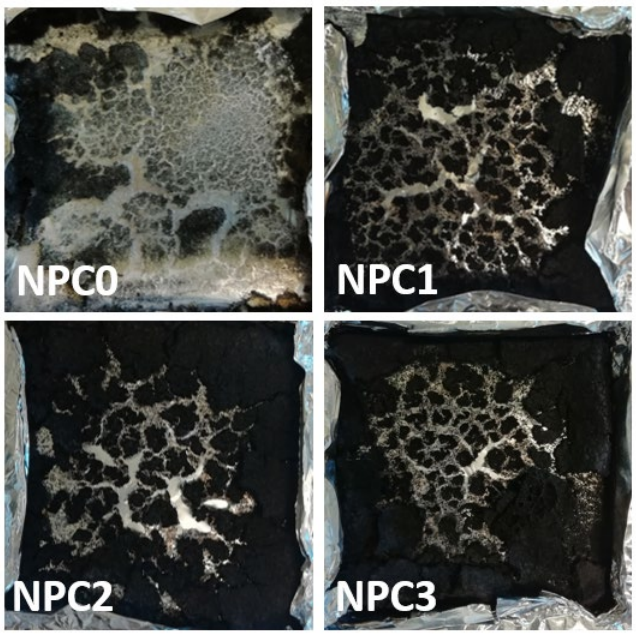

Fig. 4-11 Digital photos of char residue for PLA-based NPCs after cone calorimeter test

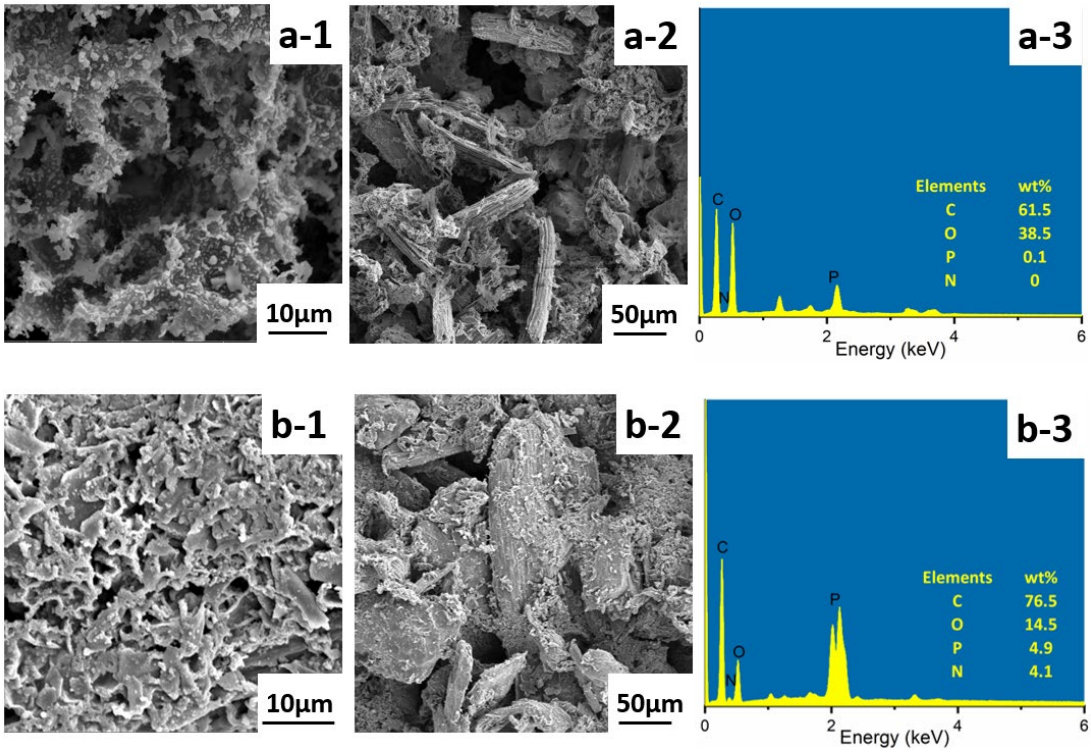

Fig. 4-12 Morphology and elements analysis of the char residue surface after cone calorimeter test for NPC0 and NPC2: a-1) external part of NPC0; a-2) internal part of NPC0; a-3) EDS for NPC0 char residue; b-1) external part of NPC2; b-2) internal part of NPC2; b-3) EDS for NPC2 char residue

Additionally, the 3D images (Fig. 4-13) from TGA-FTIR for NPC0 and NPC2 showed that there was no change for volatile species but a remarkable reduction for total volatile amount after introducing PA-THAM into natural fiber reinforced PLA composite. Combination with the mass of char residue, it can be concluded that the presence of PA-THAM prevented the premature degradation of cellulose owning to catalytic effect rather than promoted charring behaviour of PLA itself. Generally, the primary flame-retardant mechanism of this biocomposite system can be probably elucidated in Fig. 4-14. At the beginning, the dehydration of both PA-THAM and cellulose occurred, which released some inert gases to dilute the concentration of volatile fuel. Simultaneously, the pyrolyzed products from PA-THAM promoted cellulose to phosphorylation to form a stable protective layer, which can act as a thermal insulator for inner material. Consequently, the flame-retardant mechanism of this ternary system was predominantly focused on both dilution and thermal insulation effects in condensed phase.

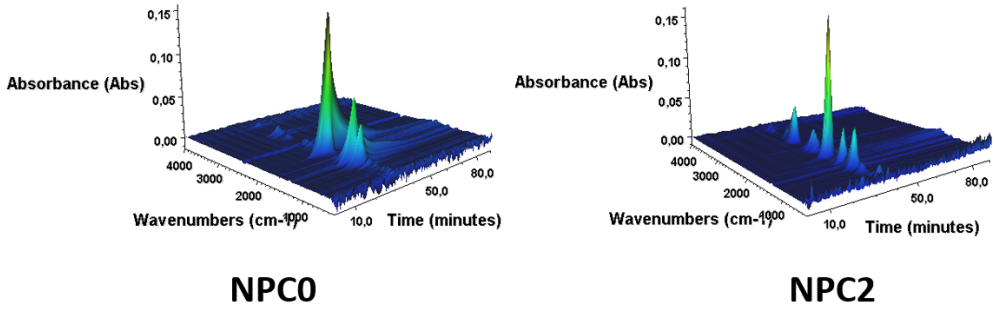

Fig. 4-13 3D images from TGA-FTIR

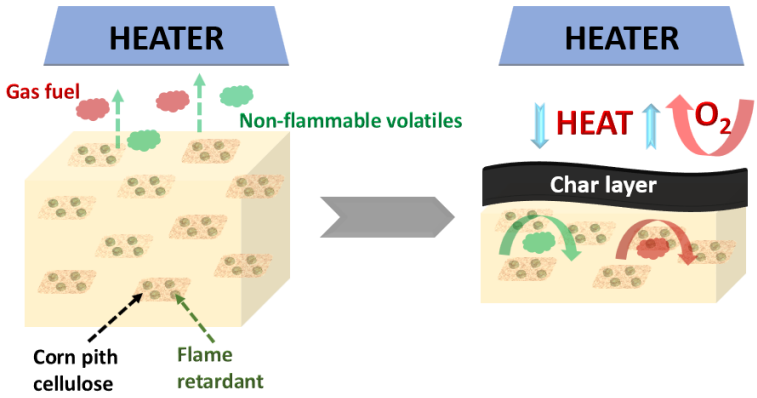

Fig. 4-14 Proposed flame-retardant mechanism

4.4 Conclusion

Based on the results in this work, a flame-retardant PLA biocomposite was prepared through the combination of oxidized corn-pith cellulose fiber (OCC) and bio-based flame retardant (PA-THAM). The natural fiber OCC was successfully coated with PA-THAM via in-situ modification, which was supported by some characterizations. The effect of combination of OCC and PA-THAM on the properties of this natural fiber reinforced plastic composite (NPC) was also investigated systematically. In comparison with the reference sample NPC0, the addition of 5 phr PA-THAM endowed sample NPC2 with a 50 °C higher $T_{10\%}$ corresponding to 10 wt% weight loss, and an increase in impact strength. The flammability of PLA-based biocomposite was improved by forming the char layer, which can prevent the premature decomposition of cellulose. For example, LOI value rose up from 19.0% to 25.2% and ratings in UL-94 increased to V-2; more achievements were observed in cone calorimeter test: 21.3 % reduction of PHRR, 6.2 wt% increase of char residue and 8 s postponement of TTI. In the wake of further 7 phr introduction of PA-THAM into material system, sample NPC3 showed a little increase

in both thermal stability and fire resistance, while the mechanical properties fell down a lot.

In conclusion, the combination of OCC and PA-THAM showed a synergistic effect during combustion, and an optimum ratio of PA-THAM and OCC was obtained, which can enable the PLA-based biocomposite to achieve acceptable mechanical properties, thermal stability, and flame retardancy simultaneously.

CHAPTER 5

Study of ecologically flame-retardant thermal insulation material: CC/AG/FR

5.1 Introduction

Issues concerned with environmental protection and energy depletion give rise to more effort to develop new nature-derived thermal insulation material applied for building industry [228,229]. In contrast to the conventional construction materials, crop by-product is becoming a promising alternative due to its eco-economic characteristic, renewable resources, and sustainable life cycle. As a widespread industrial crop, corn leaves a large amount of corn stalks after harvest every year. Consequently, recycling utilization is considered as an effective and economical way to avoid wasting resources, which can be seen in the application for thermal insulation material field [31,230].

There are already some achievements that corn by-product was utilized as thermal insulation material in construction sector. M. Palumbo et al. [231,232] found that corn pith indicated a more potential than other crop by-products to be used as a thermal insulation material due to lower density. Besides, in comparison with the reference sample without additives, sample prepared with corn pith and alginate showed a reduction of heat release rate and lower propagation speed in smouldering behavior. A. Paiva [233,234] analyzed the thermal insulation performance of a particleboard with corn cob, and considered that corn cob can become an attractive raw material for building purpose due to its microstructure and chemical composition. A nature-based composite combined corn cob with sawdust was prepared by A. Banjo Akinyemi group [235] and presented potential application for indoor uses.

Nevertheless, this promising thermal insulation material fabricated from natural materials also has the issue of fire risk related to the safety of life and property, and thus should be paid much attention to. As different forms of combustion, smouldering and flaming combustion should be concerned for building materials and the relevant properties can be improved simultaneously. It is generally known that incorporation of halogen-free flame retardant, such as phosphorus-containing and boron-containing, is considered as an efficient and economical way not only to enhance the flame retardant but also to avoid the adverse effect on health and environment.

In our previous work, several phosphorus-containing compounds were proved to be efficient additives that can endow PLA-based biocomposite with good flame-retardant properties. A biocomposite mixed with PLA and ammonium polyphosphate (solid: APP) exhibited an increase in fire resistance with a 30.8% reduction of peak of heat release rate [218]; another novel flame retardant P-AA was loaded into PLA by 0.5% percentage, which also improved the flame retardancy, passing UL-94 V-0 rating, delaying the ignition time from 66 s to 111 s [158]. Moreover, boron-containing chemicals were also investigated for the application in flame retardant purpose. An epoxy material system cured by boron-containing phenolic resin showed an excellent flame-retardant performance due to form a continuous and thicker char barrier [236]. After coating boron-containing chemicals onto cotton fabrics, these modified fabrics demonstrated a self-extinguishing behavior and good flame retardant properties because of physical obstruction of intumescent char layer [237].

However, as an effective flame retardant in many cases, some boron-containing chemicals such as boric acid and sodium borate are pointed out to have reproductive toxicity potential and restricted for building application by European Union's REACH SVHC Candidate [238]. As a consequence of the usage limitation, the combination of

boron and phosphorus was proposed to be an efficient way, which can achieve the requirement of both reducing boron-containing compounds loading and increasing fire resistance contributed by the synergistic effect between these two substances [239,240].

This work is aiming to prepare a bio-based thermal insulation material, therefore corn pith consisted of parenchymatic tissue with higher porosity was chosen as the raw material, and three types of flame retardants involved boron-containing and phosphorus-containing compounds were utilized to enhance the flame-retardant properties of this thermal insulation material. In this system, one of the flame retardants is PA-THAM that was presented in previous work, and other two chemicals were DOT and APP.

5.2 Preparation and characterization of thermal insulation particleboard

5.2.1 Pretreatment of corn pith

Same as the previous work, corn pith cellulose derived from the interior part of corn stalk was granulated into particles with 2-3 mm size by mechanical method, which were used as the raw material for thermal insulation boards. On the basis of standard TAPPI, the chemical composition of corn pith cellulose was analyzed and summarized in Table 5-1 as well.

Table 5-1 Chemical composition of corn pith

	Lignin/ (wt%)	α-cellulose/ (wt%)	Hemicellulose/ (wt%)	Ash/ (wt%)	Moisture/ (wt%)	Extractables/ (wt%)
Corn Pith	17.58	30.31	27.96	6.17	2.57	15.41

With regard to the preparation of thermal insulation particleboards, several steps were followed. Firstly, corn pith cellulose was soaked by a little deionized water; then mixed the wetted cellulose with alginate solution, which was used as the binder for this board

system, containing flame retardant and gel-accelerator agent. After obtained a well-dispersion, the mixture was transferred into relevant mold and pressed for 30 min. Afterwards, these precursors were removed from molds and put into an oven at 50 ℃ for 2 days. Finally, all the specimens were kept for another 2 days in a constant condition at 25 ± 1 ℃ and 50% ± 3 R.H before testing. Moreover, additional alginate films were prepared with same content of flame retardant as corresponding particleboards, and the formulation with only 8 wt% APP was designed to compare the flame-retardant efficiency of PA-THAM and APP. Table 5-2 and 5-3 were the formulations of thermal insulation particleboards and corresponding alginate films, respectively.

Table 5-2 Formulations of corn pith particleboards

Sample	Corn Pith/ (wt%)	Alginate/ (wt%)	Plater/ (wt%)	Citrate/ (wt%)	Flame Retardant/ (wt%) *
PB0	92	4	2	2	0
PB1	92	4	2	2	PA-THAM/ 8
PB2	92	4	2	2	PA-THAM+ DOT/ (6+2)
PB3	92	4	2	2	PA-THAM+ DOT/ (10+5)
PB4	92	4	2	2	APP/ 8

* The percentage of flame retardant is confirmed by the total amount of material system.

Table 5-3 Formulations of alginate films corresponding to respective particleboard

Sample	Alginate/ (wt%)	PA-THAM/ (wt%)	PA-THAM+DOT/ (wt%)	APP/ (wt%)
F0	4	0	0	0
F1	4	8	0	0
F2	4	0	6+2	0
F3	4	0	10+5	0
F4	4	0	0	8

5.2.2 Thermal properties of corn pith particleboards

Thermal insulation

Table 5-4 showed the thermal conductivity (λ), thermal diffusivity (α), corresponding parameter (C_ρ) for specific heat capacity (ρC_ρ), and density which were related to thermal insulation properties. It was obvious that the variations of these parameters between all the samples were within the experimental error, which indicated that the incorporation of these additives did not change the thermal insulation properties as well as the density, which played an important role in insulation materials [241]. These data elucidated that this corn pith alginate system can be used for thermal insulation application, because materials with the conductivity lower than 0.07 W/m·K can be regarded as a thermal insulator [31].

Table 5-4 Thermal properties of corn pith particleboards

Sample	λ/ (c)	Cρ/ (10^6 J/m^3·K)	α/ (10^{-6} m^2/s)	Density/ (kg/m^3)
PB0	0.036±0.002	0.037±0.003	0.96±0.05	58±1
PB1	0.037±0.001	0.046±0.002	0.87±0.04	59±2
PB2	0.035±0.001	0.032±0.003	1.08±0.07	59±1
PB3	0.034±0.002	0.032±0.001	1.07±0.05	62±2
PB4	0.037±0.002	0.045±0.002	0.88±0.07	59±2

Thermal stability

The thermal degradation behavior of alginate films and particleboards were investigated through thermogravimetric analysis and listed in Fig. 5-1. Fig. 5-1 a) showed the thermal degradation process of alginate films, in which the reference sample F0 consisted of two stages. The initial degradation temperature at 80 ℃ was attributed to moisture evaporation and loss of coordinated water, and the other one occurred at 200 ℃ was corresponding to the dehydration, decarboxylation, and decarbonylation of alginate. After incorporation of flame retardants, some improvements were observed in both decomposition temperature and remaining residue, especially for the samples F2 and F3.

The increased thermal stability was because of a catalyzed interaction between alginate and flame retardant, which promoted to form thermal stabile char-layer and improved the charring ability of alginate during the whole degradation process [242,243].

From the Fig. 5-1 b), particleboards also demonstrated a similar trend in degradation process containing three stages. Firstly, the decomposition appeared around 100 ℃ was due to the volatilization of moisture and acid-catalyzed dehydration of cellulose. Along with the increased temperature, effects of depolymerization, hydrolysis, dehydration and oxidation led to the second degradation stage. The final degradation was derived from char oxidation. In comparison of PB0, PB3 with 15 wt% mixture of flame retardants showed 60 ℃ higher value for T_{max} corresponding to maximum weight loss, whilst the maximum decomposition rate declined remarkably and char residue increased from 0 to 15 wt%. This phenomenon elucidated the effect of synergism from PA-THAM and DOT on the flame retardancy, where PA-THAM promoted cellulose to phosphorylate and carbonize by dehydration and dihydroxylation, and meanwhile, DOT stabilized char layer and prevented oxidation of char by suppressing premature weight loss. Therefore, the combination of both flame retardants can favor to form a thermal stable protective layer at the early stage, which improved the thermal stability of particleboard [43,244].

Additionally, sample PB1 with 8 wt% of PA-THAM presented higher thermal stability than PB4 with same percentage of APP, which indicated that the effect of PA-THAM was better than that of APP on flame retardant properties for corn pith thermal insulation material.

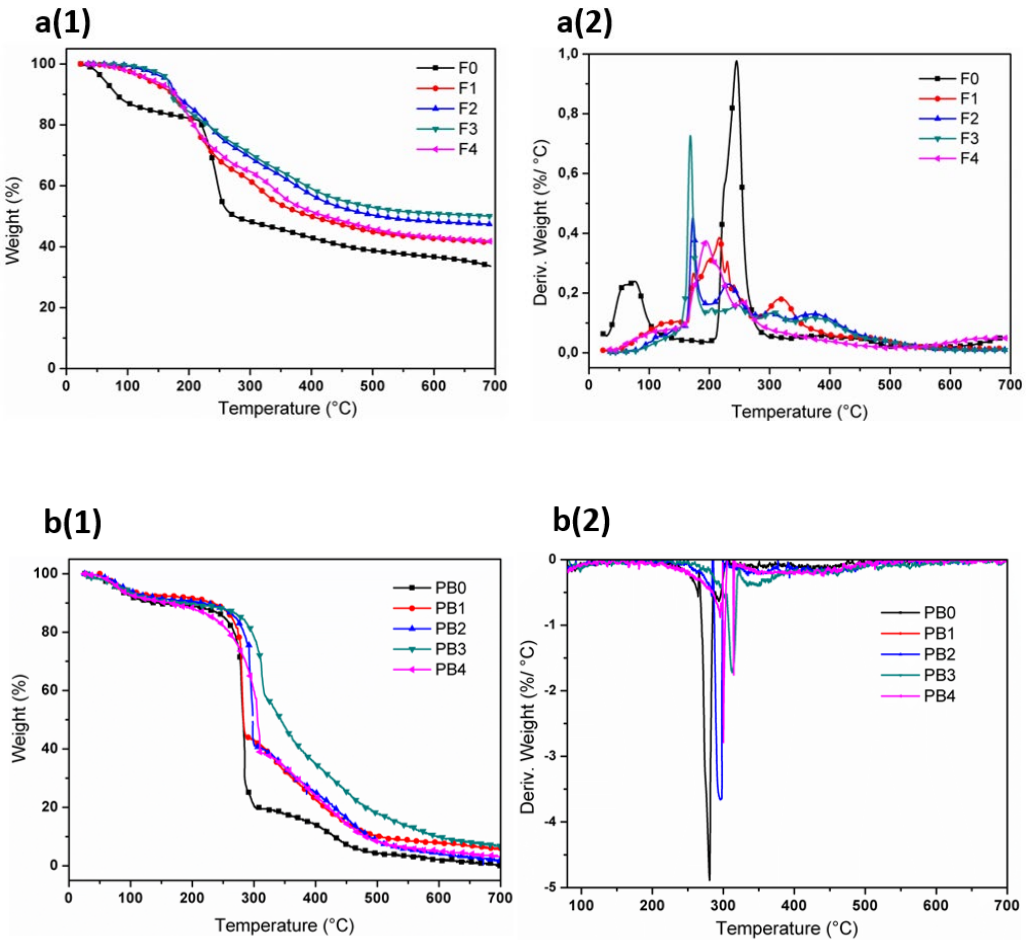

Fig. 5-1 Results from TGA test: a) alginate films; b) corn-pith alginate particleboards

5.2.3 Smouldering performance of corn pith particleboards

As an important form of combustion, smouldering, which was the leading reason of substantial deaths and economic losses, was defined as a slow, flameless phenomenon sustained by the heat generated by oxidation reaction between oxygen and condensed phase of porous materials [84,85]. Thus, smouldering test was carried out to study this flameless combustion of thermal insulation boards with corn pith cellulose, which contained large amounts of porosity.

Fig. 5-2 and Fig. 5-3 were the temperature evolutions curves of thermocouples, digital photos and infrared images for samples PB0, PB1, and PB4 during smouldering process. The reference sample PB0 without flame retardant started to smolder at 280 ℃ and

propagated at the speed of 13.0 mm/ min, in which little change was observed at another initial setting temperature 310 ℃ and same results were recorded by other researchers [231]. In contrast, samples incorporated with flame retardant showed a delayed initial temperature at which smouldering started to take place. Therefore, a higher value 310 ℃ was chosen as the onset temperature to compare the different smouldering behaviors of these three particleboards. Sample PB0 smouldered at the 40th min and smouldering was detected at other positions in 10 min, and this meant the whole sample burnt out in this short time, which was supported by the digital photo and infrared image of PB0. After introducing 8 wt% flame retardant APP into thermal insulation material, the smouldering behavior was postponed to 50th min, as well as other positions started to smoulder at a higher temperature accordingly. The whole sample combusted completely in 80 min at a speed of 3.3 mm/ min. On the contrary, the 8 wt% loading of PA-THAM enabled sample PB1 to exhibit a much better flame-retardant performance, in which a lower propagation speed of 1.5 mm/ min was recorded. Moreover, this flameless combustion ceased after 60 min although the first position started to smolder at close to 60 min.

Furthermore, smouldering performance of specimens with mixture of PA-THAM and DOT was also investigated and showed in Table 5-5. These two thermal insulation boards PB2 and PB3 with respective 8 wt% and 15 wt% of mixed flame retardants demonstrated an increased initial smouldering temperature by 350 ℃ and 370 ℃, whilst self-extinguishing phenomenon was observed in both samples. These improvements can be elucidated as the synergistic effect between PA-THAM and DOT. On the basis of similar density and thermal conductivity, the existence of flame retardants caused a high quality of char layer, as physical obstruction for oxygen supply and heat passage, to decrease propagation speed and depress further smouldering [245,246]. More flame-retardant behaviors were analyzed by in the following text.

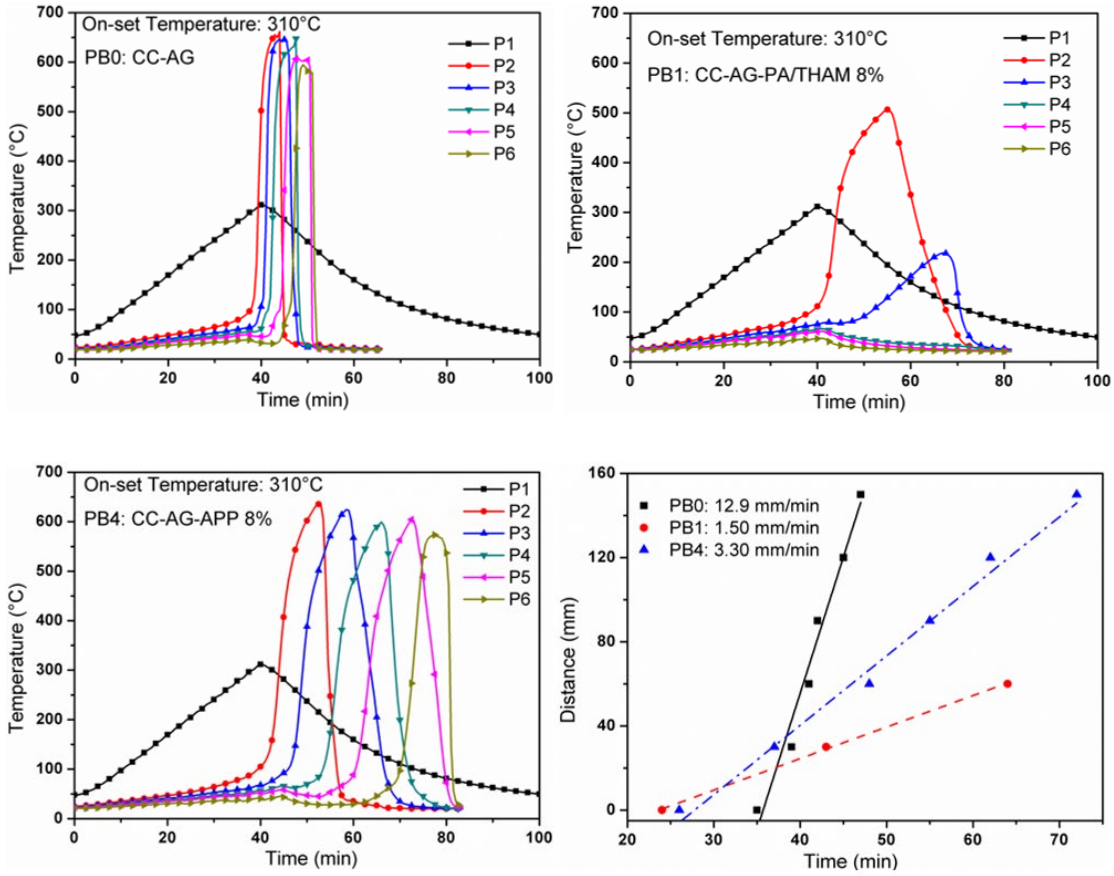

Fig. 5-2 Temperature evolutions of thermocouples located each 3cm along for corn pith alginate particleboards, P1: site of hot-plate temperature; P2-P6: the locations of six thermocouples

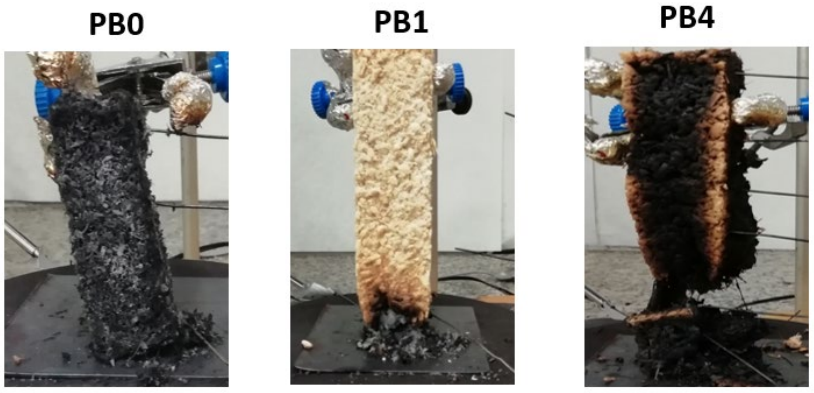

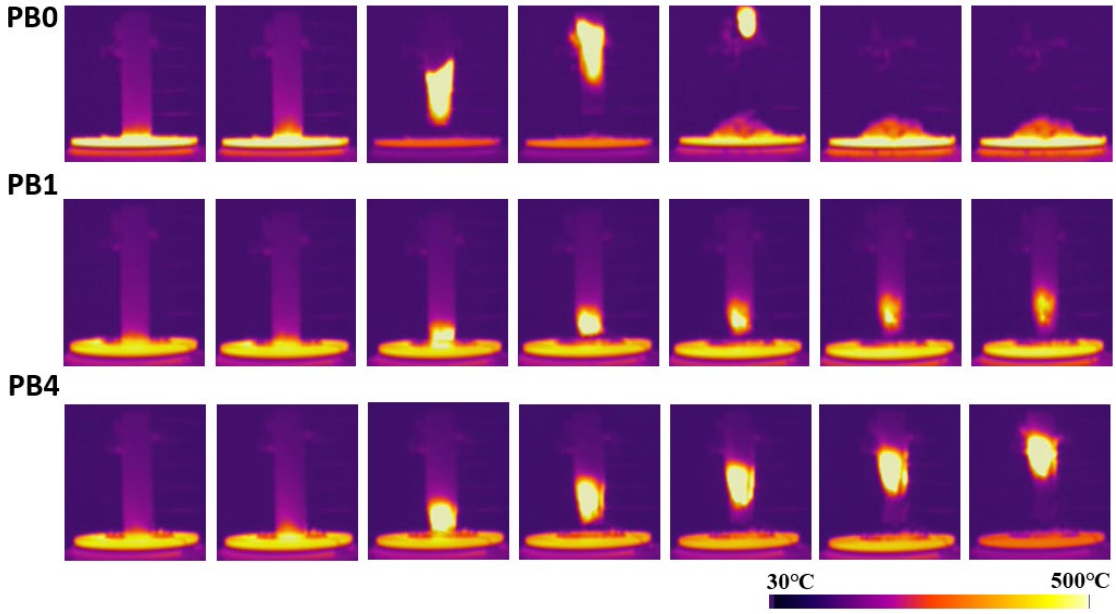

Fig. 5-3 Digital photos after smouldering combustion and infrared images for corn pith particleboards (PB0: CP/AG; PB1: CP/AG/PA-THAM (8 wt%); PB4: CP/AG/APP (8 wt%)) at times=30, 35, 40, 45, 50, 55, 60 min. White color represents the combustion region.

Table 5-5 Speed (mm/ min) of the smouldering for the corn pith particleboards at different onset temperatures

Sample	280/ (℃)	290/ (℃)	300/ (℃)	310/ (℃)	320/ (℃)	330/ (℃)	340/ (℃)	350/ (℃)	370/ (℃)
PB0	13.0	-	-	12.9	-	-	-	-	-
PB2	NO*	NO	NO	NO	NO	NO	NO	YES*	-
PB3	NO	NO	NO	NO	NO	NO	NO	NO	YES

YES*: Smouldering occurred but not burnt out.

NO*: No smouldering occurred.

5.2.4 Flaming combustion of corn pith particleboards

Ignition time and extinguishabiility test

The ignition and extinction properties of corn pith alginate particleboards were reported in this test. Some relative parameters involved first ignition time (t_1), number of ignitions in 5 min (N_{ig}), and average duration of flame (Δt_{ig}) were listed in Table 5-6 [232].

As for the controlled board, PB0 was ignited within 2s, and the ignition was observed 8 times in 5 min with 6s value for average flame duration. Nevertheless, it was noticed

that the presence of flame retardants made little effect on these properties. In comparison with PB0, specimens treated with PA-THAM and APP separately demonstrated value for t_l and N_{ig} at the same level as well as a longer time for Δt_{ig}. Besides, the retarding effect of mixture of PA-THAM and DOT was only to conserve the same level with that of particleboard without any flame retardant, which agreed with the results in other papers [247].

This no effect of flame retardants on ignition and extinction properties was because the carbonization rate along the surface of sample did not meet the combustion speed in thickness direction under this heat source; then the under unignited material was not protected by char layer. Additionally, higher Δt_{ig} value occurred in PB1 and PB4 was contributed by the faint flame observed at the edge, which was also counted into the result. In contrast, the control board PB0 was observed that the entire surface was covered with extended flame after each ignition.

Table 5-6 Ignitions and extinction properties

Sample	t_l/ (s)	N_{ig}/ (times)	Δt_{ig}/ (s)
PB0	2	8	6
PB1	4	6	18
PB2	4	8	8
PB3	4	9	8
PB4	3	9	12

Calorimeter test

Microscale combustion calorimeter test (MCC) and Cone calorimeter test (CCT) were performed to further investigate the flame-retardant properties of corn-pith alginate thermal insulation material, which were characterized by some important parameters: heat release rate (HRR), peak heat release rate (PHRR), total heat release (THR), time to

ignition (TTI), average effective heat combustion (Av-EHC), total smoke production (TSP) and char residue.

From Table 5-7, it can be noticed that the flame-retardant properties were improved due to the incorporation of additives. Sample PB0 without flame retardant was ignited in 3 seconds and left 17.9 wt% residue with the values of 188 kW/m², 7.5 MJ/ m², and 0.22 m^2 for PHRR, THR and TSP, respectively. After introducing the flame retardants, these associated parameters were enhanced accordingly, especially for the formulations with mixture of PA-THAM and DOT. Although TTI only delayed by 1s in PB2 and PB3, PHRR declined by 25.5% and 38.8% as well as THR reduced by 22.7% and 33.3%, respectively, shown in Fig. 5-4 a) and b). Additionally, the TSP fell down to 0.07 m² and 0.05 m² as well; char residue increased and became denser, which was supported by the digital photos from Fig. 5-4 c). In comparison with PB1 and PB4, there were almost no obvious change in fire resistance. With regard to Av-EHC, which was considered as an indicator of combustion efficiency of volatiles [216], little change was observed for all the thermal insulation particleboards.

Table 5-7 Results from cone calorimeter test for flame retardant corn particleboards

Sample	PHRR/ (kW/m²)	TTI/(s)	THR/ (MJ/ m²)	Av-EHC/ (MJ/kg)	Residue/ (wt%)	TSP/ (m^2)
PB0	188±3	3	7.5±0.1	31.7±0.2	17.9±0.2	0.22±0.02
PB1	171±3	4	7.0±0.2	32.9±0.1	21.7±0.3	0.18±0.01
PB2	140±2	4	5.8±0.2	31.7±0.3	20.4±0.2	0.07±0.01
PB3	115±2	4	5.0±0.1	33.5±0.1	25.5±0.2	0.05±0.01
PB4	165±4	3	6.3±0.3	32.0±0.1	19.2±0.3	0.12±0.03

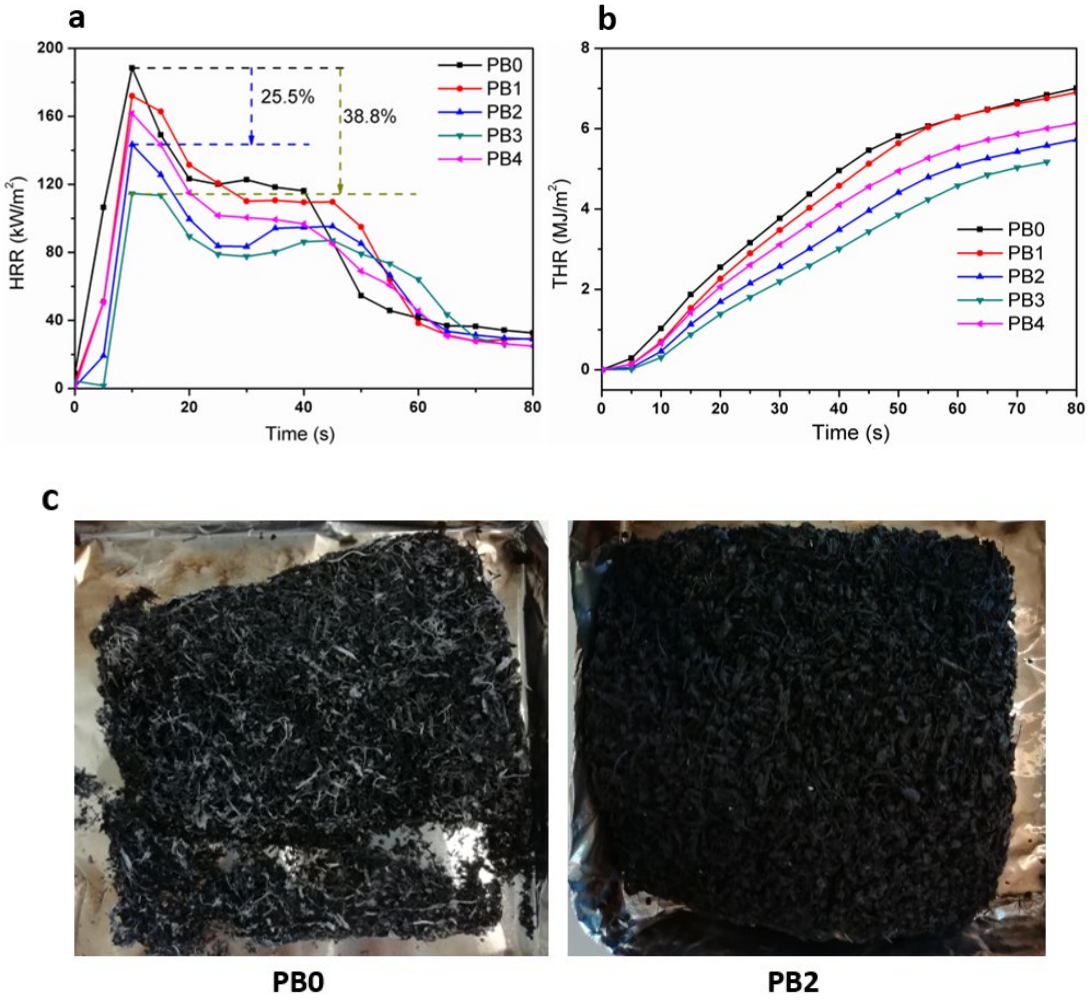

Fig. 5-4 Results of flame retardant corn pith particleboards' after cone calorimeter test: a) HRR vs Times curves; b) THR vs Times curves; c) digital photos after combustion: PB0) CP/AG, PB2) CP/AG/(PA-THAM/ DOT) (6/2) wt%

Furthermore, the relevant alginate films with different additives were also studied by MCC, shown in Fig 5-5. Pure alginate film exhibited two peaks corresponding to thermal degradation stages, which appeared at 250 ℃ with 60 W/ g PHRR and 460 ℃ with 16 W/ g accordingly. However, presence of PA-THAM and DOT altered this behavior, where the first peak almost disappeared and the second one took place at a lower temperature. This phenomenon can be associated with catalysis of PA-THAM and DOT to favor the formation of char layer to protect the alginate at early stage, while led to alginate to premature decomposition along with the increased temperature [243,248].

Based on the comprehensive analysis from combustion behavior, it elucidated that the improvement in flammability was attributed to the synergistic effect of PA-THAM and DOT. The predominant flame-retardant effect focused on the condensed phase, in which the accelerated formation of char layer can act as an obstruction to inhibit further combustion and suppress the smoke [43,249,250].

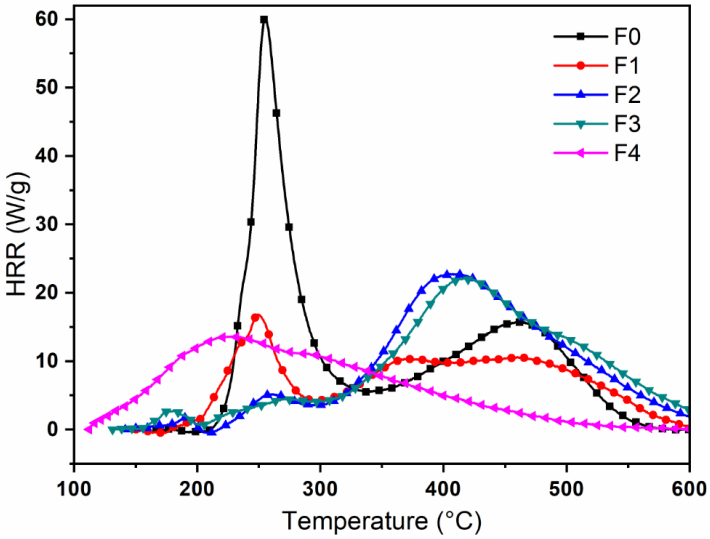

Fig. 5-5 HRR data from micro cone calorimeter for flame retardant alginate films

5.3 Study flame-retardant mechanism of corn pith particleboards

In order to investigate the flame-retardant mechanism of the combination of PA-THAM and DOT, TGA-FTIR and SEM/ EDS were performed to analyze volatile products during thermal degradation and char residue after combustion.

Fig. 5-6 a) and b) illustrated the evolution of involved gas products for PB0 and PB2 during thermal degradation process. The main pyrolysis products of reference sample PB0 were listed in Fig. 5-6 c), which was consistent with previous papers [251,252],

including C-O (1245 cm^{-1}), carbonyl compounds (1780 cm^{-1}), CO (2100 and 2190 cm^{-1}), CO_2 (2358 cm^{-1}), hydrocarbons (2850-3100 cm^{-1}), and H_2O (3577 cm^{-1}). The decomposition products from PB0 was detected at 100 °C, absorbance intensity of which reached maximum at 150 °C, and there was almost no signal at 300 °C. However, the maximum degradation behaviour was delayed to 200 °C for PB2; moreover, the intensity of absorption peaks related with the concentration of corresponding composition was much weaker than that of PB0. Especially, amounts of the compounds from hydrocarbons and carbonyl compounds reduced, which were corresponding to the restricted degradation of hemicellulose and cellulose [253]. This illustrated that the synergistic effect of PA-THAM and DOT induced to form a protective layer at early stage, preventing PB2 from further degradation. Besides, it should be explained that the downward peaks in the spectra were attributed to the instrument error instead of the gas products.

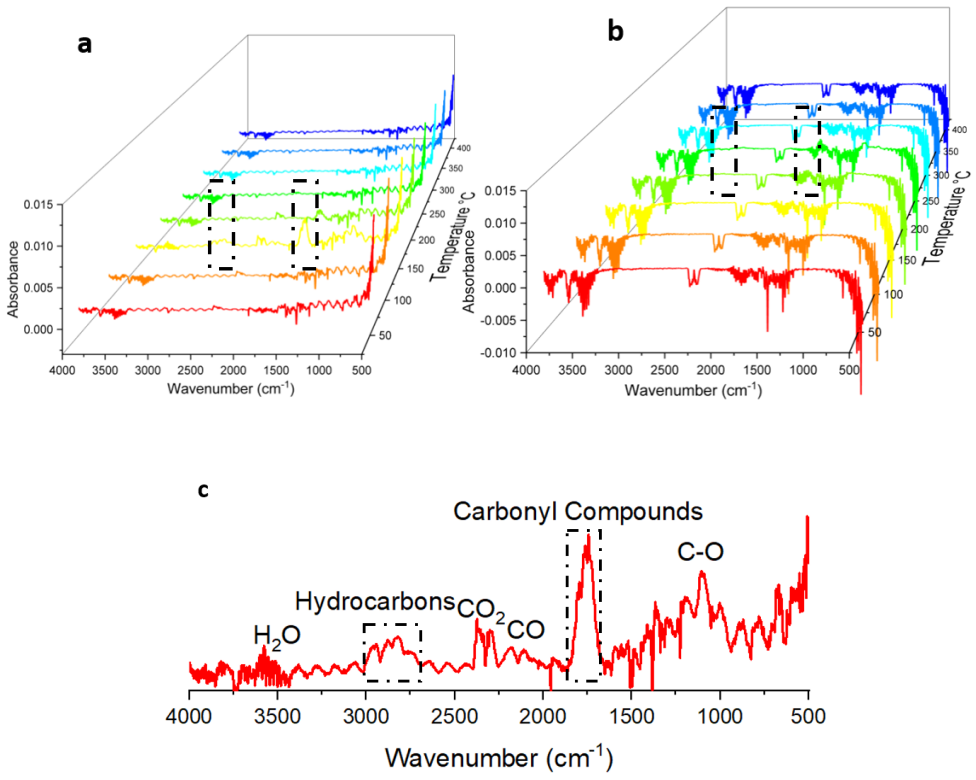

Fig. 5-6 Curves from TGA/ FTIR test for PB0 and PB2: a) 3-D image of evolution of chemical composition for PB0; b) 3-D image of evolution of chemical composition for PB2; c) FTIR spectra of total volatile products at max degradation rate from PB0 and PB2.

Analysis of residue after combustion was important to investigate fire resistance behavior on condensed phase, therefore technique of SEM connected with EDS was carried out to observe the chemical composition of residue for PB0 and PB2. From Fig. 5-7, quite small amounts of elements were detected in the residue of PB0, which were owing to the ash produced by corn pith cellulose. In contrast, the morphology of residue from PB2 became more compact as well as more elements including extra boron and phosphorus can be observed, where the small overlap of boron was because of small dosage and similar displacement with that of carbon. This indicated that the incorporation of PA-THAM and DOT led to catalytic reaction between these two compounds in the condensed phase; then promoted the formation of char layer with good quality, which acted as a physical barrier for oxygen supply and heat transfer [239,254–257].

On the basis of the results prementioned above, a proposed flame-retardant mechanism was listed in Fig. 5-8. At the early stage, some inert volatiles such as H_2O were released due to the dehydration process, as well as the decomposition of additives occurred to form the phosphorus/ boron-containing compounds, which can favor the charring process. Along with the increasing temperature, a stable char layer formed to prevent the further decomposition of inner material. In the combination of the dilution and barrier effect during the thermal degradation process, PA-THAM and DOT can function in both gaseous and condensed phases, while mainly focused on condensed phase mechanism [252,258].

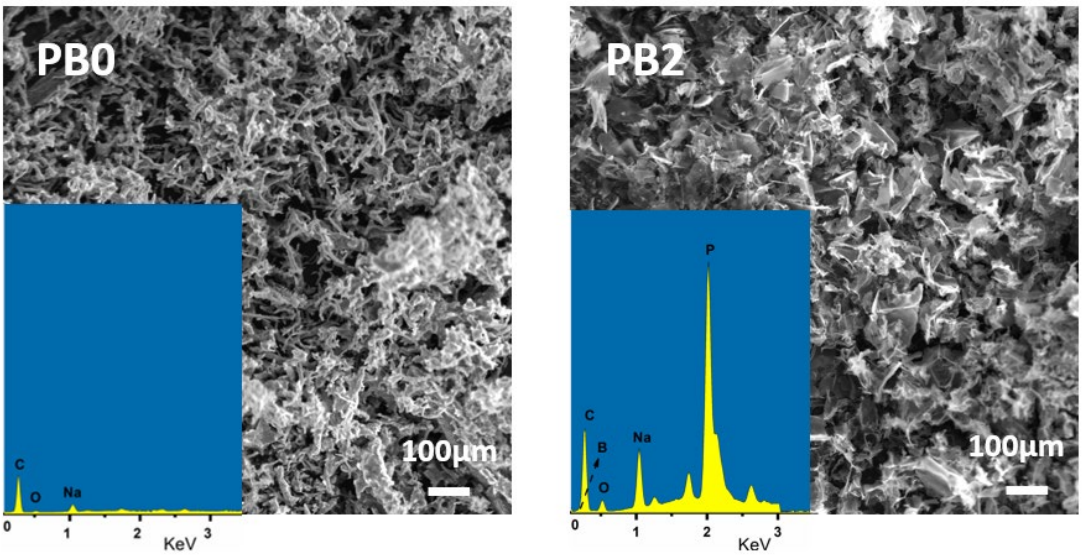

Fig. 5-7 SEM images of char residues after cone calorimeter test for particleboards: a) PB0: CP/AG; b) PB2: CP/AG/PA-THAM/DOT (6/2) wt%

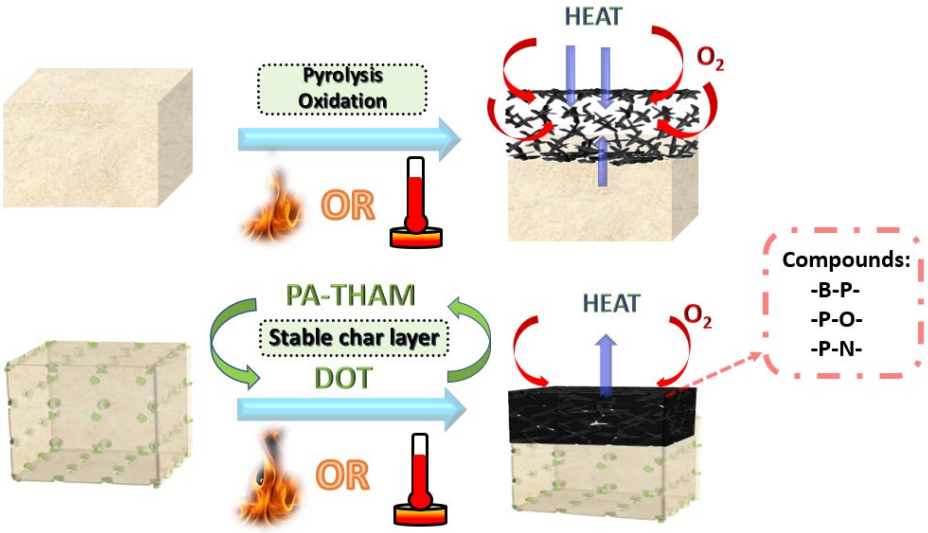

Fig. 5-8 Scheme diagram of proposed flame-retardant mechanism

5.4 Conclusion

In consequence, the combination of PA-THAM and DOT was introduced into corn-pith thermal insulation material, and the fire resistance was improved significantly due to the synergistic effect from these two additives.

Among the formulations with flame retardants, the addition of 8 wt% mixture of PA-THAM and DOT in thermal insulation particleboard PB2 exhibited much better flame-retardant properties than the one without additives. In the premise of little change in thermal conductivity and increased thermal stability, the initial smouldering temperature rose from 280 °C to 350 °C with a much reduction of propagation speed; the char residue increased in cone calorimeter test with decreased value by 25.5%, 22.7% and 68.2% for PHRR, THR, and TSP, respectively. With respect to the 15 wt% content of combined flame retardants, PB3 only showed a little enhancement in general properties compared with PB2.

On account of low toxic reproduction and general properties, this green particleboard with 8 wt% mixture of PA-THAM and DOT can be an optimum formulation to be used as thermal insulation material.

CHAPTER 6

Conclusion and future work

6.1 Conclusion

This study developed bio-based materials with improved flame-retardant properties and the corresponding flame-retardant mechanisms were investigated simultaneously. Some bio-based substances were chosen as the raw materials, for example PLA as the matrix, corn-pith cellulose as the natural fiber, sodium alginate as the binder, phytic acid as one reactant to synthesize novel flame retardant (PA-THAM), and other eco-friendly compounds as the contrastive additives. After a series of systematical investigations, this PA-THAM can be combined with other additives to improve the fire resistance of bio-based materials by some physical actions, and the primary conclusions are summarized into the following parts.

6.1.1 PLA/PA-THAM biocomposites: Structure-properties relationship

As raw materials, phytic acid derived from many plant tissues and trometamol known as buffers in medical use were chosen to synthesize the novel bio-based flame retardant (PA-THAM), the chemical structure of which was determined by some characterizations. As a comparative small molecule, the incorporation of small amount of PA-THAM into PLA caused a two-phases structure with discrete PA-THAM and continuous PLA, and the incompatibility in this binary system led to a reduction of molten viscosity as well as an optimum loading for maintaining mechanical properties. In contrast to neat PLA, biocomposite with 3 wt% content of PA-THAM exhibited 90% less complex viscosity and little change in mechanical properties.

Besides, although the introduction of 3 wt% PA-THAM did not improve the charring ability of PLA in thermal degradation, an increased ignition-resistance was observed during the combustion tests, such as an increased value 25.8% for LOI, V-0 rating with self-extinguish ability for UL-94, and postponed ignition time by 10s. This enhancement in flammability was owing to a combination of physical properties including "heat transfer" effect, slight dilution and barrier action in condensed phase. Therefore, as a multifunctional additive, an optimum loading level of PA-THAM can act as both synergist and lubricant to achieve a good balance of mechanical properties and fire resistance, as well as a decreased processing temperature for PLA-based biocomposite system.

6.1.2 PLA/OCC/PA-THAM biocomposites: Improvement of flame retardancy

As a bio-based functional additive, PA-THAM was proposed to improve the thermal stability and flame-retardant properties of natural reinforced plastic biocomposite. After pretreating OCC with PA-THAM via in-situ modification, the biocomposite illustrated a better thermal stability and flame retardancy than the control sample without additive. Especially for the formulation with the content of 5 phr PA-THAM, not only the degradation temperature increased by 50 °C, but also fire resistance improved with a 25.2% LOI value and a reduction of PHRR by 21.3%. This was attributed to a synergistic effect between PA-THAM and OCC, which catalyzed to form a good protective layer to prevent further degradation.

However, this obstructing protection in condensed phase endowed the formulation with 7 phr addition of PA-THAM with slight change in flame-retardant performances and decreased mechanical properties. Consequently, the combination of OCC and PA-THAM

can give PLA-based biocomposite good fire resistance, thermal stability, and acceptable other properties at an optimum loading level.

6.1.3 CC/AG/FR biocomposites: Ecological thermal insulation material

PA-THAM and DOT, existed as a mixture, were proportionally introduced into corn-pith alginate thermal insulation materials, which presented an excellent improvement in both smouldering and flame combustion performances. Compared with the reference sample without flame retardant, in consequence of the mixture with 6 wt% PA-THAM and 2 wt% DOT, this thermal insulation material demonstrated an increase in the initial smouldering temperature from 280 °C to 350 °C with a lower propagation speed of smouldering front, and better improvement in CCT with a reduction by 25.5%, 22.7% and 68.2% for PHRR, THR, and TSP, respectively. A formation of good quality of charring layer due to a synergistic effect from flame retardants can account for this significant enhancement in fire behaviours.

Additionally, the thermal stability increased as well, while thermal conductivity maintained the same level, which can satisfy the requirement of thermal insulation application. However, further 15 wt% loading of this mixed flame-retardant system only led to a little enhancement in the general properties. In consideration of the toxic reproduction and general properties, this thermal insulation material with combination of 8 wt% mixture of PA-THAM and DOT can be used as a good flame-retardant thermal insulation material.

In conclusion, this novel bio-based flame retardant (PA-THAM) can be used as synergist for fire-safety material systems. The predominant flame-retardant mechanism for these biocomposite systems can be elucidated by condensed-phase actions, which was mainly comprised of physical properties, such as increased “heat transfer” rate to improve

ignition-resistance, and good charring layer to obstruct the heat and oxygen during the whole combustion processing. Moreover, a good balance between fire resistance and other properties of these flame-retardant materials can achieve at optimum loadings.

6.2 Future work

On the basis of the results as above, the future work is to design and prepare a bio-based flame retardant material with sandwich structure (listed in Fig. 6-1), which is proposed as a substitute to be applied in construction field, such as building cladding and roof slabs [259–262], by using the PLA/OCC/FR as face-sheet part and CC/AG/FR as foam-core part. Three issues need to be investigated for further research.

6.2.1 Selection of adhesive

As sandwich structure material, adhesive plays an important and difficult role to meet the application requirements [263]. In order to achieve good properties, the adhesive should have a good compatibility with PLA and corn-pith cellulose, which can form an adequate joining between face-sheet and foam-core materials. In terms of the thermal insulation and flame-retardant properties, the thermal performances of the adhesive need to be analyzed, which should not result in a negative effect on thermal conductivity and decrease the thermal stability on the sandwich-structure material. The panel PLA/OCC/FR started to decompose around 280 °C and the core CC/AG/FR exhibited degradation behavior at 305 °C, therefore, the initial degradation temperature of the interfacial material should not be lower than 280 °C, which could lead to a premature degradation of bio-based material with sandwich structure [264].

6.2.2 Manufacturing processing

It is well known that the final performance of sandwich composite depends on the conditions' control during production process, which is correlative with the failure modes [265]. In this case, the bio-based composite would be proposed to fabricate by layup process with less forming pressure at a moderate temperature. Besides, some factor should be considered for designing mold, such as mold material, surface roughness, and mold release, which also impact the final performance of sandwich composite.

6.2.3 Study of related properties

In consideration of flame-retardant properties, although the flammability of both face-sheet and foam-core materials were studied in this work, it is not sufficient to guarantee the improvement in fire resistance for bio-based composite with sandwich structure. This is because there is some difference of thermal degradation between each part and integrated sandwich structure, as well as the adhesive would also illustrate extra combustion products. Consequently, the flame retardancy of sandwich material should be investigate in detail by some measurements, such as TGA, CCT/FTIR, smouldering, CCT, UL-94. With regard to the mechanical properties, tensile properties, bending stiffness, compressive strength, and impact loading would be analyzed; meanwhile the failure behavior would be investigated as well. Furthermore, other parameters should also be investigated, such as thermal conductivity, hygroscopic properties, and environmental impact, should also be analyzed due to incorporation of adhesive and new structure.

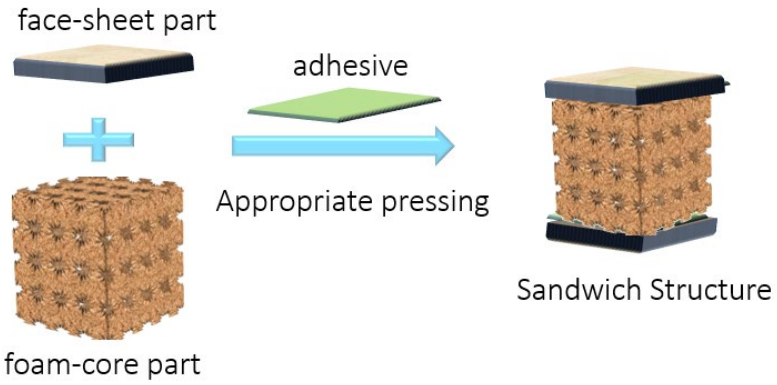

Fig. 6-1 Scheme of bio-based flame-retardant material with sandwich structure

Publications and conferences

1) Journal papers

Yunxian Yang, Laia Hauriea, Jianheng Wen, Shuidong Zhang, Arthur Ollivier, De-Yi Wang. Effect of oxidized wood flour as functional filler on the mechanical, thermal and flame-retardant properties of polylactide biocomposites. ***Industrial Crops & Products***, 2019 (130): 301–309.

Zhi-Qi Liu, Zhi Li, **Yun-Xian Yang**, Yan-Ling Zhang, Xin Wen, Na Li, Can Fu, Rong-Kun Jian, Li-Juan Li and De-Yi Wang. A Geometry Effect of Carbon Nanomaterials on Flame Retardancy and Mechanical Properties of Ethylene-Vinyl Acetate/Magnesium Hydroxide Composites. **Polymers**, 2018 (10): 1028(1-14).

Yunxian Yang, Laia Haurie, Jing Zhang, Xiu-Qin Zhang, De-Yi Wang. Effect of novel bio-based flame retardant on the properties of polylactide (PLA) (Submitted)

Yunxian Yang, De-Yi Wang, Zhiqi Liu, Ana Maria Lacasta, Laia Haurie. A green thermal insulation material with improved smoldering and flaming combustion properties. (Submitted)

Zhang, Jing; Li, Zhi; Zhang, Lu; **Yang, Yunxian**; Wang, De-Yi. Green Synthesis of Biomass Phytic Acid Functionalized UiO66-NH_2 Hierarchical Hybrids Towards Fire safety of Epoxy Resin. (Submitted)

Yunxian Yang, Laia Haurie, De-Yi Wang, Lu Zhang. Combination of corn pith fiber and bio-based flame retardant: effect of an in-situ modification method on the mechanical, thermal properties and flame retardancy of polylactide biocomposite. (To be submitted)

2) Conferences proceedings

Yunxian Yang, Laia Haurie, De-Yi Wang. Bio-based polymer composites. In: Congreso sobre Construcción con Madera y otros Materiales Lignocelulósicos (LIGNOMAD17). ***Poster communication***, Barcelona, Spain: 29/06/17 – 01/07/17.

Yunxian Yang, Laia Haurie, De-Yi Wang. Bio-based composites with good mechanical properties and flame retardancy. In: 2nd Asia-Oceania Symposium for Fire Safety Materials Science and Engineering (AOFSM 2017). ***Oral communication***, Shenzhen, China: 27-29 Oct. 2017

Yunxian Yang, Laia Haurie, De-Yi Wang. Effect of oxidized wood flour as carbonization agent on the flame-retardant properties of polylactide. In: 5th Multi-Functional Materials and Structures (MFMS 2018). ***Poster communication***, Shenyang, China: 10-13 Jun. 2018

Yunxian Yang, Laia Haurie, De-Yi Wang, Ana M Lacasta. Use of a bio-based flame retardant for lignocellulosic insulation boards. In: 6th EPNOE International Polysaccharide Conference (EPNOE 2019). ***Oral communication***, Aveiro, Portugal: 22-25 Oct. 2019.

Reference

[1] M. Yılmaz, A. Bakış, Sustainability in Construction Sector, Procedia - Soc. Behav. Sci. 195 (2015) 2253–2262. doi:10.1016/j.sbspro.2015.06.312.

[2] R.K. Singh, H.R. Murty, S.K. Gupta, A.K. Dikshit, An overview of sustainability assessment methodologies, Ecol. Indic. 15 (2012) 281–299. doi:10.1016/j.ecolind.2011.01.007.

[3] E. Ostrom, A General Framework for Analyzing Sustainability of Social-Ecological Systems, Science (80-.). 325 (2009) 419–422. doi:10.1126/science.1172133.

[4] A. Kylili, P.A. Fokaides, Policy trends for the sustainability assessment of construction materials: A review, Sustain. Cities Soc. 35 (2017) 280–288. doi:10.1016/j.scs.2017.08.013.

[5] Y. Zhong, P. Wu, Economic sustainability, environmental sustainability and constructability indicators related to concrete- and steel-projects, J. Clean. Prod. 108 (2015) 748–756. doi:10.1016/j.jclepro.2015.05.095.

[6] A. Windapo, O. Ogunsanmi, Construction sector views of sustainable building materials, Proc. Inst. Civ. Eng. - Eng. Sustain. 167 (2014) 64–75. doi:10.1680/ensu.13.00011.

[7] D. Jones, Introduction to the performance of bio-based building materials, in: Perform. Bio-Based Build. Mater., Elsevier Ltd., 2017: pp. 1–19. doi:10.1016/B978-0-08-100982-6.00001-X.

[8] T. Väisänen, O. Das, L. Tomppo, A review on new bio-based constituents for natural fiber-polymer composites, J. Clean. Prod. 149 (2017) 582–596. doi:10.1016/j.jclepro.2017.02.132.

[9] J.K. Pandey, S.H. Ahn, C.S. Lee, A.K. Mohanty, M. Misra, Recent advances in the application of natural fiber based composites, Macromol. Mater. Eng. 295 (2010) 975–989. doi:10.1002/mame.201000095.

[10] K.P. Ashik, R.S. Sharma, A Review on Mechanical Properties of Natural Fiber Reinforced Hybrid Polymer Composites, J. Miner. Mater. Charact. Eng. 03 (2015) 420–426. doi:10.4236/jmmce.2015.35044.

[11] C. Elanchezhian, B.V. Ramnath, G. Ramakrishnan, Review on mechanical properties of natural fiber composites., in: Mater. Today Proc., Elsevier Ltd, 2018: pp. 1785–1790. doi:10.1016/j.matpr.2017.11.276.

[12] M.R. Sanjay, G.R. Arpitha, B. Yogesha, Study on Mechanical Properties of Natural - Glass Fibre Reinforced Polymer Hybrid Composites: A Review, in: Mater. Today Proc., Elsevier Ltd., 2015: pp. 2959–2967. doi:10.1016/j.matpr.2015.07.264.

[13] K.M. Zia, A. Noreen, M. Zuber, S. Tabasum, M. Mujahid, Recent developments and future prospects on bio-based polyesters derived from renewable resources: A review, Int. J. Biol. Macromol. (2015). doi:10.1016/j.ijbiomac.2015.10.040.

[14] A. Hiroe, K. Ushimaru, T. Tsuge, Characterization of polyhydroxyalkanoate (PHA) synthase derived from Delftia acidovorans DS-17 and the influence of PHA production in Escherichia coli, J. Biosci. Bioeng. 115 (2013) 633–638. doi:10.1016/j.jbiosc.2012.12.015.

[15] C. Yang, W. Zhang, R. Liu, C. Zhang, T. Gong, Q. Li, S. Wang, C. Song, Analysis of polyhydroxyalkanoate (PHA) synthase gene and PHA-producing bacteria in activated sludge that produces PHA containing 3-hydroxydodecanoate, FEMS Microbiol. Lett. 346 (2013) 56–64. doi:10.1111/1574-6968.12201.

[16] Q. Chen, C. Zhu, G.A. Thouas, Progress and challenges in biomaterials used for

bone tissue engineering: bioactive glasses and elastomeric composites, Prog. Biomater. 1 (2012) 1–22. doi:10.1186/2194-0517-1-2.

[17] D.Y. Zhang, P. Liu, C.F. Ouyoung, Q. Gao, K.S. Zheng, H.F. Hu, Z.J. Li, Influence of PNA012 on Crystallization and Mechanical Properties of Polybutylene Terephthalate, Adv. Mater. Res. 624 (2012) 264–268. doi:10.4028/www.scientific.net/amr.624.264.

[18] D.E. Della-Giustina, Fire Safety Management Handbook, 2014. doi:10.1201/b16480.

[19] and Y.O. William D. Walton, Philip H. Thomas, Estimating Temperatures in Compartment Fires Handbook, 2016. doi:10.1007/978-1-4939-2565-0_30.

[20] L. W.McKeen, Plastics Used in Medical Devices Handbook, Elsevier Inc., 2014. doi:10.1016/B978-0-323-22805-3.00003-7.

[21] Ingeo TM Biopolymer 4043D Technical Data Sheet, NatureWorks, USA. (n.d.) 1–3. doi:www.natureworksllc.com.

[22] V. Ivanov, V. Stabnikov, Construction Biotechnology Plastics, Springer Science & Business Media Singapor, 2017. doi:10.1007/978-981-10-1445-1.

[23] F. Asghari, M. Samiei, K. Adibkia, A. Akbarzadeh, S. Davaran, Biodegradable and biocompatible polymers for tissue engineering application: a review, Artif. Cells, Nanomedicine Biotechnol. 45 (2017) 185–192. doi:10.3109/21691401.2016.1146731.

[24] W. Serrano, A. Meléndez, I. Ramos, N.J. Pinto, Poly(lactic acid)/poly(3-hexylthiophene) composite nanofiber fabrication for electronic applications, Polym. Int. 65 (2016) 503–507. doi:10.1002/pi.5081.

[25] A. Marra, C. Silvestre, D. Duraccio, S. Cimmino, Polylactic acid/zinc oxide biocomposite films for food packaging application, Int. J. Biol. Macromol. 88

(2016) 254–262. doi:10.1016/j.ijbiomac.2016.03.039.

[26] N. Ploypetchara, P. Suppakul, D. Atong, C. Pechyen, Blend of polypropylene/poly(lactic acid) for medical packaging application: Physicochemical, thermal, mechanical, and barrier properties, in: Energy Procedia, Elsevier B.V., 2014: pp. 201–210. doi:10.1016/j.egypro.2014.07.150.

[27] T. Mukherjee, N. Kao, PLA Based Biopolymer Reinforced with Natural Fibre: A Review, J. Polym. Environ. 19 (2011) 714–725. doi:10.1007/s10924-011-0320-6.

[28] S. Chaitanya, I. Singh, Processing of PLA/sisal fiber biocomposites using direct- and extrusion-injection molding, Mater. Manuf. Process. 32 (2017) 468–474. doi:10.1080/10426914.2016.1198034.

[29] I. Spiridon, R.N. Darie, H. Kangas, Influence of fiber modifications on PLA/fiber composites. Behavior to accelerated weathering, Compos. Part B Eng. 92 (2016) 19–27. doi:10.1016/j.compositesb.2016.02.032.

[30] V. Mazzanti, R. Pariante, A. Bonanno, O. Ruiz de Ballesteros, F. Mollica, G. Filippone, Reinforcing mechanisms of natural fibers in green composites: Role of fibers morphology in a PLA/hemp model system, Compos. Sci. Technol. 180 (2019) 51–59. doi:10.1016/j.compscitech.2019.05.015.

[31] F. Asdrubali, F. D'Alessandro, S. Schiavoni, A review of unconventional sustainable building insulation materials, Sustain. Mater. Technol. 4 (2015) 1–17. doi:10.1016/j.susmat.2015.05.002.

[32] J. Vejeliene, A. Gailius, S. Vejelis, S. Vaitkus, G. Balčiunas, Evaluation of structure influence on thermal conductivity of thermal insulating materials from renewable resources, Mater. Sci. 17 (2011) 208–212. doi:10.5755/j01.ms.17.2.494.

[33] M. Palumbo, J. Avellaneda, A.M. Lacasta, Availability of crop by-products in Spain: New raw materials for natural thermal insulation, Resour. Conserv. Recycl.

99 (2015) 1–6. doi:10.1016/j.resconrec.2015.03.012.

[34] M. Palumbo Fernández, Contribution to the development of new bio-based thermal insulation materials made from vegetal pith and natural binders : hygrothermal performance, fire reaction and mould growth resistance, Thèse Dr. Univ. Politècnica Catalunya. 61–68 (2016) 187 pages.

[35] X. yan Zhou, F. Zheng, H. guan Li, C. long Lu, An environment-friendly thermal insulation material from cotton stalk fibers, Energy Build. 42 (2010) 1070–1074. doi:10.1016/j.enbuild.2010.01.020.

[36] K. Wei, C. Lv, M. Chen, X. Zhou, Z. Dai, D. Shen, Development and performance evaluation of a new thermal insulation material from rice straw using high frequency hot-pressing, Energy Build. 87 (2015) 116–122. doi:10.1016/j.enbuild.2014.11.026.

[37] M. Boonterm, S. Sunyadeth, S. Dedpakdee, P. Athichalinthorn, S. Patcharaphun, R. Mungkung, R. Techapiesancharoenkij, Characterization and comparison of cellulose fiber extraction from rice straw by chemical treatment and thermal steam explosion, J. Clean. Prod. 134 (2016) 592–599. doi:10.1016/j.jclepro.2015.09.084.

[38] S. Bourbigot, G. Fontaine, Flame retardancy of polylactide: An overview, Polym. Chem. 1 (2010) 1413–1422. doi:10.1039/c0py00106f.

[39] L. Chen, Y.Z. Wang, A review on flame retardant technology in China. Part I: Development of flame retardants, Polym. Adv. Technol. 21 (2010) 1–26. doi:10.1002/pat.1550.

[40] G.E. ZAIKOV, Ecological Aspects of Polymer Flame Retardancy, 1999. doi:10.1201/b11960.

[41] J.T. Yeh, S.H. Hsieh, Y.C. Cheng, M.J. Yang, K.N. Chen, Combustion and smoke emission properties of poly(ethylene terephthalate) filled with phosphorous and

metallic oxides, Polym. Degrad. Stab. 61 (1998) 399–407. doi:10.1016/S0141-3910(97)00225-5.

[42] S. Bourbigot, M. Le Bras, R. Leeuwendal, K.K. Shen, D. Schubert, Recent advances in the use of zinc borates in flame retardancy of EVA, Polym. Degrad. Stab. 64 (1999) 419–425. doi:10.1016/S0141-3910(98)00130-X.

[43] B.K. Kandola, A.R. Horrocks, D. Price, G. V. Coleman, Flame-Retardant Treatments of Cellulose and Their Influence on the Mechanism of Cellulose Pyrolysis, 1996. doi:10.1080/15321799608014859.

[44] J. Green, A review of phosphorus-containing flame retardants, J. Fire Sci. 10 (1992) 470–487. doi:10.1177/073490419201000602.

[45] L.A. Savas, T.K. Deniz, U. Tayfun, M. Dogan, Effect of microcapsulated red phosphorus on flame retardant, thermal and mechanical properties of thermoplastic polyurethane composites filled with huntite&hydromagnesite mineral, Polym. Degrad. Stab. 135 (2017) 121–129. doi:10.1016/j.polymdegradstab.2016.12.001.

[46] J. Pallmann, Y.L. Ren, B. Mahltig, T.G. Huo, Phosphorylated sodium alginate/APP/DPER intumescent flame retardant used for polypropylene, J. Appl. Polym. Sci. 136 (2019) 1–10. doi:10.1002/app.47794.

[47] I. van der Veen, J. de Boer, Phosphorus flame retardants: Properties, production, environmental occurrence, toxicity and analysis, Chemosphere. 88 (2012) 1119–1153. doi:10.1016/j.chemosphere.2012.03.067.

[48] D. Goedderz, L. Weber, D. Markert, A. Schießer, C. Fasel, R. Riedel, V. Altstädt, C. Bethke, O. Fuhr, F. Puchtler, J. Breu, M. Döring, Flame retardant polyester by combination of organophosphorus compounds and an NOR radical forming agent, J. Appl. Polym. Sci. 47876 (2019) 1–11. doi:10.1002/app.47876.

[49] J.P. Malval, F. Morlet-Savary, X. Allonas, J.P. Fouassier, S. Suzuki, S. Takahara,

T. Yamaoka, On the cleavage process of the N-trifluoromethylsulfonyloxy-1,8-naphthalimide photoacid generator, Chem. Phys. Lett. 443 (2007) 323–327. doi:10.1016/j.cplett.2007.06.082.

[50] S. Jin, L. Qian, Y. Qiu, Y. Chen, F. Xin, High-efficiency flame retardant behavior of bi-DOPO compound with hydroxyl group on epoxy resin, Polym. Degrad. Stab. 166 (2019) 344–352. doi:10.1016/j.polymdegradstab.2019.06.024.

[51] H. Horacek, R. Grabner, Advantages of flame retardants based on nitrogen compounds, Polym. Degrad. Stab. 54 (1996) 205–215. doi:10.1016/S0141-3910(96)00045-6.

[52] F. Laoutid, L. Bonnaud, M. Alexandre, J.M. Lopez-Cuesta, P. Dubois, New prospects in flame retardant polymer materials: from fundamentals to nanocomposites, Mater. Sci. Eng. R Reports. 63 (2009) 100–125. doi:10.1016/j.mser.2008.09.002.

[53] Shui-Yu Lu, Recent developments in the chemistry of halogen-free flame retardant polymers, Prog. Polym. Sci. 27 (2002) 1661–1712. doi:10.1016/S0079-6700(02)00018-7.

[54] S.M.L. and G.E. Zaikov, Ecological Aspects of Polymer Flame Retardancy, 1999.

[55] M.A. and R.F. A.De Chirico, Q.Audisio*, F.Provasoli, Flame retardant polymeric additives for polyolefines. Different role of phosphoric and boric acids as FR agents in their reacton products with triglycidyl isocyanurate, Makrqmol. Chem., Macromol. Symp. 348 (1993) 343–348.

[56] B. Tawiah, B. Yu, R.K.K. Yuen, Y. Hu, R. Wei, J.H. Xin, B. Fei, Highly efficient flame retardant and smoke suppression mechanism of boron modified graphene Oxide/Poly(Lactic acid)nanocomposites, Carbon N. Y. 150 (2019) 8–20. doi:10.1016/j.carbon.2019.05.002.

[57] S. Huo, J. Wang, S. Yang, J. Wang, B. Zhang, B. Zhang, X. Chen, Y. Tang, Synthesis of a novel phosphorus-nitrogen type flame retardant composed of maleimide, triazine-trione, and phosphaphenanthrene and its flame retardant effect on epoxy resin, Polym. Degrad. Stab. 131 (2016) 106–113. doi:10.1016/j.polymdegradstab.2016.07.013.

[58] Y.Y. Gao, C. Deng, Y.Y. Du, S.C. Huang, Y.Z. Wang, A novel bio-based flame retardant for polypropylene from phytic acid, Polym. Degrad. Stab. 161 (2019) 298–308. doi:10.1016/j.polymdegradstab.2019.02.005.

[59] F. Laoutid, H. Vahabi, M. Shabanian, F. Aryanasab, P. Zarrintaj, M.R. Saeb, A new direction in design of bio-based flame retardants for poly(lactic acid), Fire Mater. 42 (2018) 914–924. doi:10.1002/fam.2646.

[60] L. Liu, G. Huang, P. Song, Y. Yu, S. Fu, Converting industrial alkali lignin to biobased functional additives for improving fire behavior and smoke suppression of polybutylene succinate, ACS Sustain. Chem. Eng. 4 (2016) 4732–4742. doi:10.1021/acssuschemeng.6b00955.

[61] L. Passauer, Thermal characterization of ammonium starch phosphate carbamates for potential applications as bio-based flame-retardants, Carbohydr. Polym. 211 (2019) 69–74. doi:10.1016/j.carbpol.2019.01.100.

[62] X.W. Cheng, J.P. Guan, R.C. Tang, K.Q. Liu, Phytic acid as a bio-based phosphorus flame retardant for poly(lactic acid) nonwoven fabric, J. Clean. Prod. 124 (2016) 114–119. doi:10.1016/j.jclepro.2016.02.113.

[63] R. Ménard, C. Negrell, M. Fache, L. Ferry, R. Sonnier, G. David, From a bio-based phosphorus-containing epoxy monomer to fully bio-based flame-retardant thermosets, RSC Adv. 5 (2015) 70856–70867. doi:10.1039/c5ra12859e.

[64] L. Passauer, Thermal characterization of ammonium starch phosphate carbamates

for potential applications as bio-based flame-retardants, Carbohydr. Polym. 211 (2019) 69–74. doi:10.1016/j.carbpol.2019.01.100.

[65] A. Twarowski, The influence of phosphorus oxides and acids on the rate of H + OH recombination, Combust. Flame. 94 (1993) 91–107. doi:10.1016/0010-2180(93)90022-U.

[66] T.M. Jayaweera, C.F. Melius, W.J. Pitz, C.K. Westbrook, O.P. Korobeinichev, V.M. Shvartsberg, A.G. Shmakov, I. V. Rybitskaya, H.J. Curran, Flame inhibition by phosphorus-containing compounds over a range of equivalence ratios, Combust. Flame. 140 (2005) 103–115. doi:10.1016/j.combustflame.2004.11.001.

[67] B. Scharte, Phosphorus-based flame retardancy mechanisms-old hat or a starting point for future development?, Materials (Basel). 3 (2010) 4710–4745. doi:10.3390/ma3104710.

[68] K.A. Salmeia, J. Fage, S. Liang, S. Gaan, An overview of mode of action and analytical methods for evaluation of gas phase activities of flame retardants, Polymers (Basel). 7 (2015) 504–526. doi:10.3390/polym7030504.

[69] M.I.J.B.A.C.M. NELSON†, Ignition properties of thermally thin plastics: The effectiveness of non-competitive char formation in reducing flammability, J. Appl. Math. Decis. Sci. 6 (2002) 155–181. doi:10.1155/S117391260200010X.

[70] and E.C. G. CAMINO,* L. COSTA, The oxygen index method in fire retardance studies of polymeric materials, J. Appl. Polym. Sci. 35 (1988) 1863–1876. doi:10.1002/app.1988.070350712.

[71] C.E. Anderson, D.E. Ketchum, W.P. Mountain, Thermal Conductivity of Intumescent Chars, J. Fire Sci. 6 (1988) 390–410. doi:10.1177/073490418800600602.

[72] I.T. Review, T. Kashiwagi, Polymer combustion and flammability-role of the

condensed phase, Rev. Lit. Arts Am. (1994) 1423–1437.

[73] E. Schmitt, Phosphorus-based flame retardants for thermoplastics, Plast. Addit. Compd. 9 (2007) 26–30. doi:10.1016/S1464-391X(07)70067-3.

[74] W. Guo, X. Wang, C.S.R. Gangireddy, J. Wang, Y. Pan, W. Xing, L. Song, Y. Hu, Cardanol derived benzoxazine in combination with boron-doped graphene toward simultaneously improved toughening and flame retardant epoxy composites, Compos. Part A Appl. Sci. Manuf. 116 (2019) 13–23. doi:10.1016/j.compositesa.2018.10.010.

[75] M.M. Velencoso, A. Battig, J.C. Markwart, B. Schartel, F.R. Wurm, Molecular Firefighting—How Modern Phosphorus Chemistry Can Help Solve the Challenge of Flame Retardancy, Angew. Chemie - Int. Ed. 57 (2018) 10450–10467. doi:10.1002/anie.201711735.

[76] Y.Q. Shi, T. Fu, Y.J. Xu, D.F. Li, X.L. Wang, Y.Z. Wang, Novel phosphorus-containing halogen-free ionic liquid toward fire safety epoxy resin with well-balanced comprehensive performance, Chem. Eng. J. 354 (2018) 208–219. doi:10.1016/j.cej.2018.08.023.

[77] E. Mikkola, Charring of wood based materials, Fire Saf. Sci. Proc. Third Int. Symp. (2006) 547–556. doi:10.4324/9780203973493.

[78] K.A. Salmeia, J. Fage, S. Liang, S. Gaan, An overview of mode of action and analytical methods for evaluation of gas phase activities of flame retardants, Polymers (Basel). 7 (2015) 504–526. doi:10.3390/polym7030504.

[79] S. Bourbigot, S. Duquesne, Fire retardant polymers: Recent developments and opportunities, J. Mater. Chem. 17 (2007) 2283–2300. doi:10.1039/b702511d.

[80] P. Jiang, S. Zhang, S. Bourbigot, Z. Chen, S. Duquesne, M. Casetta, Surface grafting of sepiolite with a phosphaphenanthrene derivative and its flame-retardant

mechanism on PLA nanocomposites, Polym. Degrad. Stab. 165 (2019) 68–79. doi:10.1016/j.polymdegradstab.2019.04.012.

[81] Boday et al., Flame-retardant polylactic acid (PLA) by grafting through of phosphorus-containing polymers directly to PLA backbone, United States Patent, US 9,187,597 B1. 11 (2015).

[82] C. Feng, M. Liang, Y. Zhang, J. Jiang, J. Huang, H. Liu, Synergistic effect of lanthanum oxide on the flame retardant properties and mechanism of an intumescent flame retardant PLA composites, J. Anal. Appl. Pyrolysis. 122 (2016) 241–248. doi:10.1016/j.jaap.2016.09.018.

[83] P. Jiang, S. Zhang, S. Bourbigot, Z. Chen, S. Duquesne, M. Casetta, Surface grafting of sepiolite with a phosphaphenanthrene derivative and its flame-retardant mechanism on PLA nanocomposites, Polym. Degrad. Stab. 165 (2019) 68–79. doi:10.1016/j.polymdegradstab.2019.04.012.

[84] T.J. Ohlemiller, Modeling of smoldering combustion propagation, Prog. Energy Combust. Sci. 11 (1985) 277–310. doi:10.1016/0360-1285(85)90004-8.

[85] G. Rein, Smouldering Combustion Phenomena in Science and Technology, Int. Rev. Chem. Eng. 1 (2009) 3–18. doi:hdl.handle.net/1842/2678.

[86] M.J. Hurley, D. Gottuk, J.R. Hall, K. Harada, E. Kuligowski, M. Puchovsky, J. Torero, Jj.M. Watts, C. Wieczorek, Smoldering combustion, Soc. Fire Prot. Eng. (2016) 581–603. doi:10.1007/978-1-4939-2565-0.

[87] X. Huang, G. Rein, Smouldering combustion of peat in wildfires: Inverse modelling of the drying and the thermal and oxidative decomposition kinetics, Combust. Flame. 161 (2014) 1633–1644. doi:10.1016/j.combustflame.2013.12.013.

[88] T. Kashiwagi, H. Nambu, Global kinetic constants for thermal oxidative

degradation of a cellulosic paper, Combust. Flame. 88 (1992) 345–368. doi:10.1016/0010-2180(92)90039-R.

[89] X. Huang, G. Rein, Smouldering combustion of peat in wildfires: Inverse modelling of the drying and the thermal and oxidative decomposition kinetics, Combust. Flame. 161 (2014) 1633–1644. doi:10.1016/j.combustflame.2013.12.013.

[90] Á. Ramírez, J. García-Torrent, A. Tascón, Experimental determination of self-heating and self-ignition risks associated with the dusts of agricultural materials commonly stored in silos, J. Hazard. Mater. 175 (2010) 920–927. doi:10.1016/j.jhazmat.2009.10.096.

[91] R.M. Hadden, S. Scott, C. Lautenberger, C.C. Fernandez-Pello, Ignition of Combustible Fuel Beds by Hot Particles: An Experimental and Theoretical Study, Fire Technol. 47 (2011) 341–355. doi:10.1007/s10694-010-0181-x.

[92] R.A. Anthenien, A.C. Fernandez-Pello, A study of forward smolder ignition of polyurethane foam, Symp. Combust. 27 (1998) 2683–2690. doi:10.1016/S0082-0784(98)80124-0.

[93] R. Hadden, A. Alkatib, G. Rein, J.L. Torero, Radiant Ignition of Polyurethane Foam: The Effect of Sample Size, Fire Technol. 50 (2014) 673–691. doi:10.1007/s10694-012-0257-x.

[94] R. Hadden, G. Rein, Burning and Water Suppression of Smoldering Coal Fires in Small-Scale Laboratory Experiments, Elsevier B.V., 2011. doi:10.1016/B978-0-444-52858-2.00018-9.

[95] B.C. Hagen, V. Frette, G. Kleppe, B.J. Arntzen, Onset of smoldering in cotton: Effects of density, Fire Saf. J. 46 (2011) 73–80. doi:10.1016/j.firesaf.2010.09.001.

[96] B.C. Hagen, V. Frette, G. Kleppe, B.J. Arntzen, Effects of heat flux scenarios on

smoldering in cotton, Fire Saf. J. 61 (2013) 144–159. doi:10.1016/j.firesaf.2013.08.001.

[97] M. Palumbo, A.M. Lacasta, A. Navarro, M.P. Giraldo, B. Lesar, 07-29-Improvement of fire reaction and mould growth resistance of a new bio-based thermal insulation material, Constr. Build. Mater. 139 (2017) 531–539. doi:10.1016/j.conbuildmat.2016.11.020.

[98] R.F. Simmons, H.G. Wolfhard, Some limiting oxygen concentrations for diffusion flames in air diluted with nitrogen, Combust. Flame. 1 (1957) 155–161. doi:10.1016/0010-2180(57)90042-1.

[99] R.E. Lyon, R.N. Walters, Pyrolysis combustion flow calorimetry, J. Anal. Appl. Pyrolysis. 71 (2004) 27–46. doi:10.1016/S0165-2370(03)00096-2.

[100] L. Costes, F. Laoutid, S. Brohez, P. Dubois, Bio-based flame retardants: When nature meets fire protection, Mater. Sci. Eng. R Reports. 117 (2017) 1–25. doi:10.1016/j.mser.2017.04.001.

[101] J. Lindholm, A. Brink, M. Hupa, Cone calorimeter - a tool for measuring heat release rate, Finnish-Swedish Flame Days 2009. (2009) 4B. doi:10.1002/fam.

[102] A. Buczko, T. Stelzig, L. Bommer, D. Rentsch, M. Heneczkowski, S. Gaan, Bridged DOPO derivatives as flame retardants for PA6, Polym. Degrad. Stab. 107 (2014) 158–165. doi:10.1016/j.polymdegradstab.2014.05.017.

[103] S. Gaan, S. Liang, H. Mispreuve, H. Perler, R. Naescher, M. Neisius, Flame retardant flexible polyurethane foams from novel DOPO-phosphonamidate additives, Polym. Degrad. Stab. 113 (2015) 180–188. doi:10.1016/j.polymdegradstab.2015.01.007.

[104] E.D. Weil, S. V. Levchik, M. Ravey, W. Zhu, A survey of recent progress in phosphorus-based flame retardants and some mode of action studies, Phosphorus,

Sulfur Silicon Relat. Elem. 144–146 (1999) 17–20. doi:10.1080/10426509908546171.

[105] G. Woodward, C. Harris, J. Manku, Design of new organophosphorus flame retardants, Phosphorus, Sulfur Silicon Relat. Elem. 144–146 (1999) 25–28. doi:10.1080/10426509908546173.

[106] J. Green, A Phosphorus-Bromine Flame Retardant for Engineering Thermoplastics - A Review, J. Fire Sci. 12 (1994) 388–408. doi:10.1177/073490419401200404.

[107] S. V. Levchik, E.D. Weil, Developments in phosphorus flame retardants, Adv. Fire Retard. Mater. (2008) 41–66. doi:10.1533/9781845694701.1.41.

[108] C. Wang, Y. Wu, Y. Li, Q. Shao, X. Yan, C. Han, Z. Wang, Z. Liu, Z. Guo, Flame-retardant rigid polyurethane foam with a phosphorus-nitrogen single intumescent flame retardant, Polym. Adv. Technol. 29 (2018) 668–676. doi:10.1002/pat.4105.

[109] K.A. Salmeia, A. Gooneie, P. Simonetti, R. Nazir, J.P. Kaiser, A. Rippl, C. Hirsch, S. Lehner, P. Rupper, R. Hufenus, S. Gaan, Comprehensive study on flame retardant polyesters from phosphorus additives, Polym. Degrad. Stab. 155 (2018) 22–34. doi:10.1016/j.polymdegradstab.2018.07.006.

[110] S. Yang, Q. Zhang, Y. Hu, Synthesis of a novel flame retardant containing phosphorus, nitrogen and boron and its application in flame-retardant epoxy resin, Elsevier Ltd, 2016. doi:10.1016/j.polymdegradstab.2016.09.023.

[111] C. Feng, M. Liang, J. Jiang, J. Huang, H. Liu, Flame retardant properties and mechanism of an efficient intumescent flame retardant PLA composites, Polym. Adv. Technol. 27 (2016) 693–700. doi:10.1002/pat.3743.

[112] Y. Chen, W. Wang, Y. Qiu, L. Li, L. Qian, F. Xin, Terminal group effects of phosphazene-triazine bi-group flame retardant additives in flame retardant polylactic acid composites, Polym. Degrad. Stab. 140 (2017) 166–175.

doi:10.1016/j.polymdegradstab.2017.04.024.

[113] P. Ding, B. Kang, J. Zhang, J. Yang, N. Song, S. Tang, L. Shi, Phosphorus-containing flame retardant modified layered double hydroxides and their applications on polylactide film with good transparency, J. Colloid Interface Sci. 440 (2015) 46–52. doi:10.1016/j.jcis.2014.10.048.

[114] C.H. Ke, J. Li, K.Y. Fang, Q.L. Zhu, J. Zhu, Q. Yan, Y.Z. Wang, Synergistic effect between a novel hyperbranched charring agent and ammonium polyphosphate on the flame retardant and anti-dripping properties of polylactide, Polym. Degrad. Stab. 95 (2010) 763–770. doi:10.1016/j.polymdegradstab.2010.02.011.

[115] K. Tao, J. Li, L. Xu, X. Zhao, L. Xue, X. Fan, Q. Yan, A novel phosphazene cyclomatrix network polymer: Design, synthesis and application in flame retardant polylactide, Polym. Degrad. Stab. 96 (2011) 1248–1254. doi:10.1016/j.polymdegradstab.2011.04.011.

[116] J. Zhan, L. Song, S. Nie, Y. Hu, Combustion properties and thermal degradation behavior of polylactide with an effective intumescent flame retardant, Polym. Degrad. Stab. 94 (2009) 291–296. doi:10.1016/j.polymdegradstab.2008.12.015.

[117] L. Barrientos, J.J. Scott, P. Murthy, Specificity of Hydrolysis of Phytic Acid by Alkaline Phytase from Lily Pollen, Plant Physiol. 106 (1994) 1489–1495. doi:10.1104/pp.106.4.1489.

[118] D.F. Li, X. Zhao, Y.W. Jia, X.L. Wang, Y.Z. Wang, Tough and flame-retardant poly(lactic acid) composites prepared via reactive blending with biobased ammonium phytate and in situ formed crosslinked polyurethane, Compos. Commun. 8 (2018) 52–57. doi:10.1016/j.coco.2018.04.001.

[119] E.T. Champagne, M.S. Fisher, O. Hinojosa, NMR and ESR studies of interactions among divalent cations, phytic acid, and N-acetyl-amino acids, J. Inorg. Biochem.

38 (1990) 199–215. doi:10.1016/0162-0134(90)84013-F.

[120] F. Pan, X. Yang, D. Zhang, Chemical nature of phytic acid conversion coating on AZ61 magnesium alloy, Appl. Surf. Sci. 255 (2009) 8363–8371. doi:10.1016/j.apsusc.2009.05.089.

[121] Y. Boonsongrit, B.W. Mueller, A. Mitrevej, Characterization of drug-chitosan interaction by 1H NMR, FTIR and isothermal titration calorimetry, Eur. J. Pharm. Biopharm. 69 (2008) 388–395. doi:10.1016/j.ejpb.2007.11.008.

[122] Bedri Erdem, Robert A. Hunsicker, Gary W. Simmons, E. David Sudol, A. Victoria L. Dimonie, M.S. El-Aasser*, XPS and FTIR Surface Characterization of TiO2 Particles Used in Polymer Encapsulation, Langmuir. 17 (2001) 2664–2669. doi:10.1021/LA0015213.

[123] L. Costes, F. Laoutid, L. Dumazert, J.M. Lopez-Cuesta, S. Brohez, C. Delvosalle, P. Dubois, Metallic phytates as efficient bio-based phosphorous flame retardant additives for poly(lactic acid), Polym. Degrad. Stab. 119 (2015) 217–227. doi:10.1016/j.polymdegradstab.2015.05.014.

[124] W. Yang, B. Tawiah, C. Yu, Y.F. Qian, L.L. Wang, A.C.Y. Yuen, S.E. Zhu, E.Z. Hu, T.B.Y. Chen, B. Yu, H.D. Lu, G.H. Yeoh, X. Wang, L. Song, Y. Hu, Manufacturing, mechanical and flame retardant properties of poly(lactic acid) biocomposites based on calcium magnesium phytate and carbon nanotubes, Compos. Part A Appl. Sci. Manuf. 110 (2018) 227–236. doi:10.1016/j.compositesa.2018.04.027.

[125] R.L. Lehman, J.S. Gentry, N.G. Glumac, Thermal stability of potassium carbonate near its melting point 10.1016/S0040-6031(98)00289-5 : Thermochimica Acta | ScienceDirect.com, 316 (1998) 1–9. http://www.sciencedirect.com/science/article/pii/S0040603198002895.

[126] O. Martin, L. Avérous, Poly(lactic acid): Plasticization and properties of biodegradable multiphase systems, Polymer (Guildf). 42 (2001) 6209–6219. doi:10.1016/S0032-3861(01)00086-6.

[127] S. Spinella, G. Lo Re, B. Liu, J. Dorgan, Y. Habibi, P. Leclère, J.M. Raquez, P. Dubois, R.A. Gross, Polylactide/cellulose nanocrystal nanocomposites: Efficient routes for nanofiber modification and effects of nanofiber chemistry on PLA reinforcement, Polymer (Guildf). 65 (2015) 9–17. doi:10.1016/j.polymer.2015.02.048.

[128] E. Piorkowska, Z. Kulinski, A. Galeski, R. Masirek, Plasticization of semicrystalline poly(l-lactide) with poly(propylene glycol), Polymer (Guildf). 47 (2006) 7178–7188. doi:10.1016/j.polymer.2006.03.115.

[129] P. Müller, J. Bere, E. Fekete, J. Móczó, B. Nagy, M. Kállay, B. Gyarmati, B. Pukánszky, Interactions, structure and properties in PLA/plasticized starch blends, Polymer (Guildf). 103 (2016) 9–18. doi:10.1016/j.polymer.2016.09.031.

[130] D. Bagheriasl, P.J. Carreau, B. Riedl, C. Dubois, W.Y. Hamad, Shear rheology of polylactide (PLA)–cellulose nanocrystal (CNC) nanocomposites, Cellulose. 23 (2016) 1885–1897. doi:10.1007/s10570-016-0914-1.

[131] B. Marosföi, S. Matko, P.A.G. Marosi, Fire retarded polymer nanocomposites, Curr. Appl. Phys. 6 (2006) 259–261. doi:10.1016/j.cap.2005.07.052.

[132] B. Wittbrodt, J.M. Pearce, The effects of PLA color on material properties of 3-D printed components, Addit. Manuf. 8 (2015) 110–116. doi:10.1016/j.addma.2015.09.006.

[133] S.M. Lebedev, O.S. Gefle, E.T. Amitov, D.Y. Berchuk, D. V. Zhuravlev, Poly(lactic acid)-based polymer composites with high electric and thermal conductivity and their characterization, Polym. Test. 58 (2017) 241–248.

doi:10.1016/j.polymertesting.2016.12.033.

[134] L.G. Krauskopf, Plasticizer structure/performance relationships, J. Vinyl Technol. 15 (1993) 140–147. doi:10.1002/vnl.730150306.

[135] B. P. Shtarkman, I. N. Razinskaya Plasticization mechanism and structure of polymers, Acta Polym. 34 (1983) 514–520. doi:10.1002/actp.1983.010340812.

[136] C.D. Han, T.C. Yu, Rheological properties of molten polymers. II. Two-phase systems, J. Appl. Polym. Sci. 15 (1971) 1163–1180. doi:10.1002/app.1971.070150512.

[137] C.D. Han, T.C. Yu, Rheological behavior of two-phase polymer melts, Polym. Eng. Sci. 12 (1972) 81–90. doi:10.1002/pen.760120203.

[138] I. Spiridon, O.M. Paduraru, M.F. Zaltariov, R.N. Darie, Influence of keratin on polylactic acid/chitosan composite properties. behavior upon accelerated weathering, Ind. Eng. Chem. Res. 52 (2013) 9822–9833. doi:10.1021/ie400848t.

[139] R.N. Darie-Niţə, C. Vasile, A. Irimia, R. Lipşa, M. Râpə, Evaluation of some eco-friendly plasticizers for PLA films processing, J. Appl. Polym. Sci. 133 (2016) 1–11. doi:10.1002/app.43223.

[140] P. Anna, G. Marosi, S. Bourbigot, M. Le Bras, R. Delobel, Intumescent flame retardant systems of modified rheology, Polym. Degrad. Stab. 77 (2002) 243–247. doi:10.1016/S0141-3910(02)00040-X.

[141] K. Fukushima, D. Tabuani, G. Camino, Nanocomposites of PLA and PCL based on montmorillonite and sepiolite, Mater. Sci. Eng. 29 (2009) 1433–1441. doi:10.1016/j.msec.2008.11.005.

[142] F. De Santis, R. Pantani, G. Titomanlio, Nucleation and crystallization kinetics of poly(lactic acid), Thermochim. Acta. 522 (2011) 128–134. doi:10.1016/j.tca.2011.05.034.

[143] H. Zhou, T.B. Green, Y.L. Joo, The thermal effects on electrospinning of polylactic acid melts, Polymer (Guildf). 47 (2006) 7497–7505. doi:10.1016/j.polymer.2006.08.042.

[144] S. Saeidlou, M.A. Huneault, H. Li, C.B. Park, Poly(lactic acid) crystallization, Prog. Polym. Sci. 37 (2012) 1657–1677. doi:10.1016/j.progpolymsci.2012.07.005.

[145] Y. Lin, K.Y. Zhang, Z.M. Dong, L.S. Dong, Y.S. Li, Study of hydrogen-bonded blend of polylactide with biodegradable hyperbranched poly(ester amide), Macromolecules. 40 (2007) 6257–6267. doi:10.1021/ma070989a.

[146] M. Yasuniwa, K. Sakamo, Y. Ono, W. Kawahara, Melting behavior of poly(l-lactic acid): X-ray and DSC analyses of the melting process, Polymer (Guildf). 49 (2008) 1943–1951. doi:10.1016/j.polymer.2008.02.034.

[147] M.A. Abdelwahab, A. Flynn, B. Sen Chiou, S. Imam, W. Orts, E. Chiellini, Thermal, mechanical and morphological characterization of plasticized PLA-PHB blends, Polym. Degrad. Stab. 97 (2012) 1822–1828. doi:10.1016/j.polymdegradstab.2012.05.036.

[148] I. Pillin, N. Montrelay, Y. Grohens, Thermo-mechanical characterization of plasticized PLA: Is the miscibility the only significant factor?, Polymer (Guildf). 47 (2006) 4676–4682. doi:10.1016/j.polymer.2006.04.013.

[149] S. Li, H. Yuan, T. Yu, W. Yuan, J. Ren, Flame-retardancy and anti-dripping effects of intumescent flame retardant incorporating montmorillonite on poly (lactic acid), Polym. Adv. Technol. 20 (2009) 1114–1120. doi:10.1002/pat.1372.

[150] M.S. Kang, Y. Yang, S.S. Jee, S.J. Kwon, E.S. Lee, J.Y. Bae, Enhanced photovoltaic performances of dye-sensitized solar cell using self-charring phosphate ester surfactant, Mater. Chem. Phys. 130 (2011) 203–210. doi:10.1016/j.matchemphys.2011.06.026.

[151] H. Qin, S. Zhang, C. Zhao, G. Hu, M. Yang, Flame retardant mechanism of polymer/clay nanocomposites based on polypropylene, Polymer (Guildf). 46 (2005) 8386–8395. doi:10.1016/j.polymer.2005.07.019.

[152] M.I. Nelson, Ignition mechanisms of thermally thin thermoplastics in the cone calorimeter, Proc. R. Soc. A Math. Phys. Eng. Sci. 454 (1998) 789–814. doi:10.1098/rspa.1998.0186.

[153] M.I. Nelson, J. Brindley, A. McIntosh, Polymer ignition, Math. Comput. Model. 24 (1996) 39–46. doi:10.1016/0895-7177(96)00137-9.

[154] J.M. Pickard, Critical Ignition Temperature, Thermochim. Acta. 392–393 (2002) 37–40. doi:10.1016/s0040-6031(02)00068-0.

[155] S.W. Lee, S.D. Park, S. Kang, I.C. Bang, J.H. Kim, Investigation of viscosity and thermal conductivity of SiC nanofluids for heat transfer applications, Int. J. Heat Mass Transf. 54 (2011) 433–438. doi:10.1016/j.ijheatmasstransfer.2010.09.026.

[156] F.C. Lai, F.A. Kulacki, The effect of variable viscosity on convective heat transfer along a vertical surface in a saturated porous medium, Int. J. Heat Mass Transf. 33 (1990) 1028–1031. doi:10.1016/0017-9310(90)90084-8.

[157] H. Zou, C. Yi, L. Wang, H. Liu, W. Xu, Thermal degradation of poly(lactic acid) measured by thermogravimetry coupled to Fourier transform infrared spectroscopy, J. Therm. Anal. Calorim. 97 (2009) 929–935. doi:10.1007/s10973-009-0121-5.

[158] X. Zhao, F.R. Guerrero, J. Llorca, D.Y. Wang, New Superefficiently Flame-Retardant Bioplastic Poly(lactic acid): Flammability, Thermal Decomposition Behavior, and Tensile Properties, ACS Sustain. Chem. Eng. 4 (2016) 202–209. doi:10.1021/acssuschemeng.5b00980.

[159] H. Xiu, X. Qi, H. Bai, Q. Zhang, Q. Fu, Simultaneously improving toughness and UV-resistance of polylactide/titanium dioxide nanocomposites by adding

poly(ether)urethane, Polym. Degrad. Stab. 143 (2017) 136–144. doi:10.1016/j.polymdegradstab.2017.07.002.

[160] T. Paragkumar N, D. Edith, J.L. Six, Surface characteristics of PLA and PLGA films, Appl. Surf. Sci. 253 (2006) 2758–2764. doi:10.1016/j.apsusc.2006.05.047.

[161] F.D. Kopinke, M. Remmler, K. Mackenzie, M. Möder, O. Wachsen, Thermal decomposition of biodegradable polyesters - II. Poly(lactic acid), Polym. Degrad. Stab. 53 (1996) 329–342. doi:10.1016/0141-3910(96)00102-4.

[162] T. Väisänen, A. Haapala, R. Lappalainen, L. Tomppo, Utilization of agricultural and forest industry waste and residues in natural fiber-polymer composites: A review, Waste Manag. 54 (2016) 62–73. doi:10.1016/j.wasman.2016.04.037.

[163] M.R. Sanjay, P. Madhu, M. Jawaid, P. Senthamaraikannan, S. Senthil, S. Pradeep, Characterization and properties of natural fiber polymer composites: A comprehensive review, Elsevier B.V., 2018. doi:10.1016/j.jclepro.2017.10.101.

[164] K.L. Pickering, M.G.A. Efendy, T.M. Le, A review of recent developments in natural fibre composites and their mechanical performance, Compos. Part A Appl. Sci. Manuf. 83 (2016) 98–112. doi:10.1016/j.compositesa.2015.08.038.

[165] A.K. Bledzki, A. Jaszkiewicz, D. Scherzer, Mechanical properties of PLA composites with man-made cellulose and abaca fibres, Compos. Part A Appl. Sci. Manuf. 40 (2009) 404–412. doi:10.1016/j.compositesa.2009.01.002.

[166] V. Barbosa, E.C. Ramires, I.A.T. Razera, E. Frollini, Biobased composites from tannin-phenolic polymers reinforced with coir fibers, Ind. Crops Prod. 32 (2010) 305–312. doi:10.1016/j.indcrop.2010.05.007.

[167] N. Saba, M. Jawaid, O.Y. Alothman, M.T. Paridah, A review on dynamic mechanical properties of natural fibre reinforced polymer composites, Constr. Build. Mater. 106 (2016) 149–159. doi:10.1016/j.conbuildmat.2015.12.075.

[168] F. Momayez, K. Karimi, M.J. Taherzadeh, Energy recovery from industrial crop wastes by dry anaerobic digestion: A review, Ind. Crops Prod. 129 (2019) 673–687. doi:10.1016/j.indcrop.2018.12.051.

[169] M.R. Ahmad, B. Chen, S. Yousefi Oderji, M. Mohsan, Development of a new bio-composite for building insulation and structural purpose using corn stalk and magnesium phosphate cement, Energy Build. 173 (2018) 719–733. doi:10.1016/j.enbuild.2018.06.007.

[170] G. Guzel Kaya, E. Yilmaz, H. Deveci, Sustainable nanocomposites of epoxy and silica xerogel synthesized from corn stalk ash: Enhanced thermal and acoustic insulation performance, Compos. Part B Eng. 150 (2018) 1–6. doi:10.1016/j.compositesb.2018.05.039.

[171] O. Aksoɬan, H. Binici, E. Ortlek, Durability of concrete made by partial replacement of fine aggregate by colemanite and barite and cement by ashes of corn stalk, wheat straw and sunflower stalk ashes, Constr. Build. Mater. 106 (2016) 253–263. doi:10.1016/j.conbuildmat.2015.12.102.

[172] A. Awal, M. Rana, M. Sain, Thermorheological and mechanical properties of cellulose reinforced PLA bio-composites, Mech. Mater. 80 (2015) 87–95. doi:10.1016/j.mechmat.2014.09.009.

[173] S.A. Hinchcliffe, K.M. Hess, W. V. Srubar, Experimental and theoretical investigation of prestressed natural fiber-reinforced polylactic acid (PLA) composite materials, Compos. Part B Eng. 95 (2016) 346–354. doi:10.1016/j.compositesb.2016.03.089.

[174] W. Ding, D. Jahani, E. Chang, A. Alemdar, C.B. Park, M. Sain, Development of PLA/cellulosic fiber composite foams using injection molding: Crystallization and foaming behaviors, Compos. Part A Appl. Sci. Manuf. 83 (2016) 130–139.

doi:10.1016/j.compositesa.2015.10.003.

[175] L. Zhang, S. Chen, Y.T. Pan, S. Zhang, S. Nie, P. Wei, X. Zhang, R. Wang, D.Y. Wang, Nickel Metal-Organic Framework Derived Hierarchically Mesoporous Nickel Phosphate toward Smoke Suppression and Mechanical Enhancement of Intumescent Flame Retardant Wood Fiber/Poly(lactic acid) Composites, ACS Sustain. Chem. Eng. 7 (2019) 9272–9280. doi:10.1021/acssuschemeng.9b00174.

[176] E.N. Kalali, A. Montes, X. Wang, L. Zhang, M.E. Shabestari, Z. Li, D.Y. Wang, Effect of phytic acid–modified layered double hydroxide on flammability and mechanical properties of intumescent flame retardant polypropylene system, Fire Mater. 42 (2018) 213–220. doi:10.1002/fam.2482.

[177] S. Yang, J. Wang, S. Huo, J. Wang, Y. Tang, Synthesis of a phosphorus/nitrogen-containing compound based on maleimide and cyclotriphosphazene and its flame-retardant mechanism on epoxy resin, Polym. Degrad. Stab. 126 (2016) 9–16. doi:10.1016/j.polymdegradstab.2016.01.011.

[178] J. Li, W. Wang, W. Zhang, S. Zhang, Preparation and characterization of microencapsulated ammonium polyphosphate with UMF and its application in WPCs, Constr. Build. Mater. 65 (2014) 151–158. doi:10.1016/j.conbuildmat.2014.04.106.

[179] F. Shukor, A. Hassan, M. Saiful Islam, M. Mokhtar, M. Hasan, Effect of ammonium polyphosphate on flame retardancy, thermal stability and mechanical properties of alkali treated kenaf fiber filled PLA biocomposites, Mater. Des. 54 (2014) 425–429. doi:10.1016/j.matdes.2013.07.095.

[180] J.M. Gould, Alkaline peroxide delignification of agricultural residues to enhance enzymatic saccharification, Biotechnol. Bioeng. 26 (1984) 46–52. doi:10.1002/bit.260260110.

[181] M. Baiardo, G. Frisoni, M. Scandola, A. Licciardello, Surface chemical modification of natural cellulose fibers, J. Appl. Polym. Sci. 83 (2002) 38–45. doi:10.1002/app.2229.

[182] Mizi Fan, Dasong Dai, B. Huang, Fourier transform infrared spectroscopy for natural fibres, Web Sci. Mater. Anal. i (2018) 45–68.

[183] S.Y. Oh, I.Y. Dong, Y. Shin, C.K. Hwan, Y.K. Hak, S.C. Yong, H.P. Won, H.Y. Ji, Crystalline structure analysis of cellulose treated with sodium hydroxide and carbon dioxide by means of X-ray diffraction and FTIR spectroscopy, Carbohydr. Res. 340 (2005) 2376–2391. doi:10.1016/j.carres.2005.08.007.

[184] S.Y. Oh, D. Il Yoo, Y. Shin, G. Seo, FTIR analysis of cellulose treated with sodium hydroxide and carbon dioxide, Carbohydr. Res. 340 (2005) 417–428. doi:10.1016/j.carres.2004.11.027.

[185] M.A. Wahab, S. Jellali, N. Jedidi, Ammonium biosorption onto sawdust: FTIR analysis, kinetics and adsorption isotherms modeling, Bioresour. Technol. 101 (2010) 5070–5075. doi:10.1016/j.biortech.2010.01.121.

[186] G. Jiang, J. Qiao, F. Hong, Application of phosphoric acid and phytic acid-doped bacterial cellulose as novel proton-conducting membranes to PEMFC, Int. J. Hydrogen Energy. 37 (2012) 9182–9192. doi:10.1016/j.ijhydene.2012.02.195.

[187] L. Costes, F. Laoutid, F. Khelifa, G. Rose, S. Brohez, C. Delvosalle, P. Dubois, Cellulose/phosphorus combinations for sustainable fire retarded polylactide, Eur. Polym. J. 74 (2016) 218–228. doi:10.1016/j.eurpolymj.2015.11.030.

[188] B. Biswas, N. Pandey, Y. Bisht, R. Singh, J. Kumar, T. Bhaskar, Pyrolysis of agricultural biomass residues: Comparative study of corn cob, wheat straw, rice straw and rice husk, Bioresour. Technol. 237 (2017) 57–63. doi:10.1016/j.biortech.2017.02.046.

[189] S.B. and R.D. C. Re´ti, M. Casetta, S. Duquesne, Flammability properties of intumescent PLA including starch and lignin, Polym. Adv. Technol. (2008) 628–635. doi:10.1002/pat.

[190] B. Prieur, M. Meub, M. Wittemann, R. Klein, S. Bellayer, G. Fontaine, S. Bourbigot, Phosphorylation of lignin to flame retard acrylonitrile butadiene styrene (ABS), Polym. Degrad. Stab. 127 (2016) 32–43. doi:10.1016/j.polymdegradstab.2016.01.015.

[191] Y. Liu, X. Zhang, C. Song, Y. Zhang, Y. Fang, B. Yang, X. Wang, An effective surface modification of carbon fiber for improving the interfacial adhesion of polypropylene composites, Mater. Des. 88 (2015) 810–819. doi:10.1016/j.matdes.2015.09.100.

[192] and F.S.H. Majid Mehrabi Mazidi, Arman Edalat, Reyhaneh Berahman, Significantly Enhanced Glass Transition and Melt Strength: Tailoring Highly-Toughened Polylactide- (PLA-) Based Ternary Blends with the Interfacial Interactions, Phase Morphology, and Performance, Macromolecules. 51 (2018) 4298–4314.

[193] E.O. Ogunsona, M. Misra, A.K. Mohanty, Impact of interfacial adhesion on the microstructure and property variations of biocarbons reinforced nylon 6 biocomposites, Compos. Part A Appl. Sci. Manuf. 98 (2017) 32–44. doi:10.1016/j.compositesa.2017.03.011.

[194] H. Liu, W. Song, F. Chen, L. Guo, J. Zhang, Interaction of microstructure and interfacial adhesion on impact performance of polylactide (PLA) ternary blends, Macromolecules. 44 (2011) 1513–1522. doi:10.1021/ma1026934.

[195] M. Maroufkhani, A.A. Katbab, W. Liu, J. Zhang, Polylactide (PLA) and acrylonitrile butadiene rubber (NBR) blends: The effect of ACN content on

morphology, compatibility and mechanical properties, Polymer (Guildf). 115 (2017) 37–44. doi:10.1016/j.polymer.2017.03.025.

[196] Z. Yang, H. Peng, W. Wang, T. Liu, Crystallization behavior of poly(ε-caprolactone)/layered double hydroxide nanocomposites, J. Appl. Polym. Sci. 116 (2010) 2658–2667. doi:10.1002/app.

[197] L. Suryanegara, A.N. Nakagaito, H. Yano, Thermo-mechanical properties of microfibrillated cellulose-reinforced partially crystallized PLA composites, Cellulose. 17 (2010) 771–778. doi:10.1007/s10570-010-9419-5.

[198] L. Suryanegara, A.N. Nakagaito, H. Yano, The effect of crystallization of PLA on the thermal and mechanical properties of microfibrillated cellulose-reinforced PLA composites, Compos. Sci. Technol. 69 (2009) 1187–1192. doi:10.1016/j.compscitech.2009.02.022.

[199] M.A.S. Anwer, H.E. Naguib, A. Celzard, V. Fierro, Comparison of the thermal, dynamic mechanical and morphological properties of PLA-Lignin & PLA-Tannin particulate green composites, Compos. Part B Eng. 82 (2015) 92–99. doi:10.1016/j.compositesb.2015.08.028.

[200] Z. Yang, H. Peng, W. Wang, T. Liu, The Effect of Maleated Polylactic Acid (PLA) as an Interfacial Modifier in PLA-Talc Composites, J. Appl. Polym. Sci. 118 (2010) 2810–2820. doi:10.1002/app.

[201] R.W. Adriana Gregorova, Marta Hrabalova, Rene Kovalcik, Surface Modification of Spruce Wood Flour and Effects on the Dynamic Fragility of PLA/Wood Composites, Polym. Eng. Sci. 51 (2011) 143–150. doi:10.1002/pen.

[202] S. Gaan, G. Sun, K. Hutches, M.H. Engelhard, Effect of nitrogen additives on flame retardant action of tributyl phosphate: Phosphorus-nitrogen synergism, Polym. Degrad. Stab. 93 (2008) 99–108.

doi:10.1016/j.polymdegradstab.2007.10.013.

[203] L. Costes, F. Laoutid, M. Aguedo, A. Richel, S. Brohez, C. Delvosalle, P. Dubois, Phosphorus and nitrogen derivatization as efficient route for improvement of lignin flame retardant action in PLA, Eur. Polym. J. 84 (2016) 652–667. doi:10.1016/j.eurpolymj.2016.10.003.

[204] T. Agag, T. Takeichi, Polybenzoxazine-montmorillonite hybrid nanocomposites: Synthesis and characterization, Polymer (Guildf). 41 (2000) 7083–7090. doi:10.1016/S0032-3861(00)00064-1.

[205] F. Shukor, A. Hassan, M. Saiful Islam, M. Mokhtar, M. Hasan, Effect of ammonium polyphosphate on flame retardancy, thermal stability and mechanical properties of alkali treated kenaf fiber filled PLA biocomposites, Mater. Des. 54 (2014) 425–429. doi:10.1016/j.matdes.2013.07.095.

[206] Monika, P. Dhar, V. Katiyar, Thermal degradation kinetics of polylactic acid/acid fabricated cellulose nanocrystal based bionanocomposites, Int. J. Biol. Macromol. 104 (2017) 827–836. doi:10.1016/j.ijbiomac.2017.06.039.

[207] Z. Ma, D. Chen, J. Gu, B. Bao, Q. Zhang, Determination of pyrolysis characteristics and kinetics of palm kernel shell using TGA-FTIR and model-free integral methods, Energy Convers. Manag. 89 (2015) 251–259. doi:10.1016/j.enconman.2014.09.074.

[208] A. Leszczyńska, J. Njuguna, K. Pielichowski, J.R. Banerjee, Polymer/montmorillonite nanocomposites with improved thermal properties. Part II. Thermal stability of montmorillonite nanocomposites based on different polymeric matrixes, Thermochim. Acta. 454 (2007) 1–22. doi:10.1016/j.tca.2006.11.003.

[209] A. Leszczyńska, J. Njuguna, K. Pielichowski, J.R. Banerjee,

Polymer/montmorillonite nanocomposites with improved thermal properties. Part I. Factors influencing thermal stability and mechanisms of thermal stability improvement, Thermochim. Acta. 453 (2007) 75–96. doi:10.1016/j.tca.2006.11.002.

[210] M.P. Arrieta, E. Fortunati, F. Dominici, E. Rayón, J. López, J.M. Kenny, Multifunctional PLA-PHB/cellulose nanocrystal films: Processing, structural and thermal properties, Carbohydr. Polym. 107 (2014) 16–24. doi:10.1016/j.carbpol.2014.02.044.

[211] Y. Yuan, H. Yang, B. Yu, Y. Shi, W. Wang, L. Song, Y. Hu, Y. Zhang, Phosphorus and Nitrogen-Containing Polyols: Synergistic Effect on the Thermal Property and Flame Retardancy of Rigid Polyurethane Foam Composites, Ind. Eng. Chem. Res. 55 (2016) 10813–10822. doi:10.1021/acs.iecr.6b02942.

[212] H.W. Zaihang Zheng, Songfeng Liu, Bingnan Wang, Ting Yang, Xuejun Cui, Preparation of a Novel Phosphorus- and Nitrogen-Containing Flame Retardant and its Synergistic Effect in the Intumescent Flame-Retarding Polypropylene System, Polym. Compos. 36 (2014) 1606–1619. doi:10.1002/pc.

[213] P. Jiang, X. Gu, S. Zhang, S. Wu, Q. Zhao, Z. Hu, Synthesis, characterization, and utilization of a novel phosphorus/nitrogen-containing flame retardant, Ind. Eng. Chem. Res. 54 (2015) 2974–2982. doi:10.1021/ie505021d.

[214] L. Costes, F. Laoutid, S. Brohez, C. Delvosalle, P. Dubois, Phytic acid–lignin combination: A simple and efficient route for enhancing thermal and flame retardant properties of polylactide, Eur. Polym. J. 94 (2017) 270–285. doi:10.1016/j.eurpolymj.2017.07.018.

[215] B. Schartel, T.R. Hull, Development of fire-retarded materials - Interpretation of cone calorimeter data, Fire Mater. 31 (2007) 327–354. doi:10.1002/fam.

[216] B. Schartel, M. Bartholmai, U. Knoll, Some comments on the use of cone calorimeter data, Polym. Degrad. Stab. 88 (2005) 540–547. doi:10.1016/j.polymdegradstab.2004.12.016.

[217] W. Yang, B. Tawiah, C. Yu, Y.F. Qian, L.L. Wang, A.C.Y. Yuen, S.E. Zhu, E.Z. Hu, T.B.Y. Chen, B. Yu, H.D. Lu, G.H. Yeoh, X. Wang, L. Song, Y. Hu, Manufacturing, mechanical and flame retardant properties of poly(lactic acid) biocomposites based on calcium magnesium phytate and carbon nanotubes, Compos. Part A Appl. Sci. Manuf. 110 (2018) 227–236. doi:10.1016/j.compositesa.2018.04.027.

[218] Y. Yang, L. Haurie, J. Wen, S. Zhang, A. Ollivier, D.Y. Wang, Effect of oxidized wood flour as functional filler on the mechanical, thermal and flame-retardant properties of polylactide biocomposites, Ind. Crops Prod. 130 (2019) 301–309. doi:10.1016/j.indcrop.2018.12.090.

[219] A. Fina, F. Cuttica, G. Camino, Ignition of polypropylene/montmorillonite nanocomposites, Polym. Degrad. Stab. 97 (2012) 2619–2626. doi:10.1016/j.polymdegradstab.2012.07.017.

[220] A. Fina, G. Camino, Ignition mechanisms in polymers and polymer nanocomposites, Polym. Adv. Technol. 22 (2011) 1147–1155. doi:10.1002/pat.1971.

[221] Z. Li, D.Y. Wang, Nano-architectured mesoporous silica decorated with ultrafine Co3O4 toward an efficient way to delaying ignition and improving fire retardancy of polystyrene, Mater. Des. 129 (2017) 69–81. doi:10.1016/j.matdes.2017.05.021.

[222] R. Hajj, B. Otazaghine, R. Sonnier, R. El Hage, S. Rouif, M. Nakhl, J.M. Lopez-Cuesta, Influence of monomer reactivity on radiation grafting of phosphorus flame retardants on flax fabrics, Polym. Degrad. Stab. 166 (2019) 86–98.

doi:10.1016/j.polymdegradstab.2019.05.025.

[223] P. Song, C. Wang, L. Chen, Y. Zheng, L. Liu, Q. Wu, G. Huang, Y. Yu, H. Wang, Thermally stable, conductive and flame-retardant nylon 612 composites created by adding two-dimensional alumina platelets, Compos. Part A Appl. Sci. Manuf. 97 (2017) 100–110. doi:10.1016/j.compositesa.2017.02.029.

[224] Y. Yu, S. Fu, P. Song, X. Luo, Y. Jin, F. Lu, Q. Wu, J. Ye, Functionalized lignin by grafting phosphorus-nitrogen improves the thermal stability and flame retardancy of polypropylene, Polym. Degrad. Stab. 97 (2012) 541–546. doi:10.1016/j.polymdegradstab.2012.01.020.

[225] L. Liu, M. Qian, P. Song, G. Huang, Y. Yu, S. Fu, Fabrication of Green Lignin-based Flame Retardants for Enhancing the Thermal and Fire Retardancy Properties of Polypropylene/Wood Composites, ACS Sustain. Chem. Eng. 4 (2016) 2422–2431. doi:10.1021/acssuschemeng.6b00112.

[226] W. Yin, L. Chen, F. Lu, P. Song, J. Dai, L. Meng, Mechanically Robust, Flame-Retardant Poly(lactic acid) Biocomposites via Combining Cellulose Nanofibers and Ammonium Polyphosphate, ACS Omega. 3 (2018) 5615–5626. doi:10.1021/acsomega.8b00540.

[227] J.C. Markwart, A. Battig, L. Zimmermann, M. Wagner, J. Fischer, B. Schartel, F.R. Wurm, Systematically Controlled Decomposition Mechanism in Phosphorus Flame Retardants by Precise Molecular Architecture: P–O vs P–N, ACS Appl. Polym. Mater. 1 (2019) 1118–1128. doi:10.1021/acsapm.9b00129.

[228] J. Adamczyk, R. Dylewski, The impact of thermal insulation investments on sustainability in the construction sector, Renew. Sustain. Energy Rev. 80 (2017) 421–429. doi:10.1016/j.rser.2017.05.173.

[229] K. Govindan, K. Madan Shankar, D. Kannan, Sustainable material selection for

construction industry - A hybrid multi criteria decision making approach, Renew. Sustain. Energy Rev. 55 (2016) 1274–1288. doi:10.1016/j.rser.2015.07.100.

[230] M. Palumbo, A.M. Lacasta, M.P. Giraldo, L. Haurie, E. Correal, Bio-based insulation materials and their hygrothermal performance in a building envelope system (ETICS), Energy Build. 174 (2018) 147–155. doi:10.1016/j.enbuild.2018.06.042.

[231] M. Palumbo, A.M. Lacasta, A. Navarro, M.P. Giraldo, B. Lesar, Improvement of fire reaction and mould growth resistance of a new bio-based thermal insulation material, Constr. Build. Mater. 139 (2017) 531–539. doi:10.1016/j.conbuildmat.2016.11.020.

[232] M. Palumbo, J. Formosa, A.M. Lacasta, Thermal degradation and fire behaviour of thermal insulation materials based on food crop by-products, Constr. Build. Mater. 79 (2015) 34–39. doi:10.1016/j.conbuildmat.2015.01.028.

[233] J. Pinto, D. Cruz, A. Paiva, S. Pereira, P. Tavares, L. Fernandes, H. Varum, Characterization of corn cob as a possible raw building material, Constr. Build. Mater. 34 (2012) 28–33. doi:10.1016/j.conbuildmat.2012.02.014.

[234] A. Paiva, S. Pereira, A. Sá, D. Cruz, H. Varum, J. Pinto, A contribution to the thermal insulation performance characterization of corn cob particleboards, Energy Build. 45 (2012) 274–279. doi:10.1016/j.enbuild.2011.11.019.

[235] A.B. Akinyemi, J.O. Afolayan, E. Ogunji Oluwatobi, Some properties of composite corn cob and sawdust particle boards, Constr. Build. Mater. 127 (2016) 436–441. doi:10.1016/j.conbuildmat.2016.10.040.

[236] P. Deng, Y. Shi, Y. Liu, Y. Liu, Q. Wang, Solidifying process and flame retardancy of epoxy resin cured with boron-containing phenolic resin, Appl. Surf. Sci. 427 (2018) 894–904. doi:10.1016/j.apsusc.2017.07.278.

[237] S.Y. Chan, L. Si, K.I. Lee, P.F. Ng, L. Chen, B. Yu, Y. Hu, R.K.K. Yuen, J.H. Xin, B. Fei, A novel boron–nitrogen intumescent flame retardant coating on cotton with improved washing durability, Cellulose. 25 (2018) 843–857. doi:10.1007/s10570-017-1577-2.

[238] ECHA, ECHA (European Chemical Agency)-Inclusion of substances of very high concern in the candidate list (Decision by the Executive Director), (2010) ED30. http://echa.europa.eu/es/candidate-list-table?

[239] M. Dočan, A. Ylmaz, E. Bayraml, Synergistic effect of boron containing substances on flame retardancy and thermal stability of intumescent polypropylene composites, Polym. Degrad. Stab. 95 (2010) 2584–2588. doi:10.1016/j.polymdegradstab.2010.07.033.

[240] L. Ai, S. Chen, J. Zeng, L. Yang, P. Liu, Synergistic Flame Retardant Effect of an Intumescent Flame Retardant Containing Boron and Magnesium Hydroxide, ACS Omega. 4 (2019) 3314–3321. doi:10.1021/acsomega.8b03333.

[241] F. Domínguez-Muñoz, B. Anderson, J.M. Cejudo-López, A. Carrillo-Andrés, Uncertainty in the thermal conductivity of insulation materials, Energy Build. 42 (2010) 2159–2168. doi:10.1016/j.enbuild.2010.07.006.

[242] J. Zhang, Q. Ji, F. Wang, L. Tan, Y. Xia, Effects of divalent metal ions on the flame retardancy and pyrolysis products of alginate fibres, Polym. Degrad. Stab. 97 (2012) 1034–1040. doi:10.1016/j.polymdegradstab.2012.03.004.

[243] Y. Liu, C.J. Zhang, J.C. Zhao, Y. Guo, P. Zhu, D.Y. Wang, Bio-based barium alginate film: Preparation, flame retardancy and thermal degradation behavior, Carbohydr. Polym. 139 (2016) 106–114. doi:10.1016/j.carbpol.2015.12.044.

[244] L. Ai, S. Chen, J. Zeng, P. Liu, W. Liu, Y. Pan, D. Liu, Synthesis and flame retardant properties of cyclophosphazene derivatives containing boron, Polym.

Degrad. Stab. 155 (2018) 250–261. doi:10.1016/j.polymdegradstab.2018.07.026.

[245] N.N. Bakhman, Smoldering wave propagation mehcanism. 1. Critical conditions, in: Combust. Explos. Shock Waves, 1993: pp. 14–17.

[246] N.N. Bakhman, Smoldering wave propagation mechanism. 2. smoldering velocity and temperature in smoldering zone, in: Combust. Explos. Shock Waves, 1993: pp. 18–24.

[247] L. Haurie, A.M. Lacasta, A. Ciudad, V. Realinho, J.I. Velasco, Addition of flame retardants in epoxy mortars: Thermal and mechanical characterization, Constr. Build. Mater. 42 (2013) 266–270. doi:10.1016/j.conbuildmat.2012.12.012.

[248] Y. Liu, J.S. Wang, P. Zhu, J.C. Zhao, C.J. Zhang, Y. Guo, L. Cui, Thermal degradation properties of biobased iron alginate film, J. Anal. Appl. Pyrolysis. 119 (2016) 87–96. doi:10.1016/j.jaap.2016.03.014.

[249] Q. Wang, J. Li, J. Winandy, Chemical mechanism of fire retardance of boric acid on wood, Wood Sci. Technol. 38 (2004) 375–389. doi:10.1007/s00226-004-0246-4.

[250] J. Zhang, Q. Ji, X. Shen, Y. Xia, L. Tan, Q. Kong, Pyrolysis products and thermal degradation mechanism of intrinsically flame-retardant calcium alginate fibre, Polym. Degrad. Stab. 96 (2011) 936–942. doi:10.1016/j.polymdegradstab.2011.01.029.

[251] Q. Liu, S. Wang, Y. Zheng, Z. Luo, K. Cen, Mechanism study of wood lignin pyrolysis by using TG-FTIR analysis, J. Anal. Appl. Pyrolysis. 82 (2008) 170–177. doi:10.1016/j.jaap.2008.03.007.

[252] M. Dogan, S. Murat Unlu, Flame retardant effect of boron compounds on red phosphorus containing epoxy resins, Polym. Degrad. Stab. 99 (2014) 12–17. doi:10.1016/j.polymdegradstab.2013.12.017.

[253] Q. Liu, Z. Zhong, S. Wang, Z. Luo, Interactions of biomass components during pyrolysis: A TG-FTIR study, J. Anal. Appl. Pyrolysis. 90 (2011) 213–218. doi:10.1016/j.jaap.2010.12.009.

[254] N.A. Isitman, C. Kaynak, Nanoclay and carbon nanotubes as potential synergists of an organophosphorus flame-retardant in poly(methyl methacrylate), Polym. Degrad. Stab. 95 (2010) 1523–1532. doi:10.1016/j.polymdegradstab.2010.06.013.

[255] U. Braun, B. Schartel, Flame retardant mechanisms of red phosphorus and magnesium hydroxide in high impact polystyrene, Macromol. Chem. Phys. 205 (2004) 2185–2196. doi:10.1002/macp.200400255.

[256] E. Wawrzyn, B. Schartel, A. Karrasch, C. Jäger, Flame-retarded bisphenol A polycarbonate/silicon rubber/bisphenol A bis(diphenyl phosphate): Adding inorganic additives, Polym. Degrad. Stab. 106 (2014) 74–87. doi:10.1016/j.polymdegradstab.2013.08.006.

[257] M.A. Fichera, U. Braun, B. Schartel, H. Sturm, U. Knoll, C. Jäger, Solid-state NMR investigations of the pyrolysis and thermo-oxidative decomposition products of a polystyrene/red phosphorus/magnesium hydroxide system, J. Anal. Appl. Pyrolysis. 78 (2007) 378–386. doi:10.1016/j.jaap.2006.09.013.

[258] Y.Y. Gao, C. Deng, Y.Y. Du, S.C. Huang, Y.Z. Wang, A novel bio-based flame retardant for polypropylene from phytic acid, Polym. Degrad. Stab. 161 (2019) 298–308. doi:10.1016/j.polymdegradstab.2019.02.005.

[259] J. Tröltzsch, K. Schäfer, D. Niedziela, I. Ireka, K. Steiner, L. Kroll, Simulation of RIM-process for Polyurethane Foam Expansion in Fiber Reinforced Sandwich Structures, Procedia CIRP. 66 (2017) 62–67. doi:10.1016/j.procir.2017.03.285.

[260] L. CoDyre, K. Mak, A. Fam, Flexural and axial behaviour of sandwich panels with bio-based flax fibre-reinforced polymer skins and various foam core densities, J.

Sandw. Struct. Mater. 20 (2018) 595–616. doi:10.1177/1099636216667658.

[261] K. Mak, A. Fam, C. MacDougall, Flexural Behavior of Sandwich Panels with Bio-FRP Skins Made of Flax Fibers and Epoxidized Pine-Oil Resin, J. Compos. Constr. 19 (2015) 04015005. doi:10.1061/(asce)cc.1943-5614.0000560.

[262] C. Atas, U. Potoğlu, The effect of face-sheet thickness on low-velocity impact response of sandwich composites with foam cores, J. Sandw. Struct. Mater. 18 (2016) 215–228. doi:10.1177/1099636215613775.

[263] C.S. Lee, D.G. Lee, J.H. Oh, Co-cure bonding method for foam core composite sandwich manufacturing, Compos. Struct. 66 (2004) 231–238. doi:10.1016/j.compstruct.2004.04.042.

[264] A. Hörold, B. Schartel, V. Trappe, M. Korzen, J. Bünker, Fire stability of glass-fibre sandwich panels: The influence of core materials and flame retardants, Compos. Struct. 160 (2017) 1310–1318. doi:10.1016/j.compstruct.2016.11.027.

[265] A. Manalo, T. Aravinthan, A. Fam, B. Benmokrane, State-of-the-Art Review on FRP Sandwich Systems for Lightweight Civil Infrastructure, J. Compos. Constr. 21 (2016) 04016068. doi:10.1061/(asce)cc.1943-5614.0000729.